

**IRON-CARBON COMPOSITES FOR THE REMEDIATION OF
CHLORINATED HYDROCARBONS**

AN ABSTRACT

SUBMITTED ON THE THIRD DAY OF APRIL 2013
TO THE DEPARTMENT OF CHEMICAL AND BIOMOLECULAR ENGINEERING
IN PARTIAL FULFILLMENT OF THE REQUIREMENTS
OF THE SCHOOL OF SCIENCE AND ENGINEERING
OF TULANE UNIVERSITY
FOR THE DEGREE
OF
DOCTOR OF PHILOSOPHY

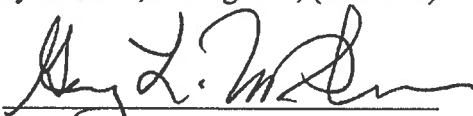
BY



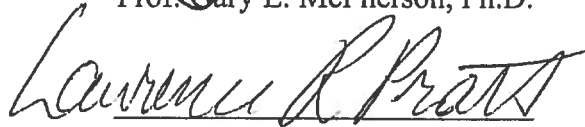
BHANU KIRAN SUNKARA

APPROVED: 


Prof. Vijay T. John, D.Eng.Sci., (Director)



Prof. Gary L. McPherson, Ph.D.



Prof. Lawrence R. Pratt, Ph.D.



Prof. Vladimir L. Kolesnichenko, Ph.D.



Prof. Noshir S. Pesika, Ph.D

ABSTRACT

This research is focused on engineering submicron spherical carbon particles as effective carriers/supports for nanoscale zerovalent iron (NZVI) particles to address the *in situ* remediation of soil and groundwater chlorinated contaminants. Chlorinated hydrocarbons such as trichloroethylene (TCE) and tetrachloroethylene (PCE) form a class of dense non-aqueous phase liquid (DNAPL) toxic contaminants in soil and groundwater. The *in situ* injection of NZVI particles to reduce DNAPLs is a potentially simple, cost-effective, and environmentally benign technology that has become a preferred method in the remediation of these compounds. However, unsupported NZVI particles exhibit ferromagnetism leading to particle aggregation and loss in mobility through the subsurface.

This work demonstrates two approaches to prepare carbon supported NZVI (iron-carbon composites) particles. The objective is to establish these iron-carbon composites as extremely useful materials for the environmental remediation of chlorinated hydrocarbons and suitable materials for the *in situ* injection technology. This research also demonstrates that it is possible to vary the placement of iron nanoparticles either on the external surface or within the interior of carbon microspheres using a one-step aerosol-based process. The simple process of modifying iron placement has significant potential applications in heterogeneous catalysis as both the iron and carbon are widely used catalysts and catalyst supports. Furthermore, the aerosol-based process is applied to prepare new class of supported catalytic materials such as carbon-supported palladium nanoparticles for *ex situ* remediation of contaminated water.

The iron-carbon composites developed in this research have multiple functionalities (a) they are reactive and function effectively in reductive dehalogenation (b) they are highly adsorptive thereby bringing the chlorinated compound to the proximity of the reactive sites and also serving as adsorption materials for decontamination (c) they are of the optimal size for transport through sediments (d) they have amphiphilic chemical functionalities that help stabilize them when they reach the DNAPL target zones. Finally, the iron-carbon composite microspheres prepared through aerosol-based process can be used for *in situ* injection technology as the process is conducive to scale-up and the materials are environmentally benign.

**IRON-CARBON COMPOSITES FOR THE REMEDIATION OF
CHLORINATED HYDROCARBONS**

A DISSERTATION

SUBMITTED ON THE THIRD DAY OF APRIL 2013

TO THE DEPARTMENT OF CHEMICAL AND BIOMOLECULAR ENGINEERING

IN PARTIAL FULFILLMENT OF THE REQUIREMENTS

OF THE SCHOOL OF SCIENCE AND ENGINEERING

OF TULANE UNIVERSITY

FOR THE DEGREE

OF

DOCTOR OF PHILOSOPHY

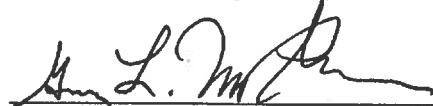
BY



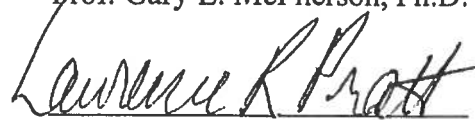
BHANU KIRAN SUNKARA

APPROVED: 

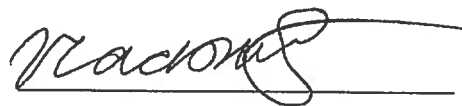
Prof. Vijay T. John, D.Eng.Sci., (Director)



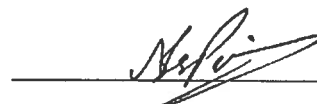
Prof. Gary L. McPherson, Ph.D.



Prof. Lawrence R. Pratt, Ph.D.



Prof. Vladimir L. Kolesnichenko, Ph.D.



Prof. Noshir S. Pesika, Ph.D.

© Copyright by Bhanu Kiran Sunkara, 2013

All Rights Reserved

ACKNOWLEDGMENTS

I would like to express my deepest gratitude to my advisor, Professor Vijay John, for being a great source of inspiration, for his excellent guidance, encouragement and support throughout my doctoral studies. I am very grateful to him for giving me the opportunity to work in his research group. He is a great mentor and I feel myself very fortunate to have him as my advisor and sincerely thank him for all his support.

I thank my thesis committee members Prof. Lawrence Pratt, Prof Gary McPherson, and Prof. Vladimir Kolesnichenko for their scientific guidance and valuable suggestions during my research work. Special thanks to Prof. Noshir Pesika for agreeing to serve on my thesis defense committee at the last moment.

This research work presented in this dissertation was made possible through several collaborations and research grants. I extend my gratitude to Dr. Vladimir Kolesnichenko (Xavier University) and Mr. Dave Culpepper (NanoFex). I would like to thank the Department of Chemical & Biomolecular Engineering, School of Science and Engineering and the Tulane University for providing all the resources for my doctoral education. Funding from the Environmental Protection Agency, the National Science Foundation and NanoFex is gratefully acknowledged.

I would like thank Dr. Jibao He for his great help with electron microscopy studies. He is excellent and very patient in training me to use the SEM and TEM

techniques. I would like to thank Dr. McPherson for all his insights and discussions in helping me analyze my research results. All the Friday meetings with him have been very helpful. Thanks to my group members (Joy, Pradeep, Jingjing, Thiru, Santosh, Yingqing, Rubo, Igor, Jaspreet, Jingjian, Sehinde, and Yuehang) for all their help in the lab. Thanks to my Lafayette buddies Lalit, Rajesh and Vijay for their help and all good times here in NOLA. Special thanks to my buddies Kalyan, Chandu, Kiran and Naveen for being there for me, for all the great road trips and their encouragement throughout my PhD.

Finally, I would like to thank my parents (Sudhakar and Kamaladevi), my brother Sai, and my sister Janapriya. They always stood by me through the good times and bad. Special thanks to my wife Anusha for being patient with me in this last year of my doctoral studies and for her moral support. I love you all very much!!

Bhanu

TABLE OF CONTENTS

ACKNOWLEDGEMENTS.....	ii
LIST OF TABLES	viii
LIST OF FIGURES	ix
CHAPTERS	
1 General Introduction	1
1.1 Soil and groundwater contamination by chlorinated hydrocarbons	1
1.2 Nanoscale zerovalent iron (NZVI) for remediation	5
1.3 Dechlorination mechanism of chlorinated hydrocarbons by NZVI	6
1.4 Factors affecting NZVI for in situ remediation technology	8
1.5 Objective	10
2 Nanoscale Zero-Valent Iron supported on Uniform Carbon Microspheres for the <i>In situ</i> Remediation of Chlorinated Hydrocarbons	14
2.1 Introduction	14
2.2 Experimental Section	19
2.2.1 Chemicals	19
2.2.2 Preparation of Fe ⁰ /C composite particles	19
2.2.3 Particle Characterization	22
2.2.4 Reaction and stability analysis	22
2.3 Results and discussion	24

2.3.1	Particle characterization	24
2.3.2	Reactivity characteristics	27
2.3.3	Adsorption characteristics	30
2.3.4	Colloidal stability and partitioning	31
2.3.5	Transport characteristics	34
2.3.6	Reaction rate enhancements	38
2.4	Summary	42
3	Modifying Metal Nanoparticle Placement on Carbon Supports using an Aerosol-Based Process, with Application to the Environmental Remediation of Chlorinated Hydrocarbons	43
3.1	Introduction	43
3.2	Experimental section	46
3.2.1	Materials	46
3.2.2	Preparation of Fe-C composite microspheres	46
3.2.3	Particle characterization	47
3.2.4	Reactivity analysis	48
3.3	Results and discussion	48
3.3.1	Particle characteristics as a function of aerosolization temperature	50
3.3.2	Reactivity characteristics of Fe-C composite particles for the reductive dechlorination of TCE	62
3.4	Summary	64

4	Iron-Carbon Microspheres Prepared through a facile Aerosol-Based Process for the Simultaneous Adsorption and Reduction of Chlorinated Hydrocarbons	66
4.1	Introduction	66
4.2	Experimental Section	68
4.2.1	Materials	68
4.2.2	Preparation of Fe-C composite microspheres	68
4.2.3	Particle characterization	69
4.2.4	Reaction analysis	69
4.3	Results and Discussion	70
4.3.1	Chemistry in a droplet	70
4.3.2	Particle characterization	73
4.3.3	Reactivity characteristics	75
4.3.4	Adsorption characteristics	79
4.4	Summary	86
5	Carbon Supported Palladium Nanoparticles prepared through a facile Aerosol-Based Process for the Catalytic Hydrodechlorination of Trichloroethylene	87
5.1	Introduction	87
5.2	Experimental Section	88
5.2.1	Materials	88
5.2.2	Preparation of Palladium-Carbon (Pd-C) composite microspheres	88

5.2.3	Characterization and Analysis	89
5.3	Results and Discussion	90
5.3.1	Chemistry in a droplet	90
5.3.2	Particle characterization	93
5.3.3	Reaction characteristics	96
5.4	Summary	99
6	Conclusions and Future work	100
Appendix: Adsorption Effect of Carbons on the Catalytic		
Hydrodechlorination of Trichloroethylene		105
1.	Introduction	105
2.	Experimental Section	106
2.1	Materials	106
2.2	Characterization and analysis	106
3.	Results	107
References		117

LIST OF TABLES

Table 1.1 Properties of the chlorinated hydrocarbons trichloroethylene (TCE) and tetrachloroethylene (PCE).

Table 4.1 Reaction rate constants for reduction of the various chlorinated ethylenes using the aerosol based Fe-C composite particles.

Table 4.2 Comparison of adsorption capacities of the aerosol-based Fe-C composites with humic acid and commercial activated carbon. In all experiments, 20 mL of a 20 ppm chlorinated ethylene ((a) PCE, (b) TCE, (c) 1, 2-DCE, (d) 1, 1-DCE, and (e) VC) solution and 0.2g of particles were used.

Table 4.3 Calculated partition coefficient of chlorinated hydrocarbons adsorption on the aerosol-based Fe-C composite particles.

Table B.1 Reaction rate constants for the reduction of trichloroethylene (TCE) using the commercial Pd/AC and Pd/Al systems with separate addition of activated carbon to the particle suspensions.

LIST OF FIGURES

Figure 1.1 Molecular structures of (a) trichloroethylene (TCE) and (b) tetrachloroethylene (PCE).

Figure 1.2 Schematic of the leakage of DNAPL from a storage tank and migration into aquifers through vadose zone. Formation of plumes of at the bottom of aquifer is also depicted.

Figure 2.1 (a) SEM (b) TEM of 500 nm carbon particles obtained from hydrothermal dehydration and pyrolysis of sucrose. (c) Schematic of the multifunctional particulate system showing a NZVI embedded carbon particle with a corona of CMC. The red dots signify TCE in solution and adsorbed on the carbon.

Figure 2.2 (a) Flow sheet for the preparation of uniform monodisperse carbon microspheres (b) Schematic for the synthesis of multifunctional particulate system.

Figure 2.3 (a) SEM and (b) TEM of Fe^0/C composite particles (carbons embedded with NZVI) (c) Cut section TEM of Fe^0/C composite particles (carbons embedded with NZVI).

Figure 2.4 (a) XRD pattern of Fe^0/C composite microsphere particles (b) Nitrogen adsorption-desorption isotherms for the carbon microspheres and Fe^0/C composite microspheres. Inset showing the BJH pore size distribution derived from the desorption branch of the isotherm of carbon microspheres and Fe^0/C composite microspheres.

Figure 2.5 TCE removal from solution and gas product evolution rates for Fe⁰/C composites (0.25 g particles, and 0.1 % Pd (w/w Fe⁰). M/M_0 is the fraction of the original TCE remaining and P/P_f is the ratio of the gas product peak to the gas product peak at the end of 9 days. The pseudo first order rate constant is 0.0145h⁻¹ and mass normalized rate constant is 4.64*10⁻³ Lg⁻¹h⁻¹.

Figure 2.6 (a) Stability of carbon microspheres (500nm) in various concentrations of carboxymethyl cellulose (b) Viscosity versus shear rate for various concentrations of carboxymethyl cellulose. (Electrolyte (NaCl) concentration in all experiments is 1mM).

Figure 2.7 (a) Stability of Fe⁰ /C + CMC in water (b) Partitioning characteristics of Fe⁰+CMC and Fe⁰ /C +CMC when contacted with a two-phase water-TCE system.

Figure 2.8 Characterization of transport through packed capillaries (a) experimental set-up. Flow rate: 0.1 mL/min, sand length: 3 cm and injected suspension volume: 0.03 mL; Photograph of capillary (b) before and (c) after water flushing. Panel i and ii show optical micrographs of sediments and particles at different locations after water flushing (all scale bars are 100 um). Arrows show the accumulated particles in the packed capillary at different locations.

Figure 2.9 TCE removal from solution and gas product evolution rates for Fe⁰/C composites prepared by incipient wetness method (20 ppm TCE, Fe⁰ concentration 10 g/L, and 0.1 % Pd (w/w Fe⁰). M/M_0 is the fraction of the original TCE remaining and P/P_f is the ratio of the gas product peak to the gas product peak at the end of 120 min. The first order rate constant is 2.95h⁻¹ and mass normalized rate constant is 295*10⁻³ Lg⁻¹h⁻¹.

Figure 2.10 Schematic of the multifunctional particulate system showing a NZVI (red cubes) embedded carbon particle surrounded by CMC containing NZVI (brown cubes). The red dots signify TCE in solution and adsorbed on the carbon.

Figure 3.1 (a) Schematic of aerosol reactor for composite particles preparation and (b) schematic of reaction in an aerosol droplet.

Figure 3.2 XRD patterns of iron species precipitated on the carbon at the various aerosolization temperatures.

Figure 3.3 FTIR spectra of the carbon showing residual functional groups which can be removed through pyrolysis.

Figure 3.4 SEM images of multiple particles prepared at the various aerosolization temperatures.

Figure 3.5 Single particle (a) SEM and (b) TEM of composite particles prepared by the aerosol-based process at various heating zone temperatures. The particles become significantly more porous when prepared at high aerosolization temperatures.

Figure 3.6 Cut-section TEM of composites at different heating zone temperatures. The evolution of iron nanoparticle placement from the external surface to the particle interior with an increase in the heating zone temperature from 300 to 1000 °C is noted.

Figure 3.7 (a) Nitrogen adsorption-desorption isotherms and (b) BJH pore size distributions of the Fe salt-C composites prepared at 300 to 1000 °C.

Figure 3.8 Proposed mechanism of morphological changes and metal nanoparticle placement with temperature.

Figure 3.9 (a) Representative GC trace of headspace analyses showing TCE degradation and reaction product evolution at various reaction times (b) TCE removal from solution and gas product evolution rates for Fe-C composites. M/M_0 is the fraction of the original TCE remaining and P/P_f is the ratio of the gas product peak to the gas product peak at the end of 4 hr.

Figure 4.1 (a) Schematic showing the aerosol process for composite particle synthesis and (b) schematic of reaction in an aerosol droplet.

Figure 4.2 (a) SEM (b) TEM and (c) High resolution TEM of Fe-C composite particles prepared by the aerosol-based process. Inset in Figure (a) is the single particle SEM of the Fe-C composite.

Figure 4.3 Representative headspace analyses using gas chromatography showing (a) PCE and (b) TCE degradation and reaction product evolution at various reaction times.

Figure 4.4 (a) PCE and (b) TCE removal from solution and gas product evolution rates for the Fe-C composites. M/M_0 is the fraction of the original chlorinated ethylene remaining and P/P_f is the ratio of the gas product peak to the gas product peak at the end of reaction.

Figure 4.5 Reaction kinetics of the intermediate chlorinated ethylenes (a) 1, 2-DCE, (b) 1, 1-DCE, and (c) VC.

Figure 4.6 Comparison of the adsorption capacities of humic acid, Fe/C from an aerosol-based process and commercial activated carbon. In all experiments, 20 mL of a 20 ppm

chlorinated ethylene ((a) PCE, (b) TCE, (c) 1, 2-DCE, (d) 1, 1-DCE, and (e) VC) solution and 0.2g of particles were used.

Figure 5.1 (a) Schematic showing the aerosol process for composite particles preparation and (b) schematic of the reaction in an aerosol droplet.

Figure 5.2 (a) SEM (b) TEM (c) high-resolution TEM of carbon supported palladium nanoparticles (Pd-C composite microspheres) prepared using aerosol-based process at 400 °C and H₂ reduction at 300 °C. (d) EDS spectrum of the Pd-C composites confirming the presence of palladium.

Figure 5.3 (a) SEM (b) single particle SEM (c) high-resolution TEM of carbon supported palladium nanoparticles (Pd-C composite microspheres) prepared using aerosol-based process at 400 °C and H₂ reduction at 400 °C. (d) EDS spectrum of the Pd-C composites confirming the presence of palladium.

Figure 5.4 TCE removals from solution and gas product evolution rates for Pd-C particles (aerosol-based process at 400 °C and H₂ reduction at 300 °C). M/M_0 is the original TCE remaining, and P/P_f is the ration of gas product peak to the gas product peak at the end of 5 h.

Figure 6.1 (a) SEM (b) TEM of carbon supported nanoscale Fe-Ni bimetallic particles (Fe-Ni/C) prepared using aerosol-based process at 700 °C. (c) TCE removal from solution and gas product evolution rates for Fe-Ni/C composite particles. M/M_0 is the fraction of the original chlorinated ethene remaining and P/P_f is the ratio of the gas product peak to the gas product peak at the end of 12 h.

Figure B.1 (a) SEM and (b) high-resolution SEM of commercial palladium on activated carbon (Pd/AC) material.

Figure B.2 (a) TEM and (b) high-resolution TEM of the commercial palladium on activated carbon (Pd/AC) material. (c) The EDS spectrum of the commercial Pd/AC confirming the presence of palladium.

Figure B.3 (a) SEM and (b) high-resolution SEM of commercial palladium on alumina (Pd/Al) material.

Figure B.4 (a) TEM and (b) high-resolution TEM of the commercial palladium on alumina (Pd/Al) material. (c) The EDS spectrum of the commercial Pd/Al material confirming the presence of palladium.

Figure B.5 TCE removal from solution Pd/AC systems with separate addition of activated carbon. M/M_0 is the original TCE remaining in the system.

Figure B.6 Gas product evolution for Pd/AC systems with separate addition of activated carbon. P/P_f is the ration of gas product peak to the gas product peak at the end of the reaction.

Figure B.7 TCE removal from solution Pd/Al systems with separate addition of activated carbon. M/M_0 is the original TCE remaining in the system.

Figure B.8 Gas product evolution for Pd/Al systems with separate addition of activated carbon. P/P_f is the ration of gas product peak to the gas product peak at the end of the reaction.

Dedicated to

My Parents (Mr. Sudhakar and Ms. Kamaladevi)

And

My grandmothers (Ms. Kanthamma and Ms. Rajyalakshmi)

Chapter 1

General Introduction

1.1. Soil and groundwater contamination by chlorinated hydrocarbons

Chlorinated solvents such as trichloroethylene (TCE) and tetrachloroethylene (also called perchloroethylene, PCE) have been extensively used in various industries since the 1920s – TCE for degreasing metals, and PCE for paint stripping and as a dry cleaning solvent.^{1, 2} The molecular structures of TCE and PCE are shown in Figure 1.1 and their properties are given in Table 1.1. These solvents are denser than water, have a low but finite solubility in water and are classified as dense non-aqueous phase liquid (DNAPL) toxic contaminants in soil and groundwater. Improper storage, handling and disposal of these solvents have led to widespread contamination of soil and groundwater.³ Figure 1.2 is a schematic showing the migration of DNAPL into aquifers through soil and sedimentary rock. Once released into environment, they transport readily in the subsurface due to their higher density and form a contaminant plume. They slowly leach into groundwater and stays as dissolved phase. The schematic also depicts the accumulation of DNAPL in bedrock. Depending on the level of human exposure, the health effects of chlorinated compounds range from nausea, headaches, and difficulty concentrating to lung cancer. Due to their toxicity and carcinogenicity, the United States Environmental Protection Agency (US EPA) has set maximum contamination level (MCL) as 5 ppb (0.005 mg L^{-1}) for both TCE and PCE in drinking water.³⁻⁵

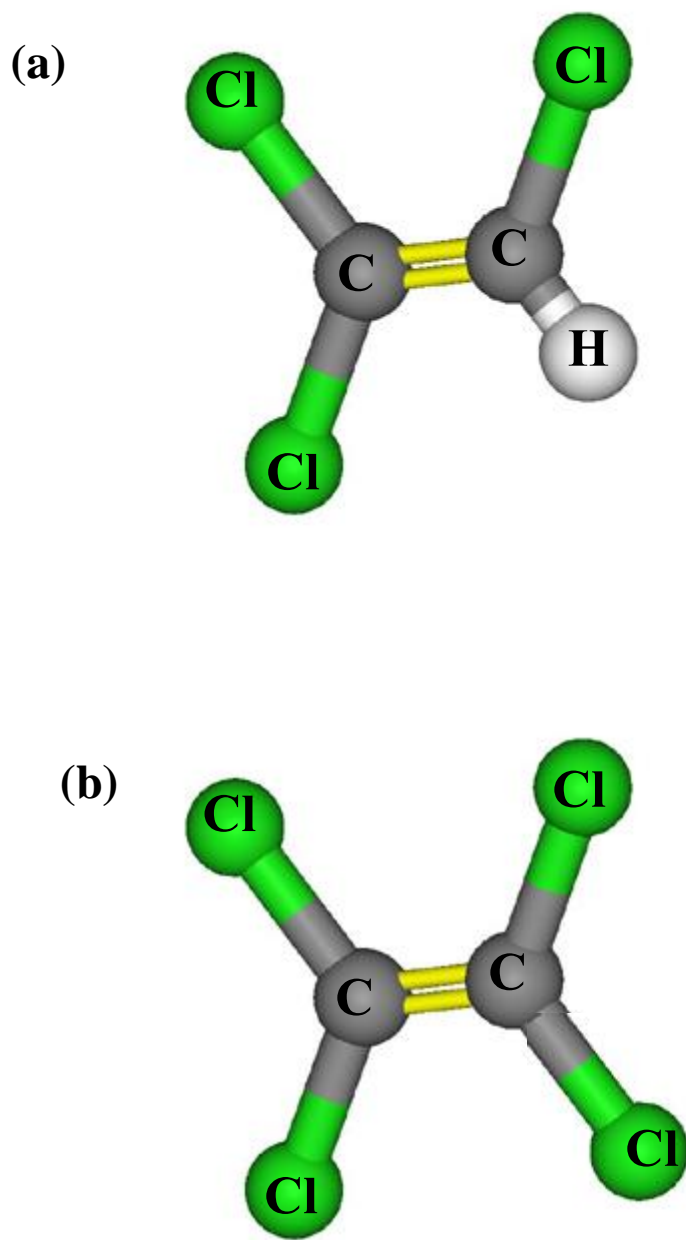


Figure 1.1 Molecular structures of (a) trichloroethylene (TCE) (b) tetrachloroethylene (PCE).

Chlorinated Solvent	Trichloroethylene	Tetrachloroethylene
Molecular formula	C_2HCl_3	C_2Cl_4
Molar Mass	$131.39 \text{ g mol}^{-1}$	165.8 g mol^{-1}
Appearance	Colorless liquid	Clear, colorless liquid
Density	1.46 g/L	1.622 g/L
Boiling point	87.2 °C	121.1 °C
Solubility in water	1100 mg/L (20°C)	150 mg/L (20 °C)

Table 1.1 Properties of the chlorinated hydrocarbons trichloroethylene (TCE) and tetrachloroethylene (PCE).

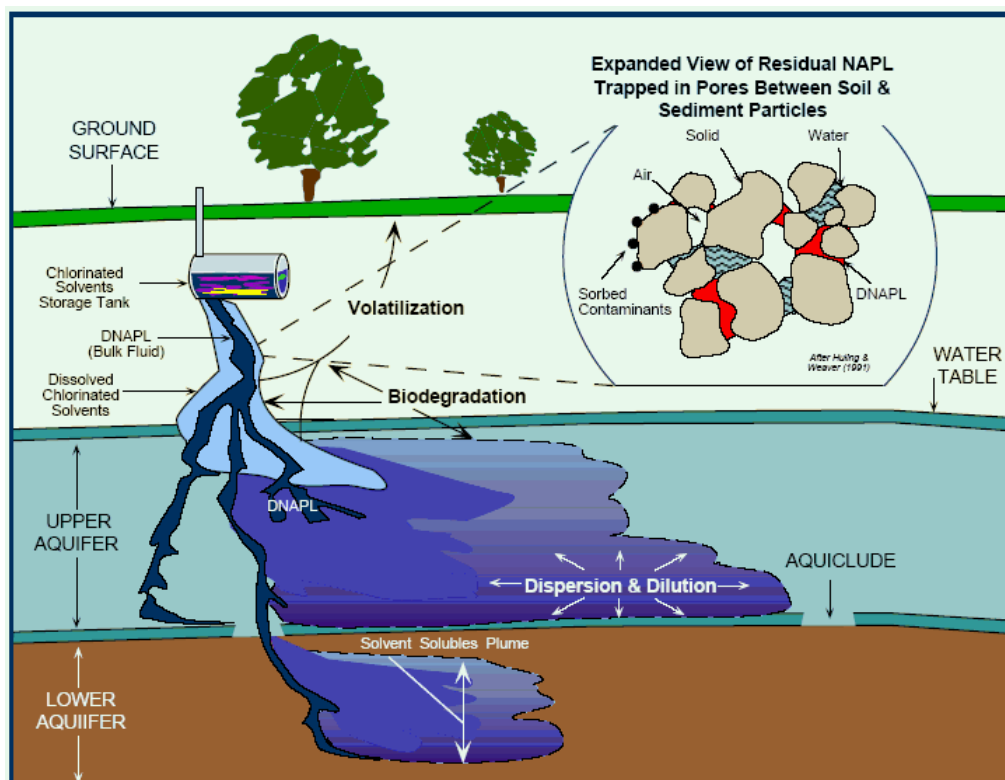


Figure 1.2 Schematic of the leakage of DNAPL from a storage tank and migration into aquifers through vadose zone. Formation of plumes of at the bottom of aquifer is also depicted.

(From:<http://oceanworld.tamu.edu/resources/environment-book/groundwaterremediation.html>)

The EPA has identified the possibility of 300,000 federal, state, and privately owned contamination sites in the United States that have some level of contamination and require remediation.⁶ Most of these contaminated sites have TCE or other chlorinated solvents that may potentially contaminate drinking water.⁶

1.2.Nanoscale zerovalent iron (NZVI) for remediation

Various methods have been developed for the remediation of DNAPLs such as soil vapor extraction, bioremediation, pump and treat methods, and the installation of permeable reactive barriers.⁷⁻¹² Compared to these methods, the *in situ* injection of NZVI particles to reduce chlorinated hydrocarbons is potentially simple, cost-effective, and environmentally benign technology that become a preferred method in the remediation of these compounds.^{13, 14} The uses of ZVI in micron-sized particles or in the form of iron filings for pump and treat methods and as reactive materials in the permeable reactive barrier technology is well established. ZVI particles prepared in nanoscale size, called as NZVI, have increased reaction rates resulting from their increased surface areas.¹⁵⁻²² Furthermore, the reaction rates can be significantly enhanced with the addition of a second metal to NZVI, typically noble metal such as palladium (Pd), nickel (Ni), or silver (Ag). These are called bimetallic nanoparticles and Pd is the most common noble metal used with NZVI, which acts as a catalyst for reductive dehalogenation reactions.²³⁻²⁶ The addition of small amounts of catalyst lowers the activation energy of the reaction and significantly enhances the reactivity through dissociative adsorption of H₂ on the catalyst surface.¹⁵ In any case, NZVI particles have gained a lot of attention for the environmental remediation of soil and groundwater contaminants due to their small size and improved properties. NZVI particles have excess surface energies and high surface areas which

lead to higher contaminant remediation rates compared to bulk ZVI materials. Several studies conducted on the treatability of chlorinated hydrocarbons using NZVI confirms that they are superior to micron-sized ZVI in reductive dechlorination and are potential reactive materials for *in situ* injection remediation technology.^{21, 27-29}

1.3. Dechlorination mechanism of chlorinated hydrocarbons by NZVI

Numerous studies were performed on the use of ZVI in both micron- and nanoscale particle sizes towards the dechlorination of PCE and TCE for more than a decade, and the fundamental reaction mechanism of ZVI in an aqueous environment is the same regardless of its particle size.^{22, 30-36} Elemental iron in its zero oxidation state or simply ZVI is a strong reducing agent with a standard reduction potential of -0.447 V.^{30, 37} As a strong reducing agent, ZVI reduces chlorinated hydrocarbons by reductive dehalogenation in the presence of a proton donor like water while being oxidized:



This is a surface mediated reaction where the contaminants gets reduced by means of electron transfer when they come in contact with the surface of iron and form mostly benign compounds such as hydrocarbons and chloride ions.²¹



The following reactions and/or pathways occur when ZVI or NZVI is present or added to the aqueous environment:^{30, 38, 39}

- Aerobic corrosion
- Anaerobic corrosion and

- Precipitation

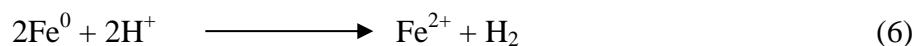
Corrosion and precipitation reactions would be required for a contaminated site remediation. Corrosion of iron increases the amount of dissolved iron present in the groundwater, thereby increasing the effectiveness of the iron to react with groundwater. During the corrosion process, iron metal is oxidized to Fe^{2+} or Fe^{3+} by giving up two or three electrons. Aerobic corrosion occurs if oxygen is present in the groundwater. It will continue until the dissolved oxygen is depleted. The reactions that occur under aerobic condition are



This reaction will be followed by the oxidation of ferrous iron (Fe^{2+}) to ferric iron (Fe^{3+}) if further oxygen is available.



Anaerobic corrosion will occur when oxygen is depleted according to the reaction



Ferric iron in solution precipitates into an amorphous ferric hydroxide by the following reaction

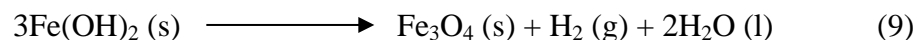


In the long term, amorphous $\text{Fe}(\text{OH})_3$ could eventually crystallize to goethite ($\alpha\text{-FeOOH}$)

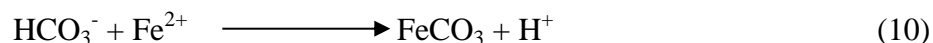
If the conditions are reducing and the pH is above 8.5, ferrous hydroxide will precipitate according to the reaction



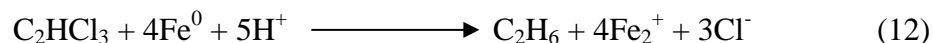
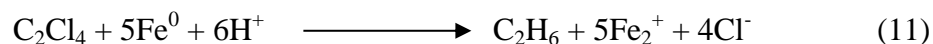
Ferrous hydroxide is a metastable phase in low temperature, anaerobic groundwater environments and will convert to magnetite by



If the conditions are reducing, the pH is neutral and the carbonate concentration is high, ferrous carbonate is precipitated according to the reaction



Irrespective of the reaction pathway, the reductive dechlorination needs electrons and can be obtained by three possible mechanisms as described by Tratnyek and co-workers.³⁰ They are (a) direct electron transfer from iron metal at the metal surface, (b) reduction by Fe^{2+} , which results from corrosion of the metal and (c) catalyzed hydrogenolysis by the H_2 that is formed by reduction of H_2O during anaerobic corrosion. The overall reactions of PCE (C_2Cl_4) and TCE (C_2HCl_3) with NZVI to form the product ethane (C_2H_6) are according to the equations (11) and (12):



1.4.Factors affecting NZVI for in situ remediation technology

The small size and colloidal nature of NZVI indicates that these particles can be used in *in situ* injection remediation technology.¹³ However, bare NZVI particles have a strong

tendency to agglomerate due to their ferromagnetic nature, forming aggregates that plug and inhibit their flow through porous media.^{24, 40-45} Our previous study showed that the commercially available bare-NZVI particles aggregate to effective sizes of 10 μm which are originally in the size range of 30-70 nm, and are ineffective for transport through soil.⁴⁶ In classical colloidal filtration theory (CFT), Brownian diffusion, interception and gravitational sedimentation are the mechanisms that govern the mobility of colloidal particles through porous media such as soil⁴⁷. The Tufenkji-Elimelech model is perhaps the most comprehensive model to describe these effects in the presence of interparticle attractive interactions⁴⁸. The mobility of particles through porous media is quantified through the collector efficiency η_0 , which is simply defined as the ability of the sediment to collect migrating particles, thus limiting transport through the subsurface. According to CFT, the optimal mobility through sediment corresponds to minimal collector efficiency, which typically occurs at a broad particle size range from about 0.2 μm to 1 μm depending on the particle physical properties and groundwater flow characteristics.^{41, 46, 48} Additionally, bare-NZVI has no affinity to partition to DNAPL phase as NZVI is hydrophilic and chlorinated solvents are hydrophobic. NZVI by itself has no preference for targeting DNAPL source and are inefficient when delivered close to the vicinity of bulk DNAPL phase. Thus the major drawbacks of using bare NZVI for in situ remediation method are poor limited mobility and nontargetability.

In summary, for successful *in situ* remediation, the injected NZVI particles should meet the following criteria: (a) travel through porous media to the contaminated zone; (b) sequester, remove or convert the contaminants in the subsurface to significantly reduce the dissolved phase concentrations and (c) partition to the DNAPL-aqueous phase^{32, 49, 50}.

This research is focused on addressing these issues of NZVI and to develop suitable materials as supports for NZVI particles which can inhibit their aggregation and effective towards the *in situ* remediation of chlorinated hydrocarbons such as TCE.

1.5.Objective

The objective of this dissertation is to develop submicron carbon spheres as effective supports/carriers for NZVI particles to address the *in situ* remediation of chlorinated hydrocarbons. The main focus is (a) to develop methods to prepare NZVI supported onto well-defined carbon materials (iron-carbon composite microspheres) in the optimal size range for transport through porous media and (b) to establish these iron-carbon composite microspheres as extremely useful materials for remediation of chlorinated hydrocarbons and suitable for the *in situ* injection technology. Our hypothesis is that (a) the carbon support will prevent the aggregation of NZVI particles by means of immobilizing them on the surface or within the matrix; (b) the NZVI particles in the iron-carbon composite particles ensure high reactivity towards the remediation of chlorinated hydrocarbons. Additionally, the carbon microspheres, much like activated carbon are expected to strongly adsorb chlorinated compounds, thereby potentially reducing dissolved phase concentrations. The optimal size range of these carbon microspheres indicates that they can be effective carriers for NZVI and can act as targeted delivery agents for the *in situ* remediation of DNAPLs.

This thesis includes six chapters. Chapter 1 is a general introduction of this research including brief introduction of soil and groundwater contamination by chlorinated solvents, use of NZVI particles for remediation, reaction mechanism of NZVI

with chlorinated hydrocarbons and thesis objective. Chapter's two to four demonstrate the approaches to prepare a new class of iron-carbon microparticulate systems towards the *in situ* remediation of soil and groundwater contaminants. Two different approaches were developed in this research for the preparation of iron-carbon composite microspheres. To differentiate the iron-carbon systems developed in this work, they are designated as Fe⁰/C (details in chapter 2) and Fe-C (details in chapter 3 and 4). However, both mean the same: NZVI particles supported on carbon microspheres. Chapter 5 expands the technology developed for the preparation of iron-carbon system (chapter 3 and 4) to the preparation of carbon-supported catalytic materials (Palladium-Carbon composite microspheres) for *ex situ* treatment of contaminated water. These comprise of material either published or prepared for publication in the peer-reviewed journals including ACS Applied Materials & Interfaces, Langmuir and Water Research. A brief description of each chapter is presented here:

In chapter 2, two existing processes (hydrothermal dehydration of simple sugars followed by carbonization and carbothermal reduction) were combined for a new approach to the preparation of engineered particles containing NZVI that are effective targeted delivery agents for the remediation of TCE. The particles contain highly uniform carbon microspheres embedded with NZVI (Fe⁰/C composite particles) with particle size around 500 nm. Supporting NZVI on carbon inhibits the aggregation of NZVI and the highly adsorptive carbon keeps the TCE in the proximity of the reactive sites and also serves as a sorptive sink for TCE removal. The Fe⁰/C composite particles are in the optimal size range for transport through soil and the polyelectrolyte carboxymethyl cellulose (CMC) is used to stabilize the composite microspheres in aqueous solution.

In chapter 3, we have developed a facile aerosol-based process to vary the placement of iron nanoparticles on the external surface of carbon microspheres or within the interior. This is accomplished through the competitive mechanisms of sucrose carbonization and the precipitation of soluble iron salts, in an aerosol droplet passing through a high temperature heating zone. The resulting iron-carbon composite (Fe-C) particles are in the size range of 100 – 1000 nm. These are highly conducive to the reductive dechlorination of TCE. The novelty of this study is the demonstration of a simple process to modify iron placement. This has significant potential applications in heterogeneous catalysis as both iron and carbon are widely used catalysts and catalyst supports.

In chapter 3, one very important observation reported from the reaction of TCE with the aerosol Fe-C particles is the lack of any detectable toxic intermediates such as dichloroethylenes (DCEs) or vinyl chloride (VC). Our hypothesis is that the highly adsorptive carbon prevents the release of any toxic intermediates. Any chlorinated intermediates generated remain adsorbed on the carbons till they are reacted away to light gases, primarily ethane and ethylene. To test this hypothesis, in chapter 4, we have applied the aerosol Fe-C particles towards the transformation of chlorinated hydrocarbons and their intermediates. We performed a systematic study of dechlorination of chlorinated ethylenes starting with PCE and its intermediate chlorinated ethylenes, TCE, DCEs and VC. The aerosol Fe-C particles are also in the optimal size range for transport through porous media and the polyelectrolyte CMC is used to provide colloidal stability in the aqueous medium.

In chapter 5, we apply the aerosol-based process for the preparation of carbon supported noble metal catalysts. Palladium (Pd) is a noble metal extensively used as a catalyst for the catalytic hydrodechlorination of chlorinated hydrocarbons. Most of the preparation techniques use multi-step processes to prepare supported Pd nanoparticles for the hydrodechlorination reactions. In the chapter 5, we describe the preparation and characterization of well-defined carbon-supported Pd nanoparticles using the aerosol-based process. These Pd-nanoparticles supported on carbon microspheres are applied towards the catalytic hydrodechlorination of trichloroethylene. This chapter emphasizes the importance of aerosol-based process towards the preparation of the supported catalyst materials for *ex situ* treatment of contaminated water.

At the end, the sixth chapter summarizes the findings of this research and provides suggestions for the future work. The results on the study of the adsorption effect of carbons on the catalytic hydrodechlorination of trichloroethylene (TCE) using commercially available supported palladium (Pd) particles are presented in the appendix section.

Chapter 2

Nanoscale Zero-Valent Iron supported on Uniform Carbon Microspheres for the *In situ* Remediation of Chlorinated Hydrocarbons

Published in the American Chemical Society Journal “ACS Applied Materials & Interfaces” as: Sunkara, B.; Zhan, J.; He, J.; McPherson, G. L.; Piringer, G.; John, V. T. *ACS Applied Materials & Interfaces* **2010**, 2 (10), 2854-2862.

2.1 Introduction

Dense nonaqueous phase liquids (DNAPLs), such as trichloroethylene (TCE) and tetrachloroethene (PCE), are widespread soil and groundwater contaminants that cause long term environmental pollution. The cleanup of DNAPL contaminated sites is of utmost importance and can be a challenging task due to subsurface heterogeneity and complex site architecture.^{43, 51} Soil vapor extraction, bioremediation, pump and treat methods, and the *in situ* placement of reactive metal barriers are some of the various methods developed for the remediation of DNAPLs.⁷⁻¹² Compared to these approaches, the *in situ* injection of nanoscale zerovalent iron (NZVI) to reduce DNAPLs is a potentially simple, cost-effective, and environmentally benign technology that become a preferred method in the remediation of these compounds.^{13, 14}

For successful *in situ* source remediation of TCE, it is important for the injected remediation agents to effectively migrate through the porous media.^{32, 49} However,

unsupported NZVI particles are chemically unstable and tend to agglomerate due to their high surface energies and intrinsic magnetic interactions, losing chemical reactivity and mobility through the subsurface. Prior studies have shown that nanoiron mobility can be increased dramatically by stabilizing the particles by adsorption of hydrophilic or amphiphilic organic species such as surfactants, vegetable oils, starches, or polyelectrolytes such as carboxymethyl cellulose (CMC) and poly (acrylic acid) (PAA), or triblock copolymers on the NZVI particle surface.^{24, 41, 42, 45, 52-54} These adsorbed organics enhance steric or electrostatic repulsions between particles to inhibit NZVI aggregation and increase solution stability. Alternatively, activated carbon granules of 1-3 mm size have been used to prevent NZVI aggregation.^{55, 56} Carbon-based composites are also advantageous because of their high adsorptive capacity. Activated carbons adsorb chlorinated compounds, and these materials have been used in the development of adsorptive-reactive barriers.⁵⁷

For effective design of multifunctional colloid particulate systems for *in situ* TCE remediation, several factors need to be met. The prepared particulate systems must be able to move through the porous media with optimal mobility, reach TCE contaminated sites, partition to the TCE phase and break down the contaminant. It would be advantageous if these particles reduce the bulk TCE concentration through sequestration by adsorption followed by reaction during mobility through the subsurface. Additional factors include the following: (1) small amounts of a catalyst, typically palladium are used to dramatically enhance reactivity through dissociative adsorption of H₂ on the catalyst surface.^{15, 31, 32, 58} and (2) the mobility of colloids in the subsurface is determined by competitive mechanisms of Brownian motion, interception by soil and sediment grains

and sedimentation effects. The Tufenkji-Elimelech model, which considers the effect of hydrodynamic forces and van der Waals interactions between colloidal particles and sediment grains is a significant improvement over earlier models and predicts that particles in the size range 0.1 to 1.0 microns have optimal transport properties at typical groundwater flow conditions^{41, 46, 48}.

In this study, we combine two existing processes for a new approach to the preparation of composite NZVI particles for effective *in situ* remediation of TCE. The first process is based on the production of highly uniform carbon microspheres through the hydrothermal dehydration of simple sugars followed by carbonization.⁵⁹⁻⁶¹ These carbon microspheres represent the support for NZVI and their relative monodispersity is shown in Figures 2.1a and 2.1b. The second process is that of carbothermal reduction where iron oxides and hydroxides on the surface of these carbons are reduced to zerovalent iron at temperatures of 800-1000⁰C with the accompanying evolution of carbon monoxide and carbon dioxide.⁶² Carbothermal processes occur during high carbon steel-making processes and have been well studied.⁶² In environmental remediation, Hoch and coworkers first applied the principle successfully by reacting soluble iron salts with carbon black to form reactive iron nanoparticles for the remediation of hexavalent chromium.⁶³

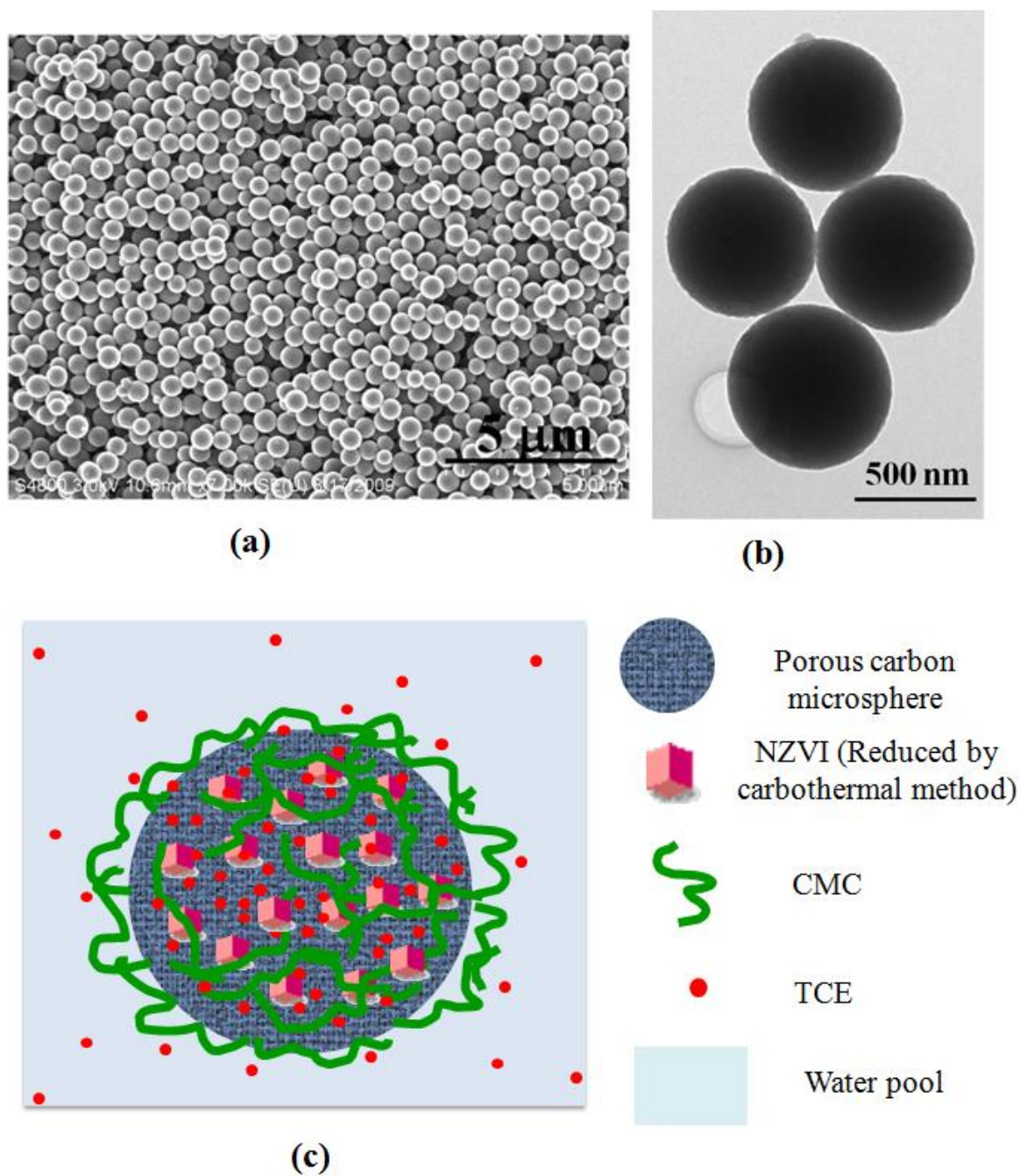


Figure 2.1 (a) SEM (b) TEM of 500 nm carbon particles obtained from hydrothermal dehydration and pyrolysis of sucrose. (c) Schematic of the multifunctional particulate system showing a NZVI embedded carbon particle with a corona of CMC. The red dots signify TCE in solution and adsorbed on the carbon.

This paper therefore describes a way to combine sugar hydrothermal dehydration and iron oxide/hydroxide carbothermal reduction to synthesize highly uniform colloidal carbon microspheres embedded with NZVI (hereafter called Fe⁰/C composite particles), which then are stabilized with a polyelectrolyte (carboxymethyl cellulose) to maintain suspension stability. There are several potentially useful properties of this new composite: (a) supporting the NZVI on carbon is expected to inhibit aggregation of NZVI (b) in analogy with the adsorptive properties of activated carbon, the carbon microspheres are expected to strongly adsorb TCE, thereby potentially reducing solution TCE content (c) the size and monodispersity of the Fe⁰/C composite particles may facilitate optimal transport in groundwater. The materials involved are easily available, expected to be environmentally benign, and relatively inexpensive. The hydrothermal dehydration synthesis of the carbon microspheres in solution, and the simple, inexpensive carbothermal reduction for the preparation of Fe⁰/C composites would indicate scalability to manufacturing volumes. In addition, the fact that the microspheres are in the optimal size range for transport as predicted by the T-E model⁴⁸ and that they can be made with high monodispersity and with inexpensive precursors provides the motivation to test their use in the *in situ* remediation of TCE.

This work is a direct extension of our recent paper where we have combined carbon microspheres with NZVI that is anchored to the stabilizing polymer (CMC)⁶⁴. The current work attempts to illustrate that NZVI can be directly supported on carbon microspheres and that reduction of precursor iron salts to zerovalent iron does not need to take place through addition of a reductant such as sodium borohydride. Instead, reduction can occur through the carbothermal step to generate NZVI and generating

porous carbons. In all experiments, we also add extremely small amounts of Pd (0.1 wt %) to catalyze the dissociative chemisorptions of H_2 .^{15, 31, 32, 58} The system therefore is based on NZVI nanoparticles on carbon microspheres which are colloidally stabilized by the addition of a polyelectrolyte such as carboxymethyl cellulose (CMC) as shown in Figure 2.1c. The characteristics of such particles as applied to TCE remediation are the focus of this work.

2.2 Experimental Section

2.2.1 Chemicals

All chemicals for synthesis were purchased from Sigma-Aldrich and used as received: Sucrose ($C_{12}H_{22}O_{11}$, ACS reagent), Iron (III) chloride hexahydrate ($FeCl_3 \cdot 6H_2O$, 97%, ACS reagent), sodium carboxymethyl cellulose (NaCMC or CMC, mean MW = 90 000, low viscosity), potassium hexachloro-palladate (IV) (K_2PdCl_6 , 99%) and trichloroethylene (TCE, 99%). Deionized (DI) water generated with a Barnstead E-pure purifier (Barnstead Co., Iowa) to a resistance of approximately 18 M Ω was used in all experiments.

2.2.2 Preparation of Fe^0/C composite particles

Uniform carbon microspheres were prepared from sucrose by hydrothermal treatment which involves two steps, the dehydration of sucrose, followed by pyrolysis (carbonization) at high temperatures. The process is similar to that reported in the literature^{59, 61} but with minor modifications, and is briefly described. In a typical preparation, a 0.15M aqueous sucrose solution was dehydrated at 190°C for 5 hours in a sealed stainless steel autoclave filled to 90% capacity. The resulting solid suspension was

centrifuged and washed three times with ethanol and air dried. The material was then pyrolyzed in a tube furnace for 10 hours at 1000 °C under flowing argon gas. The resulting carbon microspheres were stored in an airtight vial. The preparation is illustrated on shown through by a flow sheet in Figure 2.2a.

Carbothermal reduction was employed to synthesize the Fe⁰/C composite particles. In a typical synthesis, 0.5 g of the carbon microspheres were first dispersed in 50 mL of water and to this 2.42g FeCl₃.6H₂O salt dissolved in 50mL water was added and stirred overnight. The solution was then heated at 80°C to remove the water and then air dried. The dried particles were pyrolyzed under flowing argon at 800°C for 3 hours to obtain the final Fe⁰/C composite particles. To stabilize these composite particles in solution and to enhance their mobility through sediments, 1% (w/w) CMC was added to 5g/L Fe⁰/C composites in water . The process is shown schematically in Figure 2.2b. Figure 2.1c illustrates the concepts behind this study, which shows a schematic of a Fe⁰/C composite surrounded by a corona of CMC.

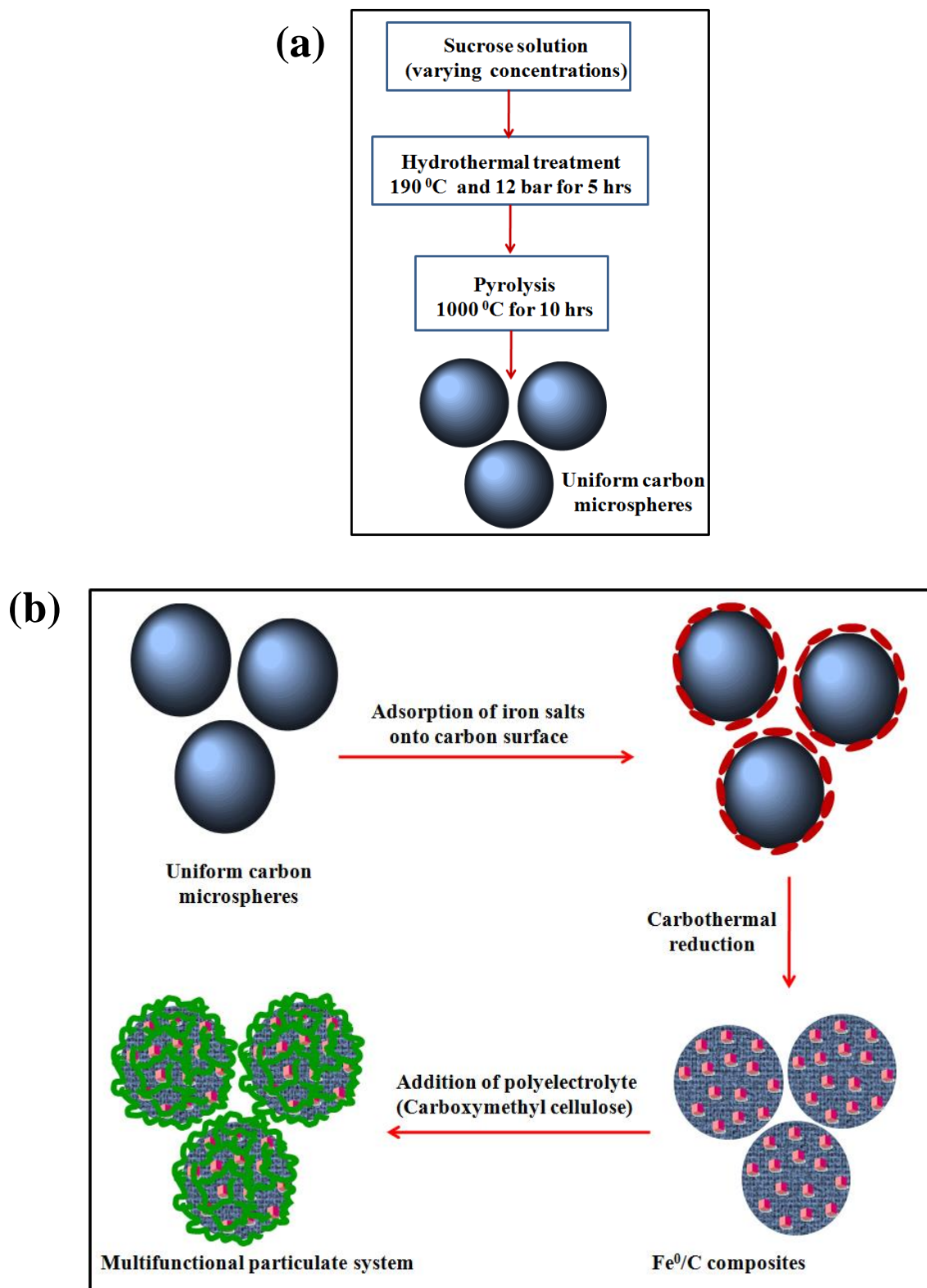


Figure 2.2 (a) Flow sheet for the preparation of uniform monodisperse carbon microspheres (b) Schematic for the synthesis of multifunctional particulate system.

2.2.3 Particle Characterization

Field emission scanning electron microscopy (SEM, Hitachi S-4800, operated at 20 kV), transmission electron microscopy (TEM; JEOL 2010, operated at 120 kV voltage), and X-ray diffraction (XRD, Rigaku, using Cu K α radiation) were used to characterize particle size, morphology and crystal structure. Nitrogen Brunauer-Emmet-Teller (BET) adsorption isotherms were obtained using a Micromeritics ASAP 2010 surface area analyzer. Optical microscopy (Olympus IX71, Japan) was used to analyze the behavior of the particles in porous media.

2.2.4 Reaction and Stability Analysis

To test the reactivity of the particles with TCE, 0.25 g of Fe⁰/C composite particles were dispersed in 10 mL of water. To this 125 μ L of 0.0047M K₂PdCl₆ was added to load the catalyst Pd onto Fe⁰/C composite particles. The catalyst loading is similar to the procedure described in literature.^{24, 45, 64-66} The particle suspension was placed in a 40 mL reaction vial capped with a Mininert valve. To this vial, 10 mL of 40 ppm TCE stock solution was added to reach an overall concentration of 20 ppm TCE. Accordingly, the final composition of Fe⁰/C composite particles used in this study is 3.125 g/L Fe⁰, 9.375g/L carbon, and 0.1% Pd (w/w of Fe⁰). TCE and reaction products were monitored through headspace analysis using a HP 6890 gas chromatograph equipped with a J&W Scientific capillary column (30m \times 0.32mm) and a flame ionization detector (FID). Samples were injected splitless at 220 °C. The oven temperature was held at 75°C for 2 min, ramped to 150°C at a rate of 25°C /min and finally held at 150°C for 10 min to ensure adequate peak separation between TCE, chlorinated and non-chlorinated reaction products.

To determine the minimum amount of CMC required stabilizing the carbon particles in solution for extended time periods, varying concentrations of CMC polyelectrolyte were added systematically to aqueous suspensions of carbon particles. The well-mixed suspensions were added to sample vials and allowed to settle while turbidity measurements were taken over time. The carbon particles were separately dispersed in water by probe sonication for 30 mins. Electrolyte (1mM NaCl) was added to the suspensions to mimic realistic groundwater conditions.^{67, 68} CMC solution was first added to the dispersed carbon particle solution and mixed for 10 min before the addition of the electrolyte. The concentration of CMC varied from 50mg/L (0.005%) to 5000mg/L (0.5%). The final composition of the colloidal suspension was 50mg/L carbon, 1mM NaCl and varying concentrations of CMC. The turbidity, measured in nephelometric turbidity units (NTU), was monitored using a benchtop turbidity meter (Model: DRT-100B, HF Scientific, Inc., Fort Myers, FL). For accuracy, each turbidity measurement was repeated several times and averaged. All turbidity measurements showed good reproducibility. The viscosities of the CMC solutions at various concentrations were measured using a laboratory rheometer (Model: AR 2000 Rheometer, TA instruments, USA). The viscosities of the CMC solutions at various concentrations with carbon (50mg/L) and electrolyte were also measured to note any changes in viscosity with the presence of the additives. Zeta potentials were measured using a Malvern Nanosizer (Malvern Instruments, USA).

2.3 Results and Discussion

2.3.1 Particle Characterization

Scanning and transmission microscopy were used to analyze the morphology and microstructure of the composite particulate system. As shown in Figures 2.1a and 2.1b, carbon particles prepared through the hydrothermal method are spherical, uniform, and monodisperse with particle size around 500 nm, consistent with the literature.⁵⁹ Figures 2.3a and 2.3b show the carbon microspheres embedded with NZVI particles (Fe^0/C composite particles) obtained after carbothermal reduction process, and 3c is the cut section TEM of an Fe^0/C composite particle showing the presence of NZVI within the porous microspheres. The presence of nanoiron with higher electron contrast inside the carbons indicates the distribution of nanoiron throughout the carbon without aggregation. The presence of zerovalent iron is confirmed by the XRD pattern in Figure 2.4a. In the XRD pattern of Fe^0/C composite particles, the $26^\circ 2\theta$ peak corresponds to 002 graphitic carbon spheres and peaks at 45° , 65° , and $82^\circ 2\theta$ correspond to zero valent iron.

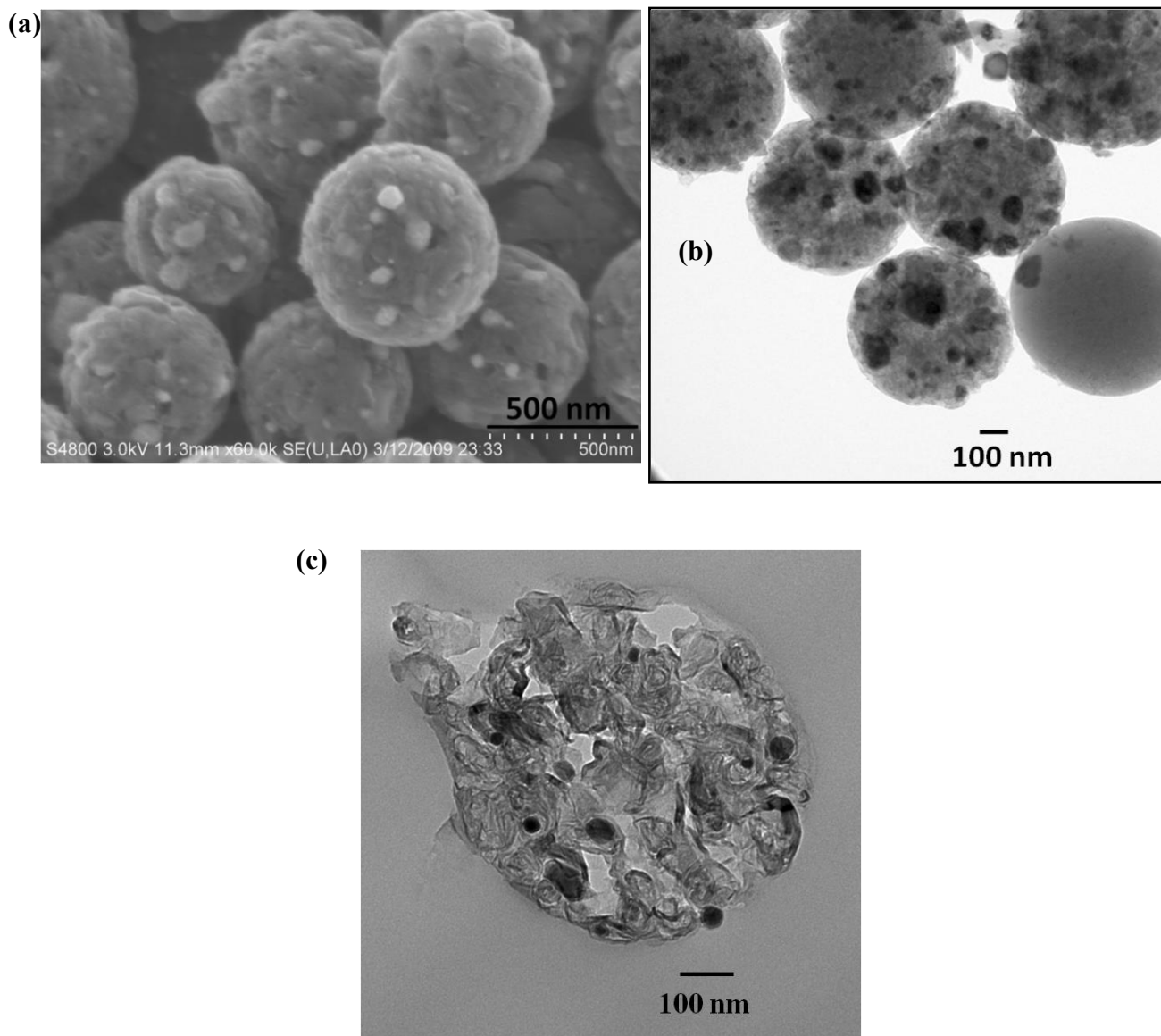


Figure 2.3 (a) SEM and (b) TEM of Fe^0/C composite particles (carbons embedded with NZVI). (c) Cut section TEM of Fe^0/C composite particles (carbons embedded with NZVI).

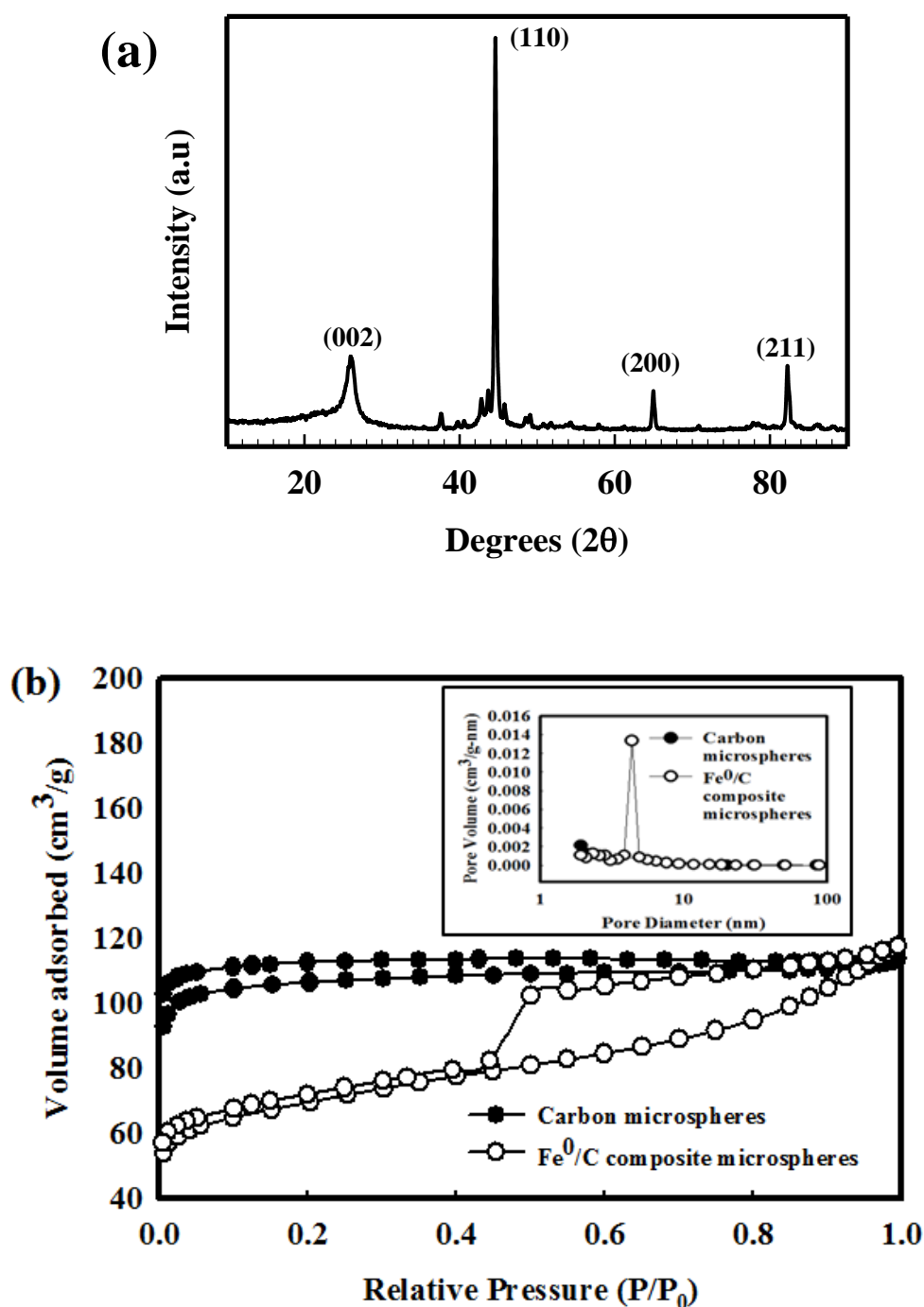


Figure 2.4 (a) XRD pattern of Fe^0/C composite microsphere particles (b) Nitrogen adsorption-desorption isotherms for the carbon microspheres and Fe^0/C composite microspheres. Inset showing the BJH pore size distribution derived from the desorption branch of the isotherm of carbon microspheres and Fe^0/C composite microspheres.

Figure 2.4b shows the N₂ adsorption isotherms obtained for these microspherical particles. Surface areas for the native carbon microspheres and Fe⁰/C composite microspheres at 77°K were calculated using Brunauer-Emmet-Teller (BET) method. The BET surface areas were found to be 320 m²/g and 221 m²/g respectively, and the corresponding Barret-Joyner-Halenda (BJH) desorption pore volumes were determined to be 0.0109 cm³/g and 0.1282 cm³/g. The adsorption isotherms are Type I for the carbon microspheres and Type IV for Fe⁰/C composite microspheres, using the Brunauer, Demming, Demming and Teller (BDDT) classification.⁶⁹ The isotherms indicate a highly microporous structure for carbon microspheres, and a transition to mesopore structure with capillary condensation for the Fe⁰/C composite microspheres.⁷⁰ The transition to mesopore structure for Fe⁰/C composite is evident from the BJH pore size distribution, shown in the inset of Figure 2.4b. The evolution of pore structure is also clearly visualized in the TEM images of Figure 2.3b and 2.3c.

2.3.2 Reactivity Characteristics

The reaction kinetics of TCE in the presence of Fe⁰/C particles with added palladium is shown in Figure 2.5. An immediate sharp reduction of the TCE peak is followed by a much slower decline in TCE concentrations. This sharp reduction is not due to reaction but to TCE adsorption on the carbon, as the product generation follows a much slower rate. The subsequent slow evolution of gas phase TCE dechlorination products indicates that dechlorination of TCE is responsible for the second, slower phase in the combined adsorption+reaction sequence. Assuming that dechlorination of TCE is rate controlling for the second step, it is possible to calculate a pseudo-first order rate constant for TCE dechlorination from the evolution rate of gas phase products. The

observed pseudo-first order rate constant was 0.0145 h^{-1} and the mass normalized rate constant, k_m was $4.64 \times 10^{-3} \text{ Lg}^{-1}\text{h}^{-1}$. While the pseudo first order rate constant is relatively low, we note that for *in situ* injection of NZVI based materials, the reaction rate alone is insufficient to make these materials good remediation candidates^{14, 44, 71}. In *in situ* injection, as long as reaction occurs over reasonable time scales, reactive systems can be used as long as they are able to come into contact with TCE saturated groundwater in an effective manner through effective transport in groundwater saturated sediments, and through contaminant sequestration. We are able to enhance the reactivity by two orders of magnitude through alternate routes of metal reduction but we will defer this discussion to the section on rate enhancements.

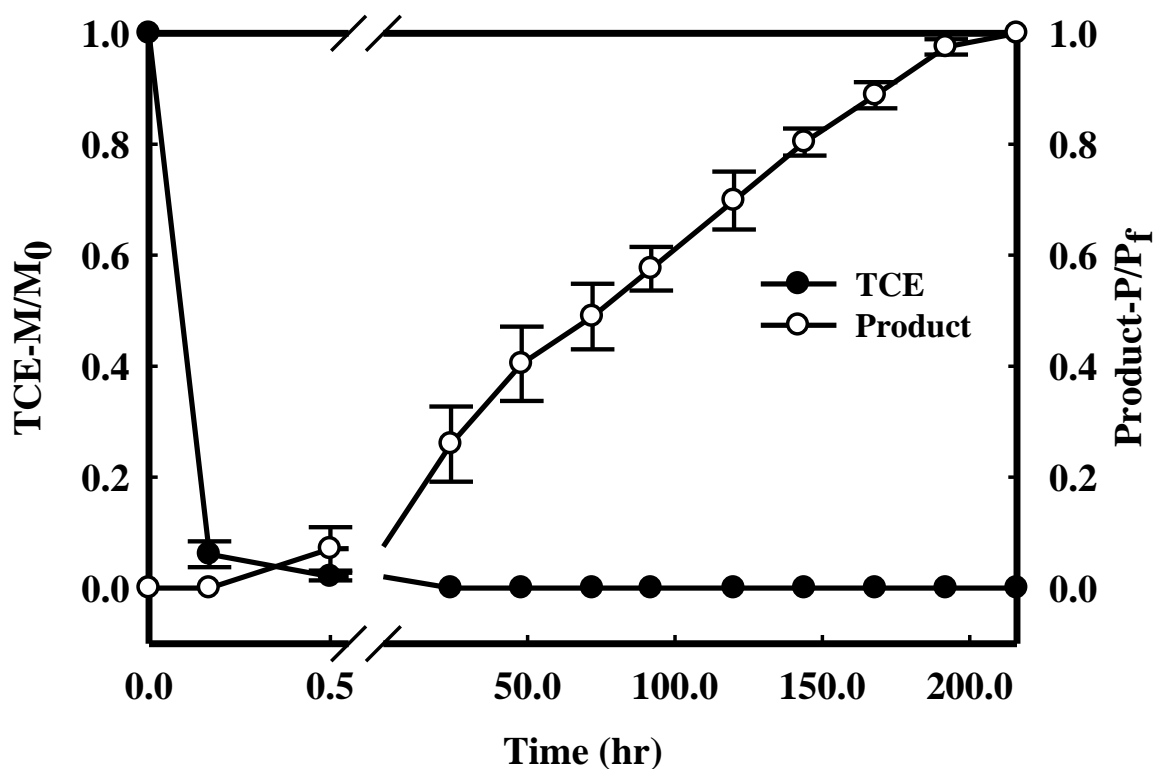


Figure 2.5 TCE removal from solution and gas product evolution rates for Fe^0/C composites (0.25 g particle, and 0.1 % Pd (w/w Fe^0)). M/M_0 is the fraction of the original TCE remaining and P/P_f is the ratio of the gas product peak to the gas product peak at the end of 9 days. The pseudo first order rate constant is 0.0145h^{-1} and mass normalized rate constant is $4.64 \times 10^{-3} \text{ Lg}^{-1}\text{h}^{-1}$

2.3.3 Adsorption Characteristics

The adsorption of TCE on the carbons is a significant advantage of the proposed technology since this property will allow sequestration of the TCE on the reactive materials. We have calculated the partition coefficient for TCE adsorption on the Fe⁰/C composite particles using the comprehensive definition of Phenrat and coworkers⁷¹

$$\frac{C_{TCE}^{ads}}{C_{TCE}^{water}} = K_p = \left\{ \frac{\left[(C_{TCE}^{Air})_{ref} V_{hs} - (C_{TCE}^{Air})_{ads} V_{hs} \right] + \left[\left(\frac{C_{TCE}^{Air}}{K_H^{TCE\bullet}} V_{water} \right)_{ref} - \left(\frac{C_{TCE}^{Air}}{K_H^{TCE\bullet}} V_{water} \right)_{ads} \right]}{\left(\frac{M_{ads}}{\rho_{ads}} \right) \left(\frac{C_{TCE}^{Air}}{K_H^{TCE\bullet}} \right)_{ads}} \right\}$$

Where C_{TCE}^{ads} is the concentration of TCE on the adsorbent (mol/L), C_{TCE}^{water} is the concentration of TCE in the water phase (mol/L), C_{TCE}^{Air} is the concentration of TCE in the headspace (mol/L), V_{hs} and V_{water} are the volumes of the headspace and water, respectively (L), M_{ads} is the mass of the adsorbent (g), ρ_{ads} is the density of the adsorbent (g/L). The subscripts *ref* and *ads* refer to the system without and with the adsorbent. $K_H^{TCE\bullet}$ is the Henry's law constant for TCE partitioning in water, with a value of 0.343 at 25°C⁷. The measured partition coefficient for TCE adsorption on CMC is 14.5, in close agreement with that measured by Phenrat and coworkers⁷¹. On the other hand, K_p for the adsorption of TCE on Fe⁰/C composite particles is 4819, constituting an almost 300 fold increase in adsorption capacity.

2.3.4 Colloidal Stability and Partitioning

The colloidal stability of nano- and micro-scale particles is a key factor in assessing their transport in groundwater.¹⁴ Results of stabilization experiments are illustrated in Figure 2.6a, showing turbidity as a function of time; NTU_0 indicates the initial turbidity at time zero. Figure 2.6a clearly shows that CMC decreases the settling rate of carbon particles, and above a CMC concentration of 2500mg/L, the carbon particles are stable for more than 24 hours. Figure 2.6b indicates the viscosity versus shear rate for various concentrations of CMC, illustrating no significant increase in viscosity with the CMC concentrations used to stabilize the carbon microspheres and implying no significant difficulty in the injection of these particles into TCE contaminated groundwater.

Figure 2.7 illustrates simple visual studies of suspension and partitioning characteristics of the carbon based systems. The samples were probe sonicated to enhance mixing and allowed to equilibrate. Figure 2.7a illustrates the suspension stability of Fe^0/C samples in water and it is clear that CMC stabilizes the carbon particles. All suspensions were stable in water for greater than four days, demonstrating the stabilizing effect of CMC as an effective colloid dispersant.^{45, 63, 72} Figure 2.7b illustrates the partitioning behavior of carbon when a bulk TCE phase is in contact with a bulk aqueous phase. On the left, the aqueous-phase solution containing $Fe^0 + CMC$ retains suspension stability in the aqueous phase. However, on the right, we see that $Fe^0/C + CMC$ particles partition to the TCE phase and a close inspection indicates that the partitioning is primarily around the TCE side of the water-TCE interface, with a dense layer near the interface.

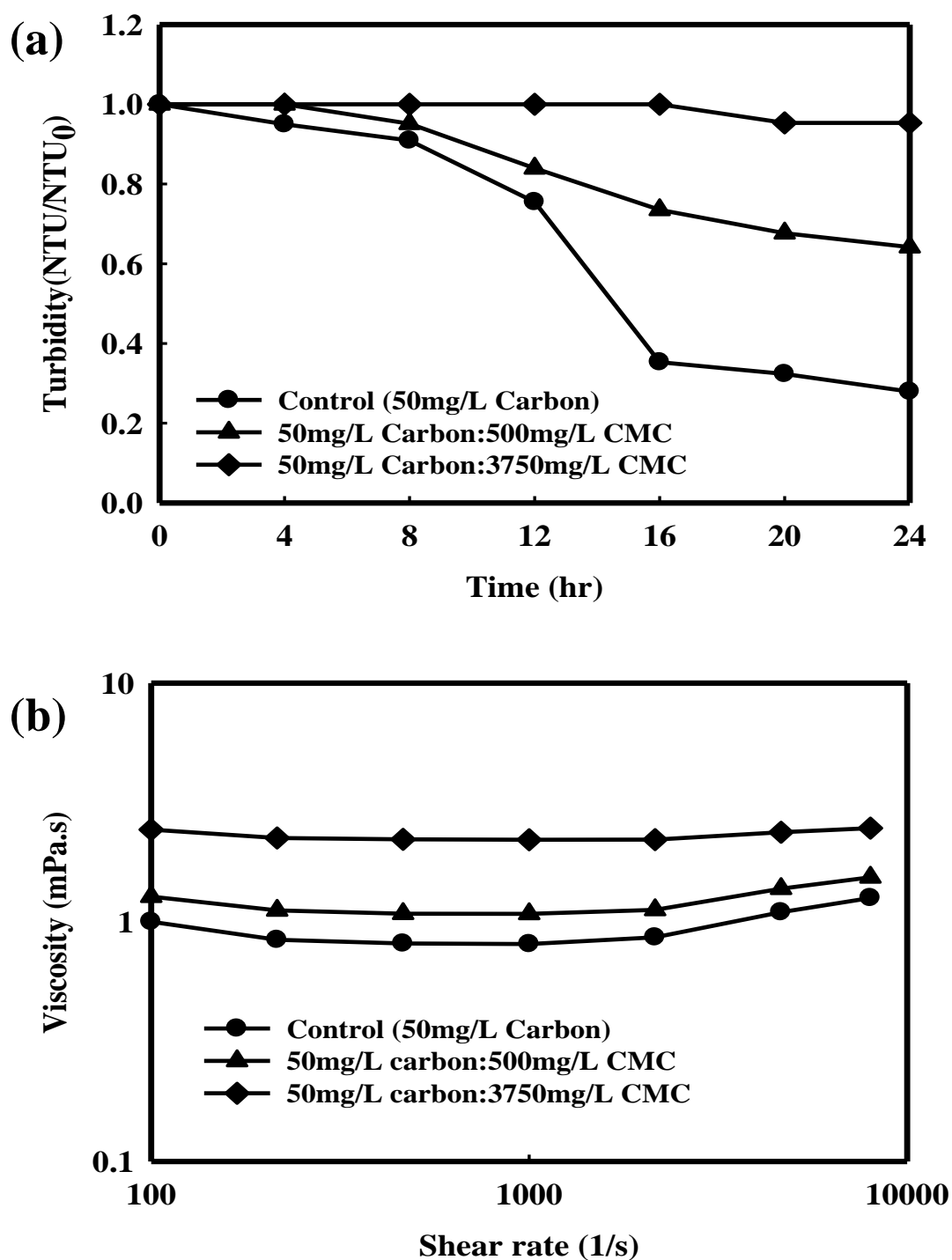


Figure 2.6 (a) Stability of carbon microspheres (500nm) in various concentrations of carboxymethyl cellulose (b) Viscosity versus shear rate for various concentrations of carboxymethyl cellulose. (Electrolyte (NaCl) concentration in all experiments is 1mM).

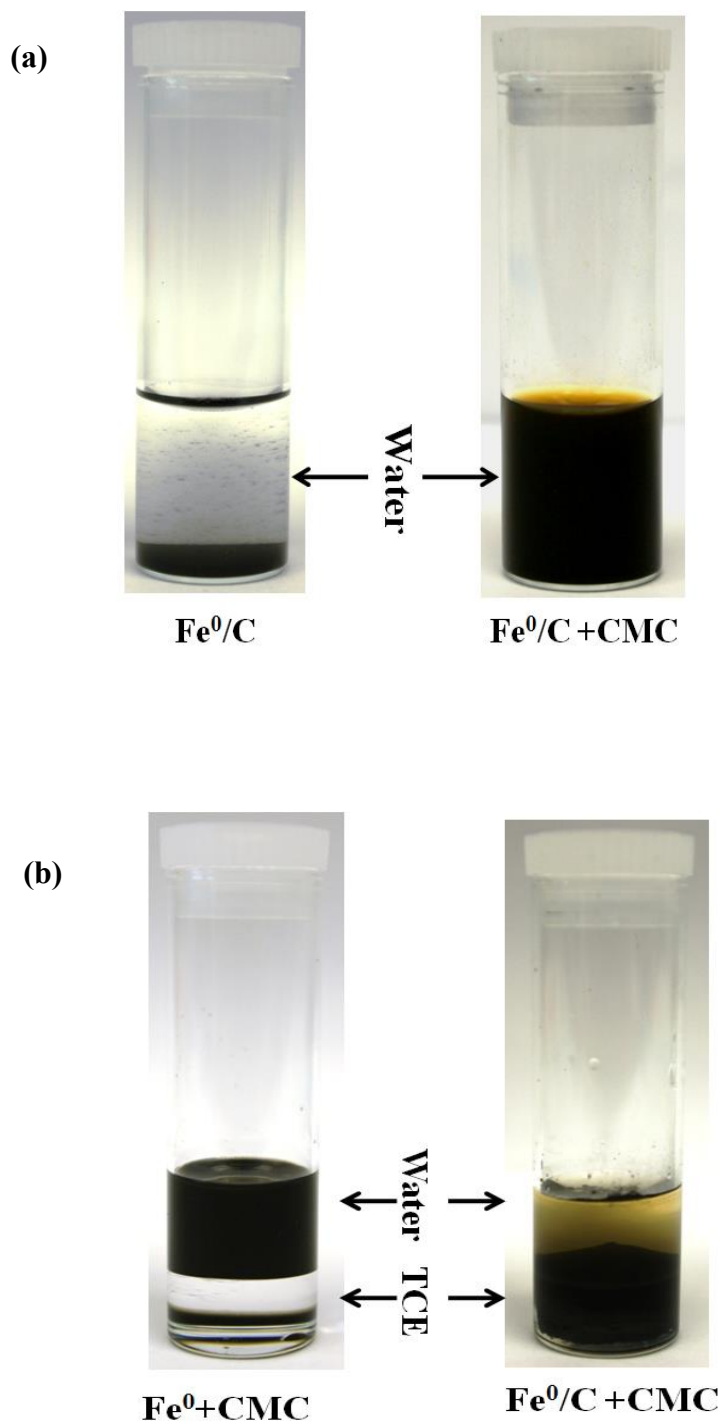


Figure 2.7 (a) Stability of $\text{Fe}^0/\text{C} + \text{CMC}$ in water (b) Partitioning characteristics of $\text{Fe}^0 + \text{CMC}$ and $\text{Fe}^0/\text{C} + \text{CMC}$ when contacted with a two-phase water-TCE system.

This is clearly a consequence of the tendency of the hydrophobic carbon to partition to the organic phase. The idealized system of a hydrophobic carbon microsphere enveloped by hydrophilic CMC approximates a 500 nm particle with amphiphilic characteristics. This property of partitioning to the interface when in contact with bulk TCE may be of specific advantage in anchoring the particles to pooled TCE at fractures along the sediment-bedrock boundary.

2.3.5 Transport characteristics

Transport characteristics of $\text{Fe}^0/\text{C}+\text{CMC}$ system were studied by capillary transport experiments. The experiment followed the procedure described by Zhan and coworkers which is a simple and intuitive method to study particle transport through porous media⁴⁶. Briefly, glass melting-point tubes with both ends open (1.5-1.8 mm i.d. \times 100 mm length, Corning, NY) were used as capillaries. The capillary tubes were packed with wet Ottawa sand over a 3 cm length and were placed horizontally to simulate groundwater flow. A continuous water flow at 0.1 mL/min (Darcy velocity: 5 cm/min) was driven by a syringe pump. The exit point of the capillary was capped with a small glass wool plug. After 30 μL of $\text{Fe}^0/\text{C}+\text{CMC}$ suspension was injected into the inlet of the capillary, water flushing was initiated and an inverted optical microscope was used to observe the pore-scale transport of the particles. Figure 2.8 illustrates photographs of the capillaries depicting the capillary containing $\text{Fe}^0/\text{C}+\text{CMC}$ colloids before and after the water flush. The images indicate that Fe^0/C composite particles readily transport through the packed capillaries and become captured in the glass wool. The effluent particle concentration was obtained by monitoring the turbidity of elutes with a nephelometric turbidimeter (DRT100B, HF Scientific, Inc., Fort Myers, FL.).

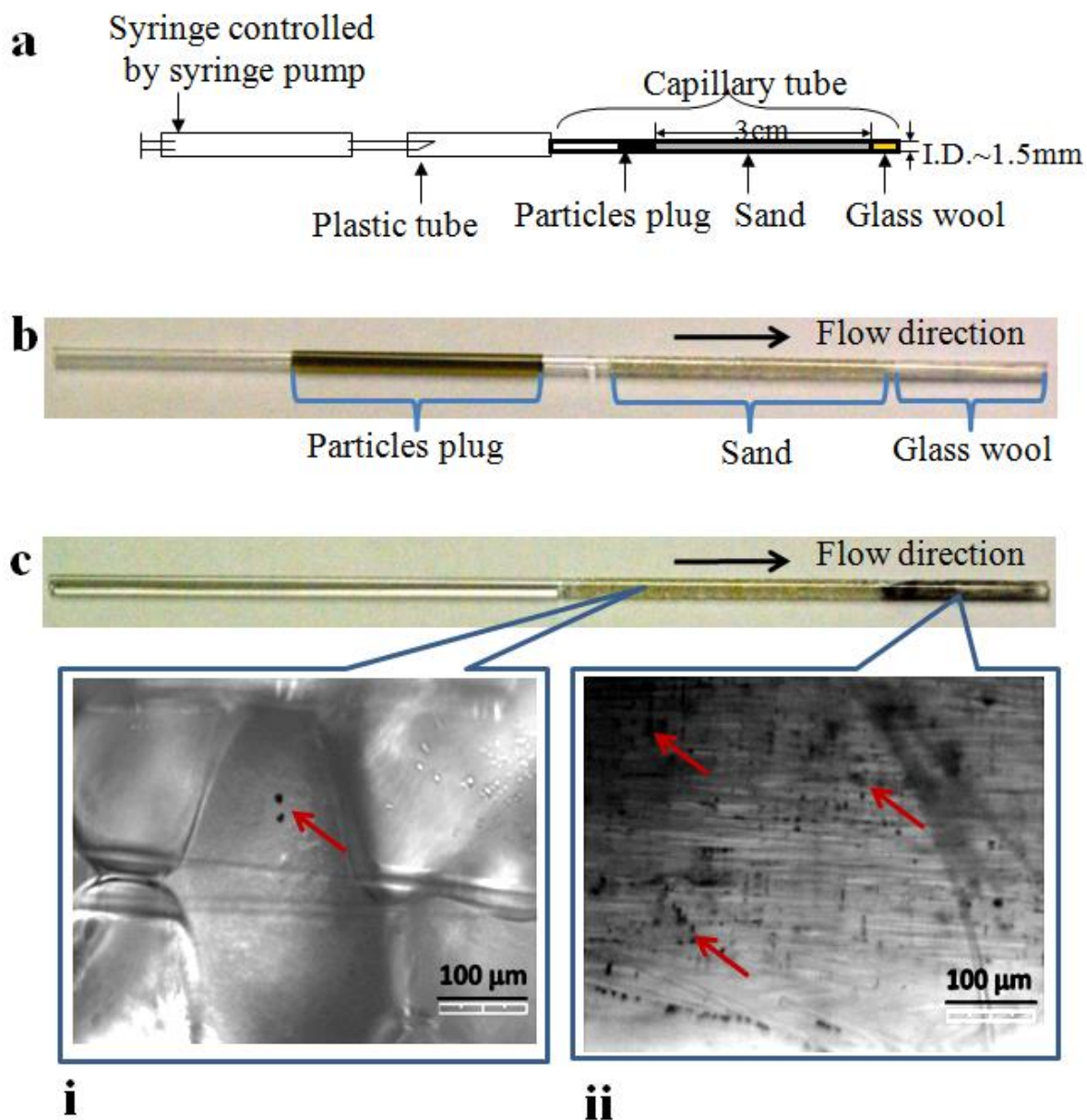


Figure 2.8 Characterization of transport through packed capillaries (a) experimental set-up. Flow rate: 0.1 mL/min, sand length: 3 cm and injected suspension volume: 0.03 mL; Photograph of capillary (b) before and (c) after water flushing. Panel i and ii show optical micrographs of sediments and particles at different locations after water flushing (all scale bars are 100 μ m). Arrows show the accumulated particles in the packed capillary at different locations.

In the experiment, particles retained by the glass wool were collected by a simple water washing method and were counted as a part of effluent. The turbidity result indicates that almost all of the Fe⁰/C composite particles were eluted from the Ottawa sand capillary under the specified conditions.

In classical colloidal filtration theory (CFT), Brownian diffusion, interception and gravitational sedimentation are the mechanisms that govern the mobility of colloidal particles through porous media such as soil.⁴⁷ The Tufenkji-Elimelech model is perhaps the most comprehensive model to describe these effects in the presence of interparticle attractive interactions.⁴⁸ The mobility of particles through porous media is quantified through the collector efficiency η_0 , which is simply defined as the ability of the sediment to collect migrating particles, thus limiting transport through the subsurface. According to CFT, the optimal mobility through sediment corresponds to minimal collector efficiency, which typically occurs at a broad particle size range from about 0.2 μm to 1 μm depending on the particle physical properties and groundwater flow characteristics.^{41, 46, 48} However, CFT can break down under conditions of deposition in the secondary minimum and surface charge heterogeneities, when consideration of repulsive DLVO interactions are accounted for, as shown by Tufenkji and Elimelech.^{73, 74} Nevertheless, it is noteworthy that our experimental results do indicate effective transport of the 500 nm composite particles. Additionally, the use of carboxymethylcellulose (CMC) as an anionic polyelectrolyte to stabilize the carbons leads to a high surface charge on the particles. The measured zeta potential is of the order of -45 mV indicating that the CMC will be able to mask the role of surface heterogeneities and provide better agreement with the modified colloid filtration theory.⁴⁸

We have calculated the attachment efficiency (α)^{48, 75} from capillary column breakthrough data for 500 nm size Fe⁰/C composite particles following the procedure of Zhan and coworkers.⁶⁴ Briefly, the attachment efficiency (α) is estimated from breakthrough data of capillary transport experiments using the following equations based on CFT.^{48, 75}

$$\alpha = \frac{-2}{3} \frac{d_c}{(1-f)L\eta_0} \ln(C/C_0)$$

Where d_c : the average diameter of sand grains, C and C_0 are effluent and influent particle concentration, f the porosity of the sand grains, and L the length of the column. η_0 , the single-collector efficiency is calculated using the T-E equation.⁴⁸

$$\eta_0 = 2.4 A_S^{1/3} N_R^{-0.081} N_{Pe}^{-0.715} N_{vdW}^{0.052} + 0.55 A_S N_R^{1.675} N_A^{0.125} + 0.22 N_R^{-0.24} N_G^{1.11} N_{vdW}^{0.053}$$

We calculated the attachment efficiency based on the following conditions:

Porosity $f = 0.32$, fluid viscosity $\mu = 1.0 \times 10^{-3}$ N.s/m², temperature, $T = 298$ K, Hamaker constant⁷⁶, $H = 1.09 \times 10^{-19}$ J, density of Fe⁰/C composite particles (calculated), $\rho = 2.74$ g/mL = 2.74×10^3 kg/m³, particle size: $d_p = 500$ nm, volumetric flow rate = 0.1 mL/min = 8.3×10^{-4} m/s

With a measured eluting fraction, $C/C_0 = 0.97$ the attachment efficiency is 0.0844 indicating effective transport through the packed capillary.

2.3.6 Reaction Rate Enhancements

The reactivity of the carbon supported nanoscale ZVI composites can be enhanced through the addition of sodium borohydride as reducing agent to obtain ZVI nanoparticles, thus avoiding the carbothermal process. First, nanoscale zero valent iron particles supported on carbon (hereafter called NZVI/C composite particles) microspheres were prepared by the incipient wetness method⁷⁷⁻⁸⁰, typically used in the preparation of supported catalysts and recently, in reactive barrier design for the dechlorination of polychlorinated biphenyls.⁸¹ In the current study, carbons obtained from the hydrothermal treatment were used and 1:1 weight ratio of carbon to iron was selected for these composite particles. In a typical preparation, 1.936 g $\text{FeCl}_3 \cdot 6\text{H}_2\text{O}$, dissolved in 5 mL water, was added to 0.4 g carbon powder. The volume of the water was kept to a minimum, sufficient enough to wet the solid carbon powder but with no excess liquid present; therefore it is assumed that all the iron salt particles are dispersed over the solid carbon. The water was then evaporated, leaving a dispersed carbon/iron salt/metal oxide mixture. The dried powder was then reduced with 10 mL of sodium borohydride solution and washed three times with water to obtain NZVI/C composite microspheres. Figure 2.9 shows the reaction characteristic of NZVI/C particles loaded with 0.1% palladium catalyst (w/w NZVI) prepared by this method. The pseudo first order rate constant is 2.95 h^{-1} and mass normalized rate constant, k_m is $295 \cdot 10^{-3} \text{ L g}^{-1} \text{ h}^{-1}$. The reactivity is greater than by a factor of about 60 compared to Fe^0/C composites prepared by the carbothermal process. In all cases, the mass normalized rate constant is calculated based on the weight of iron in the system.

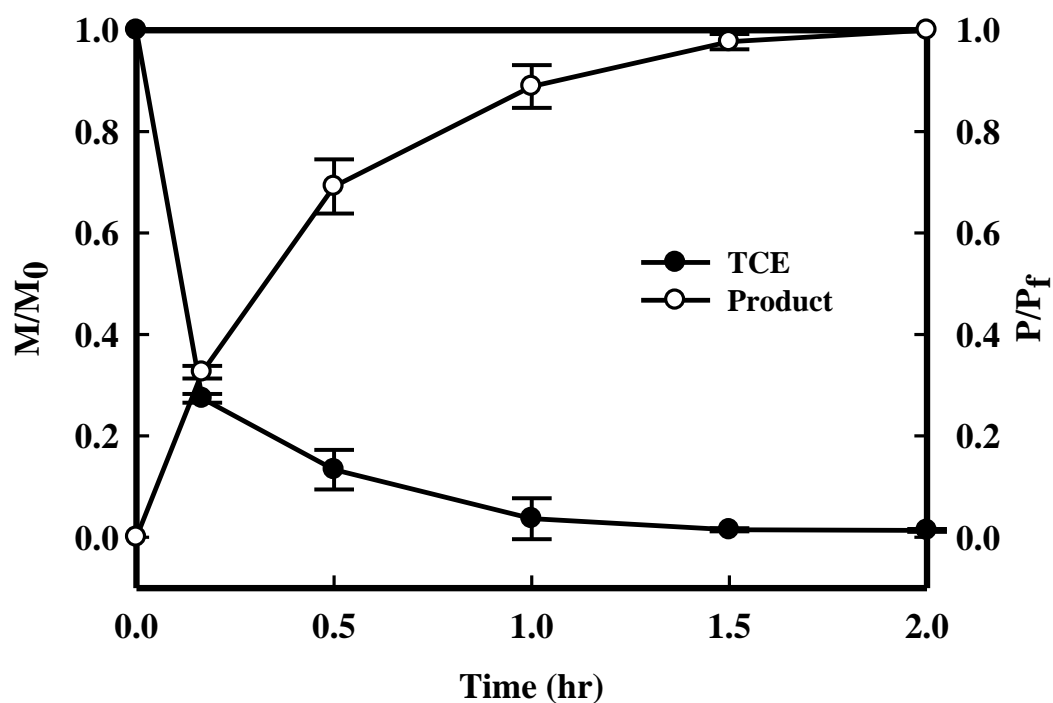


Figure 2.9 TCE removal from solution and gas product evolution rates for Fe^0/C composites prepared by incipient wetness method (20 ppm TCE, Fe^0 concentration 10 g/L, and 0.1 % Pd (w/w Fe^0)). M/M_0 is the fraction of the original TCE remaining and P/P_f is the ratio of the gas product peak to the gas product peak at the end of 120 min. The first order rate constant is 2.95h^{-1} and mass normalized rate constant is $295 \times 10^{-3} \text{ Lg}^{-1}\text{h}^{-1}$.

While the use of NaBH_4 enhances reaction rate, the cost of the reductant makes is perhaps less economical than the carbothermal method. In continuing work, we seek to understand the variations in reactivity using various reduction methods using detailed X-ray diffraction and X-ray Photoelectron Spectroscopy (XPS) to understand bulk and surface characteristics of the different iron species.

Figure 2.10 summarizes the various configurations of NZVI placement. From our earlier work⁶⁴ following the remarkable concepts of Zhao and coworkers⁴⁵ we have shown that it is possible to attach NZVI directly to carboxymethyl cellulose (the brown cubes in Figure 2.10) with high rate constants in the order of $2100 \times 10^{-3} \text{ Lg}^{-1}\text{h}^{-1}$. The current work describes the placement of NZVI directly on the carbon but with accompanying lower reaction rates. Figure 2.10 illustrates that it is possible to couple the various configurations to maximize loading. Since NZVI is not a catalyst but becomes gradually oxidized, the combination of slow and fast reacting NZVI may be of advantage in tuning the remediation to contaminant site characteristics.

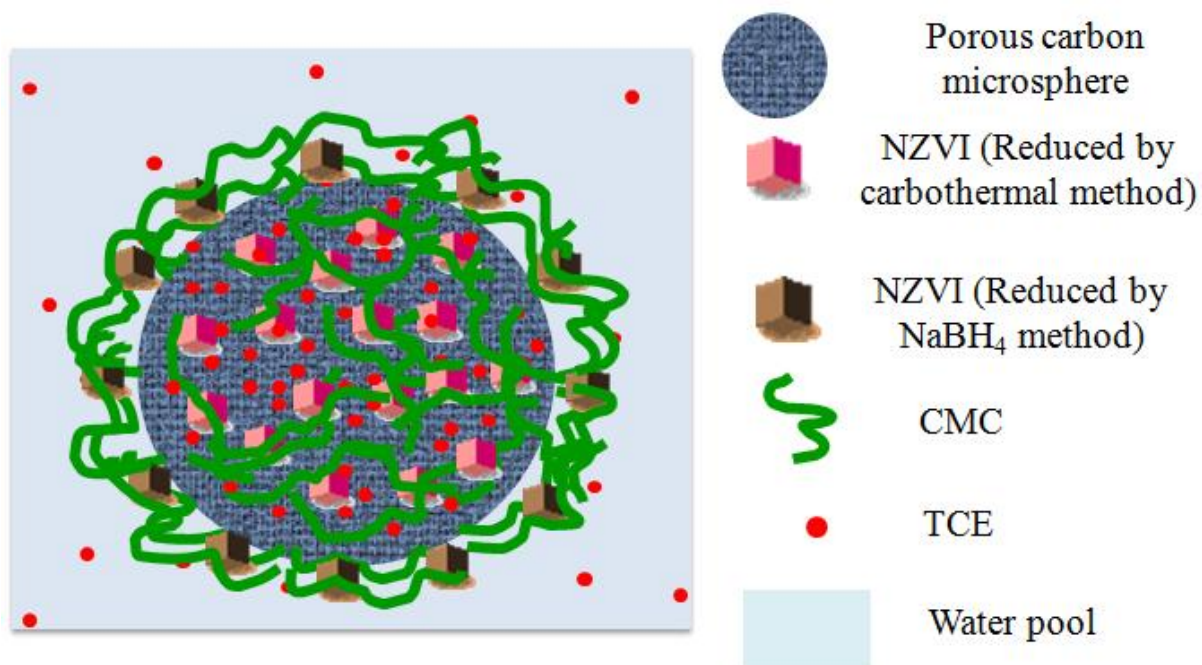


Figure 2.10 Schematic of the multifunctional particulate system showing a NZVI (red cubes) embedded carbon particle surrounded by CMC containing NZVI (brown cubes). The red dots signify TCE in solution and adsorbed on the carbon.

2.4 Summary

In all cases described in this work, the composite materials have multiple functionalities (a) they are reactive and function effectively in reductive dehalogenation (b) they are highly adsorptive thereby bringing the chlorinated compound to the proximity of the reactive sites and also serving as adsorption materials for decontamination (c) they are in the optimal size range predicted by colloidal filtration theory for optimal transport through sediments (d) the composite with a hydrophilic corona and a hydrophobic core may possess amphiphilic properties to stabilize the particles when they reach target zones of bulk DNAPLs. These multiple functionalities can be designed at low cost and the materials are intuitively environmentally innocuous since they contain carbon, iron and a biodegradable polymer. While this work is a follow up to our earlier work where NZVI was attached to the polyelectrolyte⁶⁴, it considerably expands the scope of the technology through placement of NZVI within the carbon and through the generation of highly adsorptive porous materials.

Chapter 3

Modifying Metal Nanoparticle Placement on Carbon Supports using an Aerosol-Based Process, with Application to the Environmental Remediation of Chlorinated Hydrocarbons

Published in the American Chemical Society Journal “Langmuir” as: Sunkara, B.; Zhan, J.; Kolesnichenko, I.; Wang, Y.; He, J.; Holland, J. E.; McPherson, G. L.; John, V. T. *Langmuir* **2011**, 27, 7854-7859.

3.1 INTRODUCTION

Chlorinated hydrocarbons such as trichloroethylene (TCE) form a class of dense non-aqueous-phase liquid (DNAPL) toxic contaminants in soil and groundwater. These are difficult to remediate since they have densities greater than water and transport deep into sediments till they reach the bedrock where they pool in cracks and fissures. They have a low but finite solubility in water and therefore slowly leach into ground water.^{43, 51, 82-84} The *in situ* injection of nanoscale zerovalent iron (NZVI) to reductively remediate DNAPLs is a potentially simple, cost-effective, and environmentally benign technology that has become a preferred method in the remediation of these compounds.^{13, 40} For successful *in situ* source remediation of DNAPLs, it is important for the injected remediation agents to effectively migrate through the porous media.^{32, 49} However, unsupported NZVI particles exhibit ferromagnetism leading to particle aggregation and a

loss in mobility through the subsurface.⁴⁰ Prior studies have shown that nanoiron mobility can be increased dramatically by stabilizing the particles through the adsorption of hydrophilic or amphiphilic organic species such as surfactants, vegetable oils, starches, or polyelectrolytes such as carboxymethyl cellulose (CMC) and poly (acrylic acid) (PAA), or triblock copolymers on the NZVI particle surface.^{24, 41, 42, 53, 54, 85, 86} These adsorbed organics enhance steric or electrostatic repulsions between particles to inhibit NZVI aggregation and increase solution stability. Alternatively, activated carbon granules of 1-3 mm size have been used to prevent NZVI aggregation.^{55, 87} Recently, well defined carbon microspheres have been studied as supports for NZVI particles to inhibit aggregation, as NZVI carriers for transport through sediments, and as effective targeted agents for DNAPLs.^{64, 88} Carbon-based composites are also advantageous because of their high adsorptive capacity. Activated carbons adsorb chlorinated compounds, and these materials have been used in the development of adsorptive-reactive barriers.⁸⁹ Porous carbon materials can be an especially effective support for environmental application because they provide high surface areas, their surfaces can be functionalized to provide controlled metal loading sites, and their pore structure can be tailored for enhanced adsorption.^{64, 87, 88, 90}

Prior studies in the synthesis of iron supported carbon composites for environmental applications typically use multi-step processes including: (a) catalyst impregnation using the incipient wetness method,^{87, 90} (b) carbothermal reduction or pyrolysis by reacting soluble iron salts with carbon products to form reactive iron nanoparticles,^{88, 91} and (c) chemical or physical adsorption methods.^{41, 64} We describe a method in this paper to design a carbon supported NZVI (Fe-C) particulate system using

a facile aerosol-based process (ABP) that effectively addresses the environmental degradation of chlorinated compounds. The particulate systems are obtained from inexpensive precursors and through a semi-continuous method which allows for large scale synthesis of the composites necessary for eventual *in-situ* application. The work follows our earlier concepts of supporting zerovalent iron on silica microspheres using an aerosol-based process.^{46, 49, 92} In an accompanying recent paper, we have demonstrated the use of the aerosol-based process to synthesize carbon-based nanomaterials, i.e. functional nanocomposites of zerovalent iron supported on the surface of carbon microspheres.⁹³ The aerosol-based carbon microspheres allow adsorption of TCE, thus removing dissolved TCE rapidly and facilitating reaction by increasing the local concentration of TCE in the vicinity of iron nanoparticles. The composite particles are in the optimal size range for transport through groundwater saturated sediments.

In this study, we focus on a remarkable characteristic of the aerosol-based process, demonstrating that it is possible to vary the placement of iron nanoparticles on carbon microspheres either on the surface of the microsphere or in the interior. Such a variation of metal placement can be accomplished simply through operation at various temperatures and are the result of modifying the relative rates of carbonization and metal precipitation in an aerosol droplet. We note that there have been recent articles in the literature on placement of iron in carbon supports.⁹⁴⁻⁹⁸ In very recent work, Atkinson and coworkers have pioneered the aerosol route to incorporating iron in carbon⁹⁴ and Zheng and coworkers have shown the preparation of hollow carbon microspheres containing iron species.⁹⁶ The distinctive aspect of the present work is to show that the aerosolization process can be adapted to control the placement of iron in carbon through

manipulating the relative rates of carbonization and metal precipitation. Additionally, this work seeks to establish that such materials are extremely useful to the environmental remediation of chlorinated hydrocarbons, as initially described in our earlier paper.⁹³

3.2 Experimental Section

3.2.1 Materials

All chemicals for synthesis were purchased from Sigma-Aldrich and used as received: Sucrose ($C_{12}H_{22}O_{11}$, ACS reagent), Iron (III) chloride hexahydrate ($FeCl_3 \cdot 6H_2O$, 97%, ACS reagent), sodium borohydride ($NaBH_4$, 99%), and trichloroethylene (TCE, 99%). Deionized (DI) water generated with a Barnstead E-pure purifier (Barnstead Co., Iowa) to a resistance of approximately 18 M Ω was used in all experiments.

3.2.2 Preparation of Fe-C Composite Microspheres

The iron-carbon composite particles were prepared from sucrose and iron chloride salt by an aerosol-based technology which involves dehydration of sucrose and precipitation of iron salts in a single step. In a typical preparation, 6.0 g of sucrose and 4.0 g of $FeCl_3 \cdot 6H_2O$ were dissolved in 30 mL of water. The resulting solution was aged for 30 min under stirring to mix the solution completely. In the aerosol-based process, the precursor is first atomized to form aerosol droplets, which are then carried by an inert gas (N_2) through a heating zone where solvent evaporation and carbonization occurs. The flow rate of the carrier gas was 2.5 L/min and the thermal treatment was carried out in a 100 cm tube (internal diameter of 4.45 cm) with a furnace length of 38 cm leading to a superficial velocity of 2.7 cm/s and a furnace residence time of 14 seconds. The flow rate of the carrier gas was obtained after bubbling the effluent gas through water at room

temperature, and the superficial velocity calculations are done with flow rate conditions at standard temperature and pressure (1 atm, 298K). The temperature of the heating zone was held at different temperatures (300, 500, 700 and 1000 °C) for each experimental run. The resulting Fe salt/carbon particles were collected over a filter maintained at 100 °C.

To obtain Fe-C particles, the as-synthesized Fe salt-carbon particles were reduced using liquid phase NaBH_4 . Specifically, 0.2 g of particles collected from the filter paper was placed in a vial followed by drop-wise addition of 10 mL of a 0.26 M NaBH_4 water solution. After cessation of visible hydrogen evolution, the particles were centrifuged and washed by water thoroughly before use.

3.2.3 Particle Characterization

Field emission scanning electron microscopy (SEM, Hitachi S-4800, operated at 20 kV), transmission electron microscopy (TEM; JEOL 2010, operated at 120 keV), and X-ray diffraction (XRD, Rigaku Instruments, Cu $K\alpha$ radiation) were used to characterize particle size, morphology and crystal structure. Nitrogen Brunauer-Emmet-Teller (BET) adsorption isotherms were obtained using a Micromeritics ASAP 2010 surface area analyzer. For cut-section TEM, the composite particles were embedded in an epoxy resin, dried overnight, and then microtomed into thin slices (approximately 70 nm) with a diamond knife. A thin slice of the microtomed sample was transferred to a copper grid and observed under the TEM. The presence of functional groups is analyzed using Fourier transform infrared spectroscopy (FTIR, PerkinElmer Spectrum GX with DTGS detector).

3.2.4 Reactivity Analysis

The dechlorination efficiency towards TCE was tested in batch experiments. In detail, 0.2 g of the aerosol-based Fe-C composites were dispersed in 20 mL water and placed in a 40 mL reaction vial capped with a Mininert valve. To this vial, 20 μ L of a TCE stock solution (20 g/L TCE in methanol) was added, resulting in an initial TCE concentration of 20 ppm. The reactions were monitored through headspace analysis using a HP 6890 gas chromatograph (GC) equipped with a J&W Scientific capillary column (30m \times 0.32 mm) and flame ionization detector (FID). Samples were injected at 220 $^{\circ}$ C and the column operated in splitless mode. The oven temperature was held at 75 $^{\circ}$ C for 2 min, ramped to 150 $^{\circ}$ C at a rate of 25 $^{\circ}$ C /min and finally held at 150 $^{\circ}$ C for 10 min to ensure adequate peak separation.

3.3 Results and Discussion

Details of the aerosol reactor and the aerosol based process have been detailed in our earlier paper⁹³ and are further summarized through a schematic here (Figure 3.1). Briefly, a homogenous precursor solution containing sucrose and iron chloride was first atomized using a commercial atomizer (Model 3076, TSI, Inc., St Paul, MN) to form aerosol droplets that undergo a heating and drying step, generating submicron particles that are collected on a filter (Figure 3.1a).

Figure 3.1b is a representation of the formation process of Fe-C composites, involving the processes occurring in an aerosol droplet. When the droplets pass through the heating zone, solvent evaporation and dehydration/carbonization of sucrose occurs. In addition, precipitation of the iron salt is concomitant with the dehydration of sucrose, generating a black powder of Fe salt-C composites.

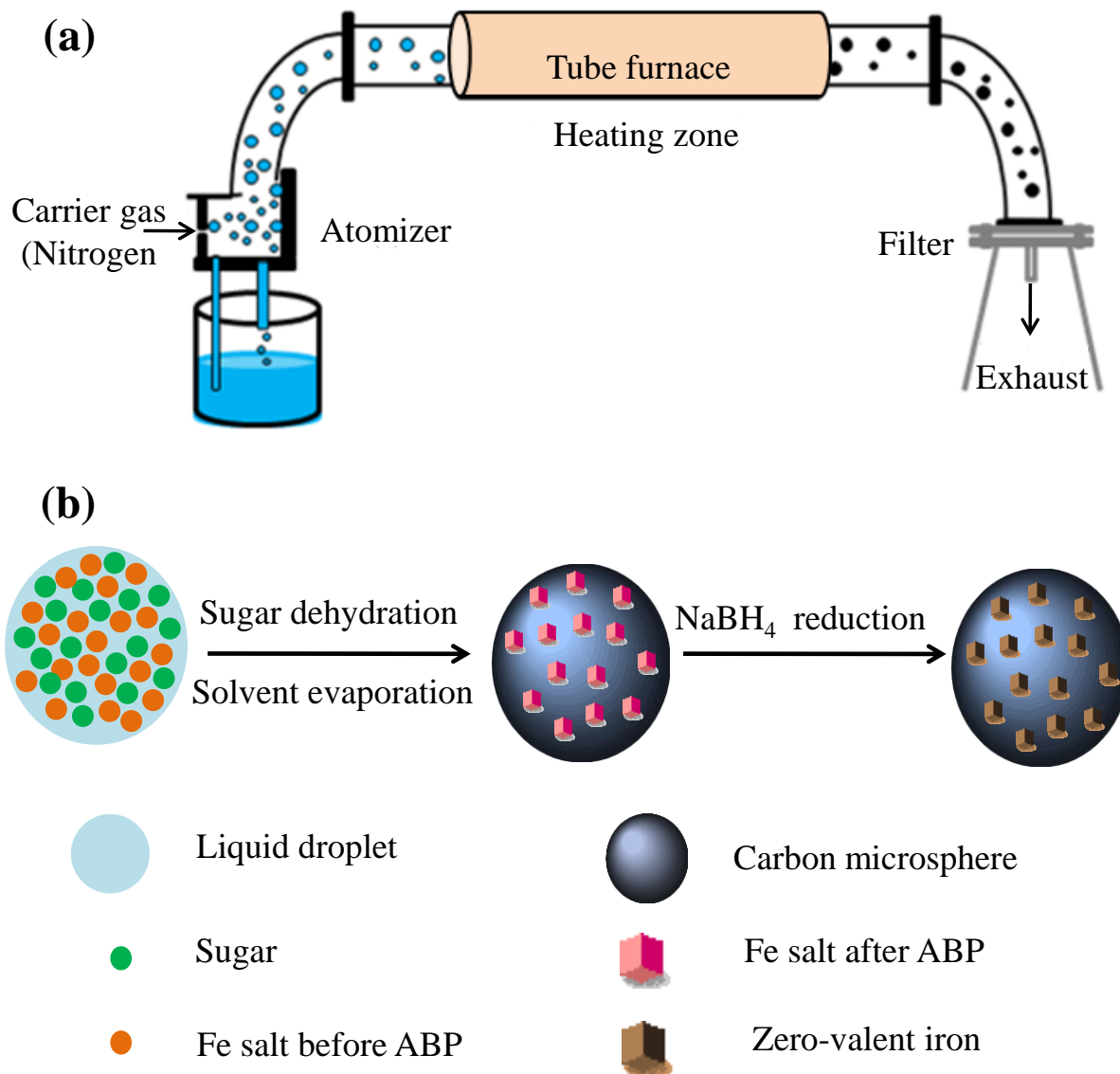


Figure 3.1 (a) Schematic of aerosol reactor for composite particles preparation and (b) schematic of reaction in an aerosol droplet.

To obtain Fe-C composites, the collected powder is treated with sodium borohydride solution in excess to reduce ferrous ion to zerovalent iron.

3.3.1 Particle Characteristics as a Function of Aerosolization Temperature.

The aerosol-based process results in well-defined carbon microspheres containing the recrystallized iron salt. Figure 3.2 provides all details on the X-ray diffraction patterns of the iron species as a function of furnace temperature. The peaks at 16.1, 22.4, 29.6, 41.3 and, 42.3° 2 θ correspond to the (001), ($\bar{2}$ 01), (021), (022) and ($\bar{4}$ 01) planes of iron chloride hydrate ($\text{FeCl}_2 \cdot 4\text{H}_2\text{O}$), respectively. At higher temperatures of aerosolization (500, 700 and 1000 °C), the presence of magnetite (Fe_3O_4) is observed with diffraction peaks at 30.1, 35.4, 56.9 and, 65.5° 2 θ corresponding to the (220), (311), (511) and (440) planes. The relative intensity of the Fe_3O_4 peaks increases as the heating zone temperature increases (500 to 1000 °C). Exposure of the iron salts to oxygen at higher temperature leads to the formation of Fe_3O_4 ,⁶³ but the short residence times encountered such oxidztion is minimal.

The short residence time in the furnace prevents full carbonization to graphitic species and the carbons are typically amorphous with remnant functional groups. The presence of functional groups is analyzed using Fourier transform infrared spectroscopy (FTIR). Figure 3.3 shows the FTIR spectrum of Fe salt/Carbon samples prepared at 300 °C (Figure 3.3a), 1000 °C (Figure 3.3b) and carbon particles pyrolyzed at 1000 °C for 3 hours under argon atmosphere (Figure 3.3c). Figure 3.3a shows the strong characteristic peak at 3425 cm^{-1} which corresponds to the O-H stretch. This absorption peak implies the existence of residual hydroxyl groups.^{99, 100}

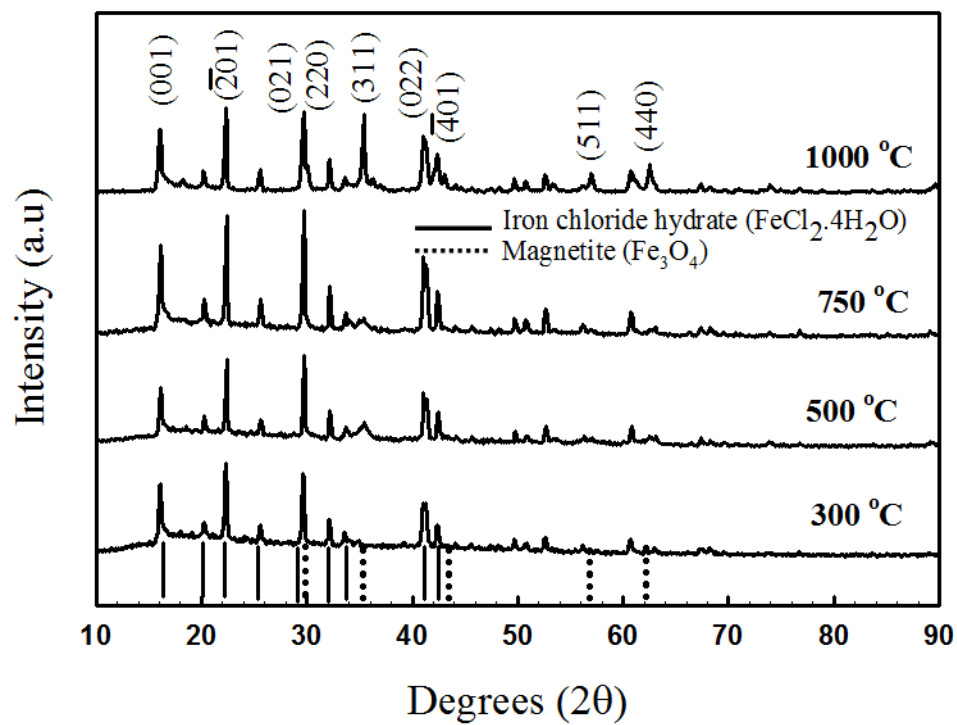


Figure 3.2 XRD patterns of iron species precipitated on the carbon at the various aerosolization temperatures.

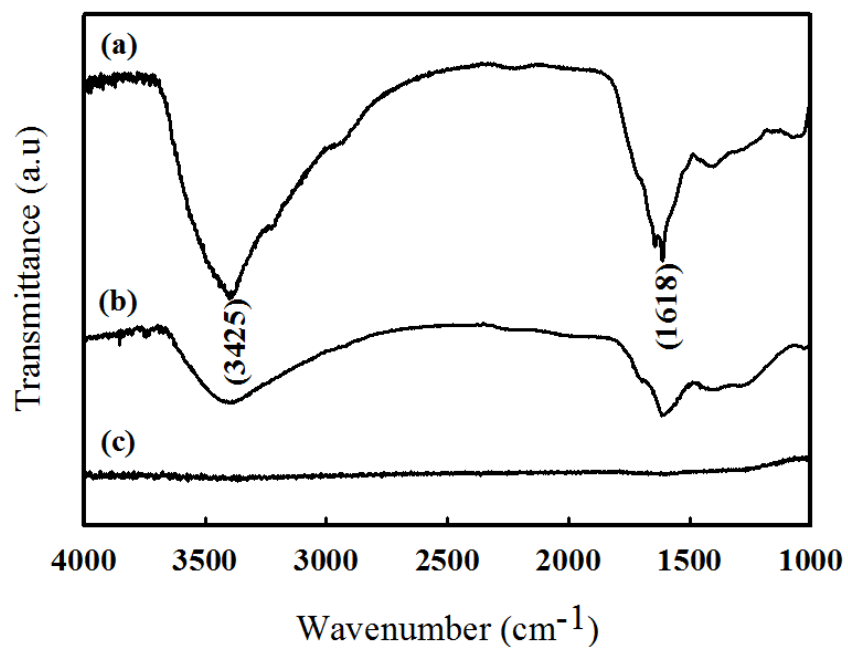


Figure 3.3 FTIR spectra of the carbon showing residual functional groups which can be removed through pyrolysis.

The absorption peak at 1618 cm^{-1} corresponds to the C=C symmetric stretch present in furanic rings resulting from the dehydration of sucrose.^{99, 101} The FTIR spectra indicate the reduction of residual functional groups with increasing temperatures of aerosolization (Figure 3.3b), and eventually a loss of all functional groups if the material is further pyrolyzed in a second step (Figure 3.3c).

The composite microspheres are typically in the submicron (100 nm to 1000 nm) size range as observed through electron microscopy (Figures 3.4, 3.5 and 3.6). Scanning (SEM) and transmission (TEM) electron micrographs of a single microsphere particle prepared at different heating zone temperatures are shown in Figure 3.5 and Figure 3.6, respectively (Figure 3.4 illustrates the SEM of multiple particles to gain an idea of the polydispersity involved). The images are of particles obtained directly from the filter, and morphology and particle structures are retained after treatment with NaBH_4 .⁹³

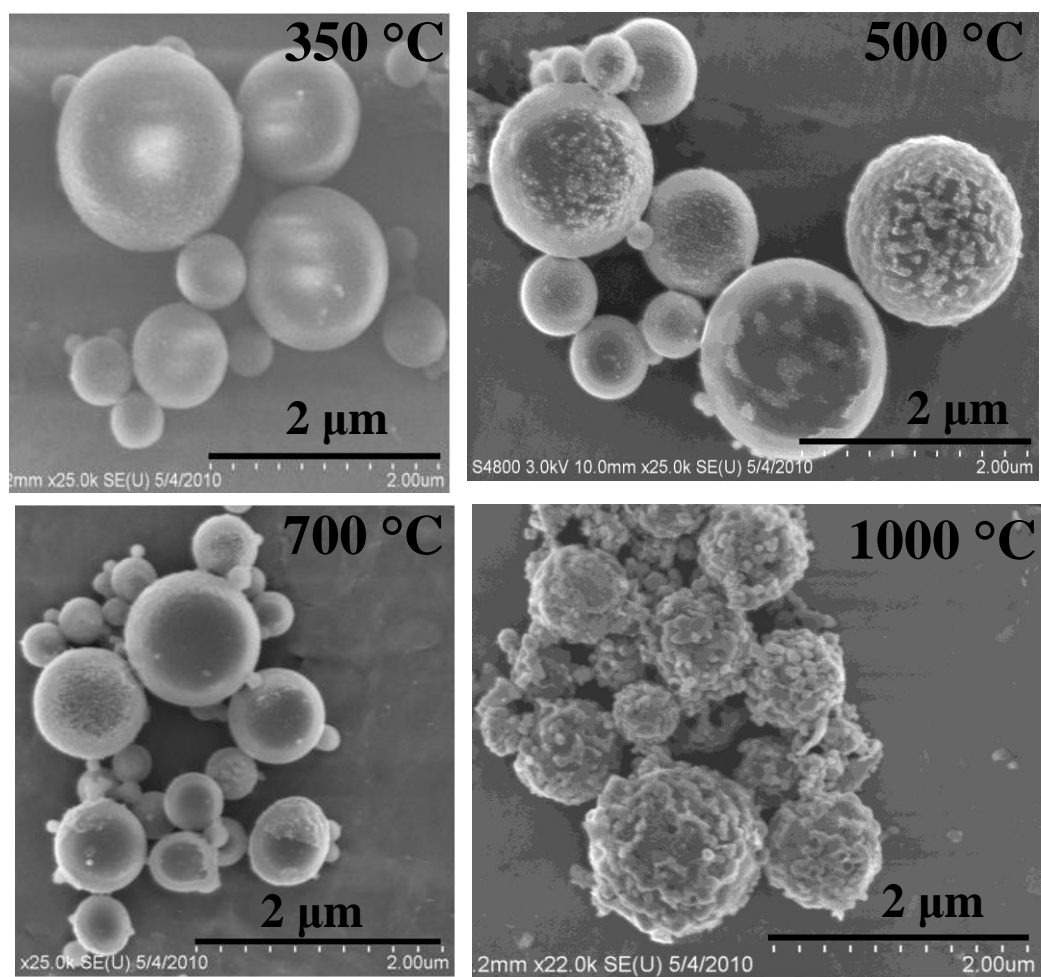


Figure 3.4 SEM images of multiple particles prepared at the various aerosolization temperatures.

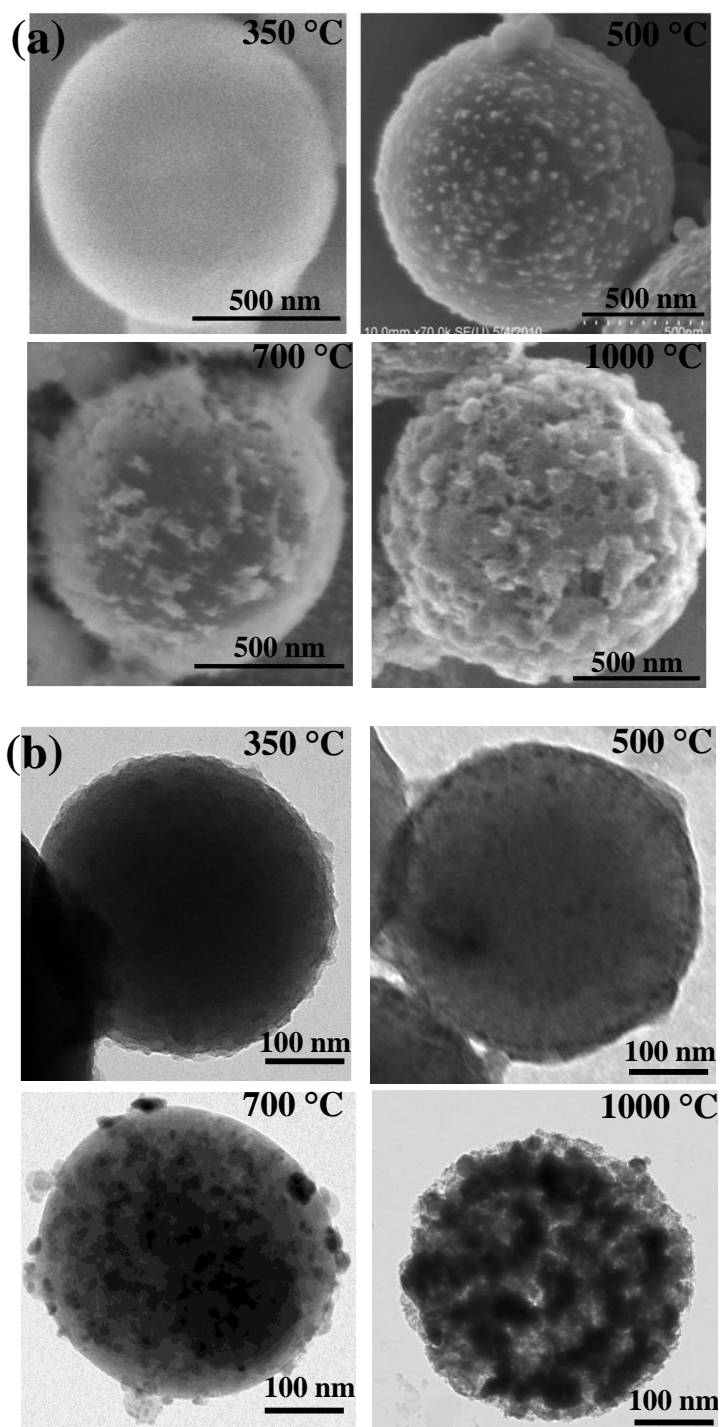


Figure 3.5 Single particle (a) SEM and (b) TEM of composite particles prepared by the aerosol-based process at various heating zone temperatures. The particles become significantly more porous when prepared at high aerosolization temperatures.

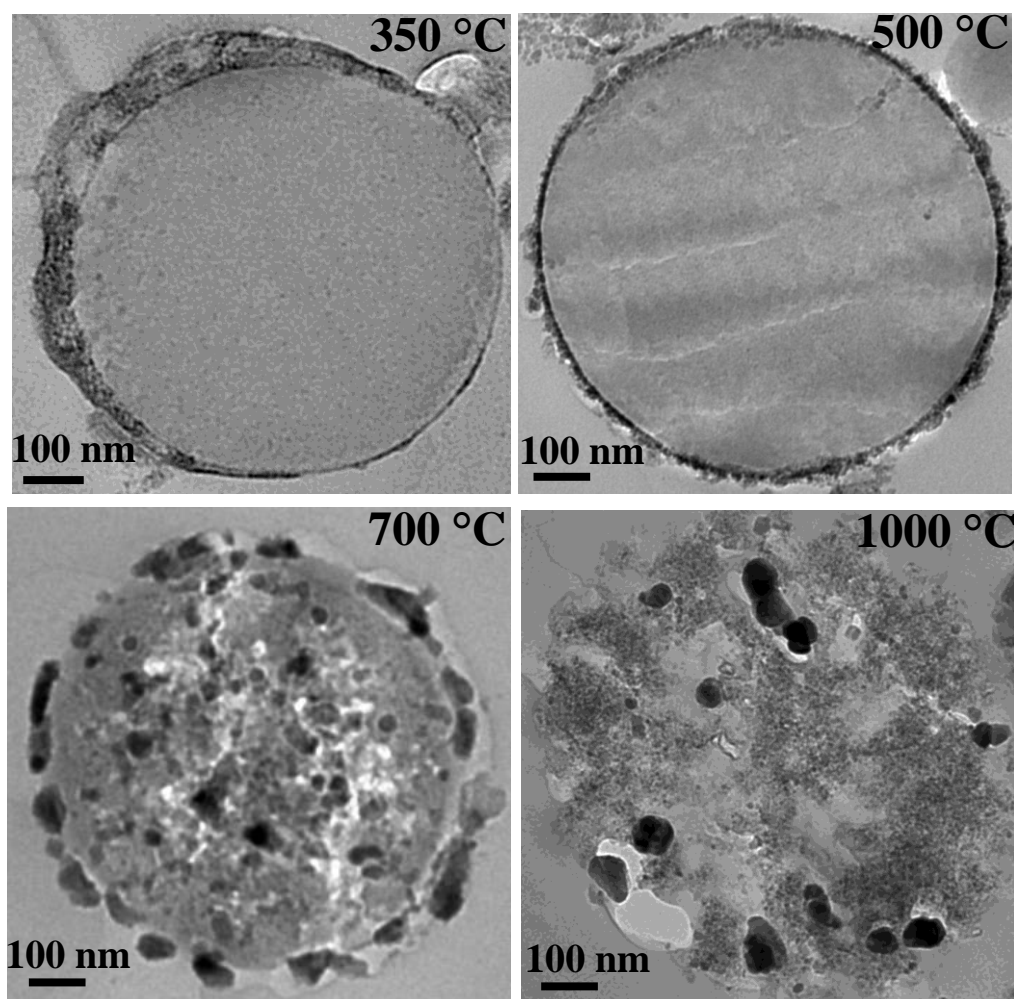


Figure 3.6 Cut-section TEM of composites at different heating zone temperatures. The evolution of iron nanoparticle placement from the external surface to the particle interior with an increase in the heating zone temperature from 300 to 1000 °C is noted.

From these images, it is clear that there is a significant change in morphology of the composites with an increase in the temperature of heating zone, maintaining the residence time characteristics. Figure 3.5b also indicates that the iron particles attached to the surface of the carbon microspheres at low temperatures (300 and 500 °C), becomes embedded within the carbon matrix as the temperature of heating zone is elevated to 700 °C and above. Cut-section TEM images of the composites were obtained to further corroborate the transition in the morphology (Figure 3.6). At the lower aerosolization temperatures, a strong contrast between the dark edge and pale core clearly implies that the iron species are attached to the carbon microsphere external surface rather than located in the interior. At 1000 °C, the iron salt particles are completely embedded within carbon microspheres, with clear evidence of larger clusters or crystallites of the iron salts. At 700 °C, iron species are present within the carbon microsphere as well as on the surface, indicating the transition.

In addition to the observed transition in placement of the iron, it is evident that the porosity of the carbon structure increases with the aerosolization temperature. N₂ adsorption-desorption isotherms of Fe salt-carbon composite microspherical particles are shown in Figure 3.7a. Surface areas for the composite microspheres, calculated using the Brunauer-Emmett-Teller (BET) method are 14, 19, 51 and 118 m²/g for the particles prepared at heating zone temperatures 300, 500, 700 and 1000 °C, respectively. The corresponding Barret-Joyner-Halenda (BJH) desorption pore volumes were determined to be 0.0284, 0.0401, 0.1156 and 0.2324 cm³/g, respectively. A clear hysteresis is seen at the higher temperatures with the Type IV isotherm (Brunauer, Demming, Demming and Teller classification (BDDT)) indicating the presence of a mesoporous structure.^{69, 70}

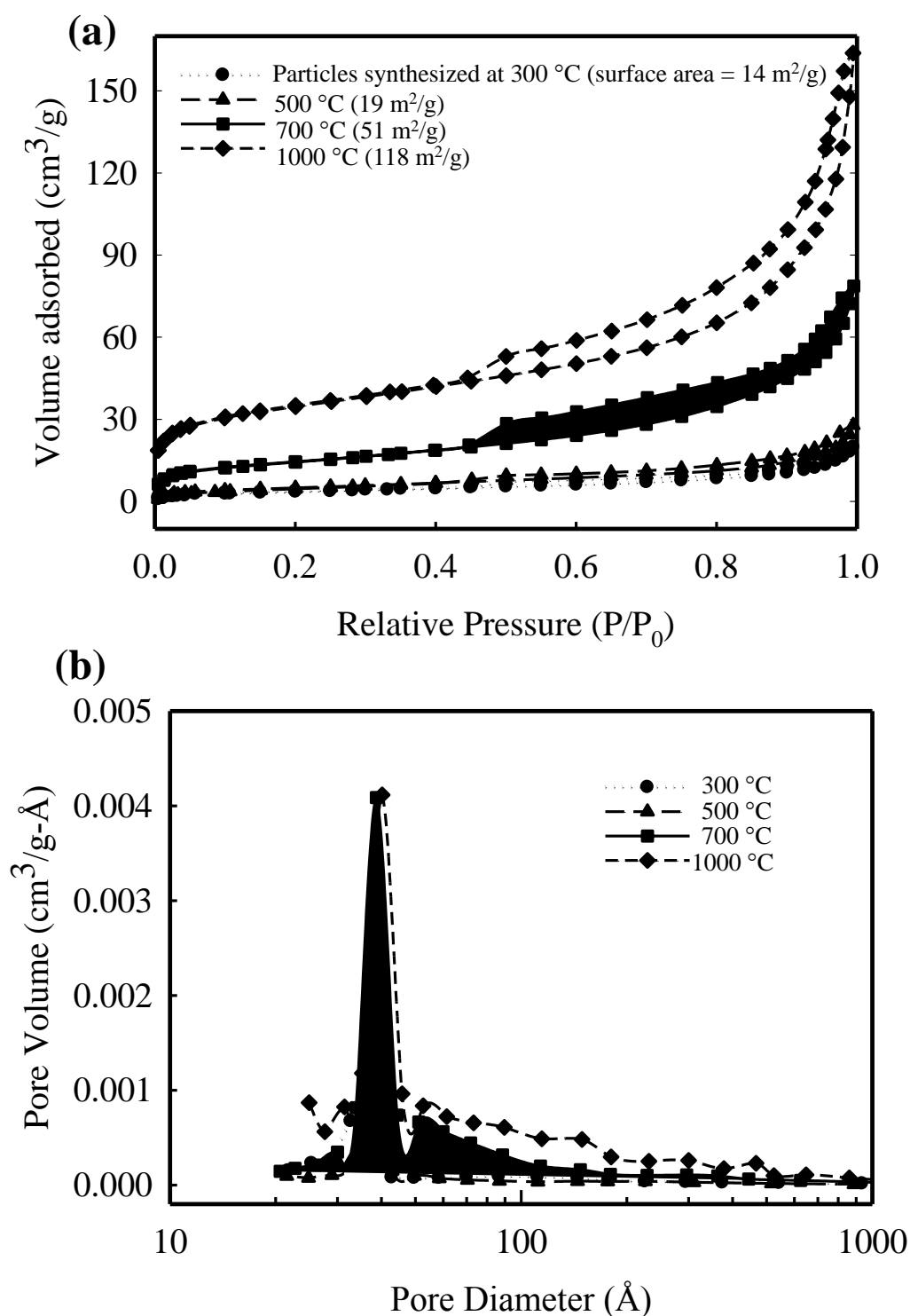


Figure 3.7 (a) Nitrogen adsorption-desorption isotherms and (b) BJH pore size distributions of the Fe salt-C composites prepared at 300 to 1000 °C.

Figure 3.7b illustrates the BJH pore size distribution as derived from the desorption branch of the isotherms. The mesoporous samples show a pronounced pore size between 3 and 5 nm.

We propose that the formation of iron-carbon microspheres with placement of iron species on the surface or within carbon microspheres is based on the relative rates of two concurrent processes: (a) the carbonization of sucrose (b) the recrystallization of iron salt as the solvent evaporates. Figure 3.8 is a schematic of these processes showing the consequences if carbonization occurs prior to recrystallization of the iron salt, and if carbonization occurs concurrent with recrystallization. At lower temperatures (300-500 °C), carbonization of sucrose precedes the crystallization of iron salt, ostensibly because the water has not fully evaporated and there is still solubilized iron chloride in the droplet that now contains a carbonized particle. As the water evaporates off, the solubilized salt recrystallizes but has no place to precipitate but on the surface of the carbon particle. At the other end of the temperature range (1000 °C), the rapid evaporation of the solvent accelerates iron salt precipitation and both processes become concurrent. This result in the formation of a highly porous structure with iron salt embedded throughout the carbon matrix. The internal porosity is created from both sucrose decomposition and crystallization of precipitated iron salts into the carbon matrix. At the intermediate temperature of 700 °C, we see a transition, where clearly some of the iron salt crystallizes out onto the surface of the carbonized sucrose.

It should be noted that at all the temperatures in this study, it is necessary to use the iron salt to facilitate the formation of carbon microspheres. Aerosolization of sucrose solution without the iron precursor did not produce carbon microspheres at any of the

temperatures used in this study. With dilute sulfuric acid (10% - w/w sucrose) however; efficient carbonization is observed indicating that the carbonization is acid-catalyzed. A recent pioneering paper by Atkinson and coworkers illustrates the formation of iron in carbon microspheres at high temperatures and under base catalyzed conditions.⁹⁴

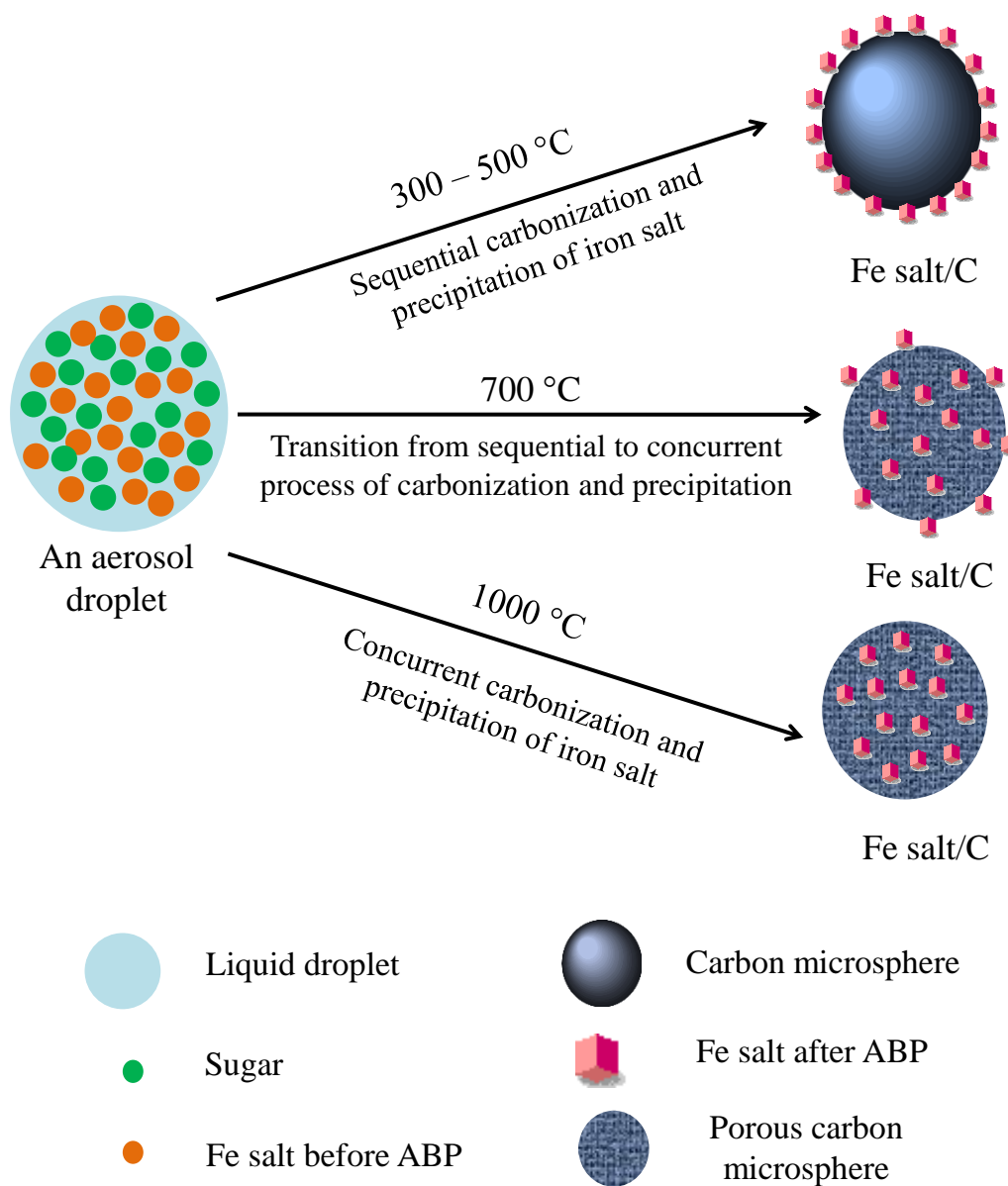


Figure 3.8 Proposed mechanism of morphological changes and metal nanoparticle placement with temperature.

The novelty of the current work is the delineation of a method to modify placement of nanoparticles of an iron species on a carbon support, either on the external surface of the support or within the interior. In our recent paper⁹³, we have shown the application of iron supported on the external surface of the carbon in reductive dechlorination of TCE. We extend this observation here to show that the iron species located in the interior of the carbon support is equally effective in the reaction.

3.3.2 Reactivity characteristics of Fe-C composite particles for the reductive dechlorination of TCE

Figure 3.9a illustrates TCE removal from solution and the time evolution of gas phase products where we have used the iron-carbon composite particles generated at 1000 °C to illustrate particle reactivities. The chromatogram is illustrative in that it shows the sharp decrease of solution TCE level as soon as the reactive particles are added, a consequence of rapid TCE adsorption on the carbon. This is a particular advantage of using carbon as a support. In addition to the inherently innocuous aspects of carbon as a support, it is possible that the dechlorination is facilitated by enhanced reactant concentrations in the vicinity of the reactive NZVI sites through strong adsorption. The subsequent slower evolution of gas phase dechlorination products as shown in Figure 3.9b indicates that the sequential dechlorination of intermediates is responsible for the second, slower phase in the combined adsorption + reaction sequence. Using the product evolution to obtain a pseudo-first order rate constant for TCE destruction independent of adsorption, we have calculated a mass normalized rate constant k_m of 0.84 Lhr⁻¹g⁻¹.

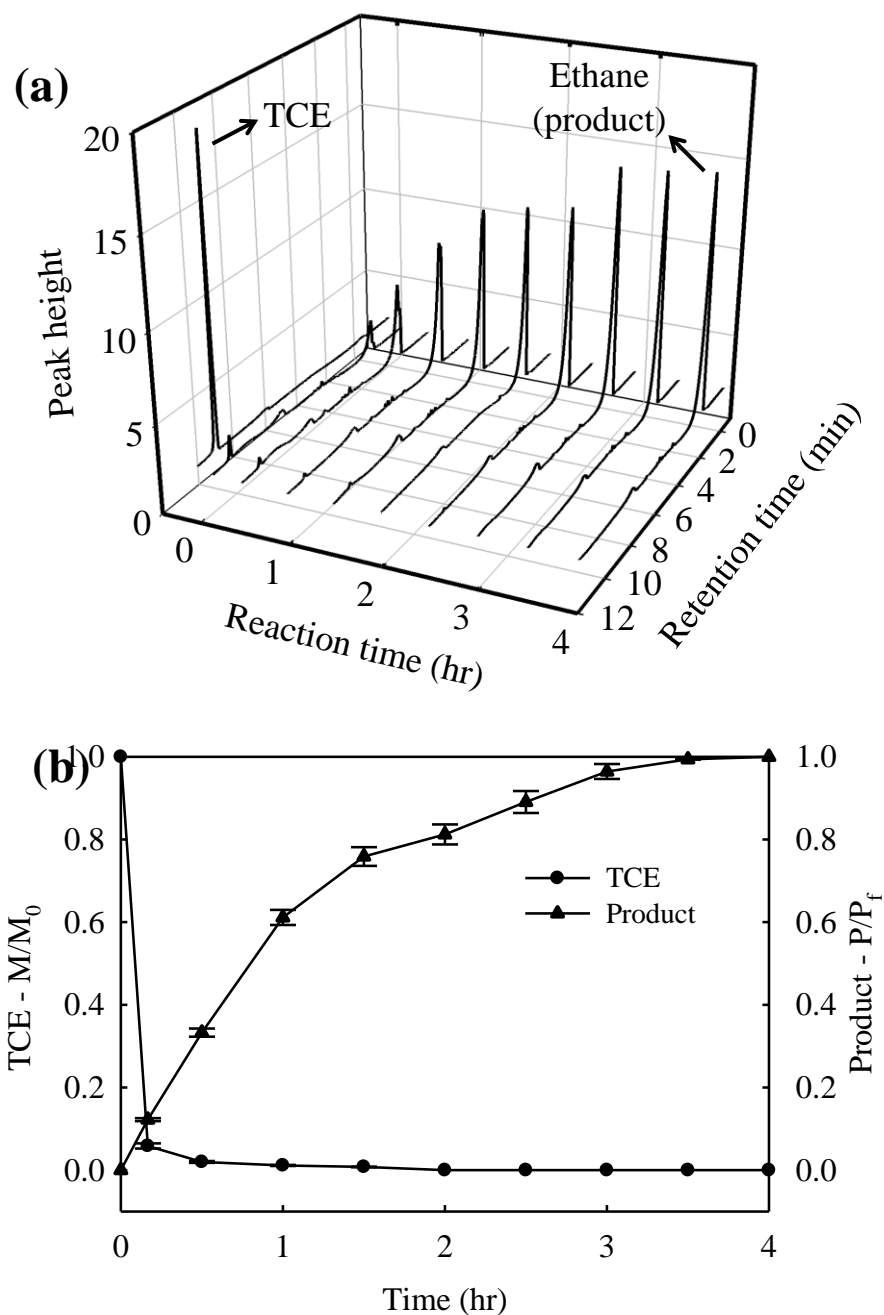


Figure 3.9 (a) Representative GC trace of headspace analyses showing TCE degradation and reaction product evolution at various reaction times (b) TCE removal from solution and gas product evolution rates for Fe-C composites. M/M_0 is the fraction of the original TCE remaining and P/P_f is the ratio of the gas product peak to the gas product peak at the end of 4 hr.

Indeed the high temperature iron-in-carbon based materials show superior reaction kinetics in comparison to the iron-on-surface based materials that we have described in our recent paper where k_m is $0.12 \text{ Lhr}^{-1} \text{ g}^{-1}$.⁹³ The increase in reaction rate with materials prepared at highest aerosolization temperature used is useful, but the more important aspect is the fact that the materials are reactive over a range of aerosolization temperatures, since *in situ* application only mandates materials that are reactive. We also note that this is not a metal-catalyzed reaction where metal particle surface characteristics define activity. On the other hand, the entire particle characteristics become important as the zerovalent iron becomes converted to iron oxide over the course of the reaction. The reactivities observed here appear to be significantly higher than that reported in the literature in a procedure involving impregnation of activated carbon with iron salts followed by reduction to zerovalent iron.¹⁰²

The most instructive aspect of the reaction is seen in the chromatogram of Figure 3.9a where three factors stand out (a) the relatively rapid complete reduction of TCE in 4 hours (b) the sharp adsorption of TCE (c) the lack of any detectable quantities of intermediates such as vinyl chloride, since these chlorinated intermediates are also strongly adsorbed till they are reacted away. Continuing work seeks to fully clarify the adsorption and reaction of all intermediates and other chlorinated compounds.

3.4 SUMMARY

In summary, nanoscale adsorptive-reactive (carbon-iron) composites were synthesized using a facile aerosol-based process and these materials are shown to have applications in the reductive dechlorination of TCE. The novelty of the current work is

the demonstration of the versatility of the aerosol-based process, and the understanding of the competitive nature of carbonization of sucrose and iron salt precipitation during evaporation of an aerosol droplet. By a simple increase of heating zone temperatures, we have shown that the relative increase in the iron precipitation rate to the carbonization rate results in iron placement in the interior of the carbon microsphere than on the external surface. Regardless of the environmental application described here, carbon is a ubiquitous catalyst support and iron is an equally ubiquitous catalytic material. Whether these concepts can be extrapolated to the preparation of other catalytic metals on carbon supports is the subject of further study. But one can imagine the possibilities of a facile method to control metal placement in catalytic supports. In highly diffusion limited reactions, external placement of the metal species may be preferred, whereas in cases where diffusion hinders transport of catalyst poisons or coke precursors, internal placement of the metal species would be preferred. The aerosol route to such placement modification is therefore of significant use to catalyst design.

Chapter 4

Iron-Carbon Composite Microspheres Prepared through a facile Aerosol-Based Process for the Simultaneous Adsorption and Reduction of Chlorinated Hydrocarbons

Based on a manuscript submitted to *Water Research* journal

4.1 Introduction

The reductive dehalogenation of chlorinated hydrocarbons such as tetrachloroethylene (PCE) and trichloroethylene (TCE) using zerovalent iron (ZVI) is a promising approach to the remediation of these persistent contaminants^{5, 30, 103-110}. Nanoscale ZVI particles (NZVI) have enhanced reaction rates resulting from their increased surface areas.¹⁵⁻²² More importantly, the colloidal nature of NZVI indicates that these particles can be used in *in situ* injection remediation technology, which is potentially a simple, cost-effective and environmentally benign method for remediation.¹³ For successful subsurface remediation, the injected NZVI particles should meet the following criteria: (a) travel through porous media to the contaminated zone; (b) sequester, remove or convert the contaminants in the subsurface to significantly reduce dissolved phase concentrations and (c) partition to the DNAPL-aqueous phase.^{32, 49, 50}

However, NZVI particles have a strong tendency to agglomerate due to their ferromagnetic nature, forming aggregates that prevent their flow through porous media.^{24, 40-45} NZVI particles stabilized by organic species such as surfactants, vegetable oils, starches, or polyelectrolytes such as carboxymethyl cellulose (CMC) and poly (acrylic

acid) (PAA), or triblock copolymers exhibit increased mobility through porous media.^{24, 41, 42, 53, 54, 86, 111} These organic species physically adsorb onto NZVI particles surface preventing their aggregation and increases solution stability by means of steric or electrostatic repulsions, thereby significantly enhancing transport characteristics.

Previous studies from our laboratory have shown silica and carbon microspheres prepared in the size range of 100-1000 nm can serve as effective supports and/or carriers for NZVI particles with improved transport and reactive properties.^{46, 49, 64, 93, 112-114} In recent work, we have described a method to develop spherical iron-carbon (hereafter designated as Fe-C) composite particles using a facile aerosol-based process.^{93, 113, 114} These Fe-C composite particles have been tested towards the dechlorination of TCE with the important observation being the lack of detectable toxic intermediates such as dichloroethylenes (DCEs) or vinyl chloride (VC). This is in contrast to earlier studies that have shown that the dechlorination of PCE and TCE with bare ZVI leads to the accumulation of the undesired intermediates.^{31, 34, 115, 116} This is a major concern for any remediation method/materials and not much attention is given to the aspect of the fate and transformation of toxic intermediate products. Our hypothesis is that the highly adsorptive carbon prevents the release of any toxic intermediates. Any chlorinated intermediate generated remain adsorbed on the carbons till they are reacted away to the light gases, primarily ethane and ethylene. To test this hypothesis, we have applied the aerosol Fe-C particles towards the transformation of chlorinated hydrocarbons and their intermediates in this present work. Our objective is the systematic study of dechlorination of chlorinated ethylenes starting with PCE and its intermediate chlorinated ethylenes, TCE, DCEs and VC. To the best of our knowledge, this is the first study focusing on the

simultaneous adsorption and reaction of chlorinated hydrocarbons PCE, TCE and their intermediates DCE (*cis*- and *trans*- 1,2-DCE, 1, 1-DCE and VC) using the iron-carbon composite particulate system.

4.2 Experimental Section

4.2.1 Materials

All chemicals for synthesis were purchased from Sigma-Aldrich and used as received: Sucrose ($C_{12}H_{22}O_{11}$, ACS reagent), Iron (III) chloride hexahydrate ($FeCl_3 \cdot 6H_2O$, 97%, ACS reagent), sodium borohydride ($NaBH_4$, 99%), tetrachloroethylene (PCE, C_2Cl_4 , 99%), trichloroethylene (TCE, C_2HCl_3 , 99%), 1, 2 dichloroethylene (mixture of *cis*- and *trans*-1, 2-DCE, $C_2H_2Cl_2$, 99%) 1,1 dichloroethylene (1,1-DCE, $C_2H_2Cl_2$, 99%), vinyl chloride (VC, C_2H_3Cl , 2000 $\mu g/mL$), potassium hexachloropalladate (IV) (K_2PdCl_6 , 99%) and sodium carboxymethyl cellulose (NaCMC or CMC, mean MW = 90 000, low viscosity). Deionized (DI) water generated with a Barnstead E-pure purifier (Barnstead Co., Iowa) to a resistance of approximately 18.2 M Ω was used in all experiments.

4.2.2 Preparation of Fe-C composite microspheres

The aerosol-based process was used to prepare Fe-C composite particles and follows the same procedure, described in our earlier work.^{93, 113, 114} Briefly, a homogeneous precursor solution containing 0.58M sucrose and 0.5M $FeCl_3 \cdot 6H_2O$ was first atomized to form aerosol droplets, which were then carried by an inert gas (nitrogen (N_2)) through a heating zone where solvent evaporation and carbonization occurs. The flow rate of the carrier gas was 2.5 L/min and the thermal treatment was carried out in a 120 cm tube (internal diameter of 4.45 cm) with a furnace length of 38 cm with a superficial

velocity of 2.7 cm/s and a furnace residence time of 14 seconds. The flow rate of the carrier gas was obtained after bubbling the effluent gas through water at room temperature, and the superficial velocity calculations are done with flow rate conditions at standard temperature and pressure (1 atm, 298K). The temperature of the heating zone was held at 700 °C. The heating zone temperature was maintained using a commercial tube furnace unit (Type F21100 Tube Furnace, Barnstead International, Dubuque, IA). The resulting iron salt-carbon (Fe salt-C) particles were collected over a filter maintained at 100 °C.

The as-synthesized Fe salt-C particles were reduced through liquid phase NaBH_4 reduction to obtain Fe-C carbon particles. Specifically, 0.2 g of particles collected from the filter paper was transferred to a vial followed by drop-wise addition of 10 mL of 0.26 M NaBH_4 water solution. After cessation of visible hydrogen evolution, the particles were centrifuged and washed with water and ethanol thoroughly before use.

4.2.3 Particle Characterization

Field emission scanning electron microscopy (SEM, Hitachi S-4800, operated at 20 kV), transmission electron microscopy (TEM; JEOL 2010, operated at 120 kV voltage), were used to characterize particle size and morphology.

4.2.4 Reaction Analysis

The dechlorination effectiveness of the Fe-C system for each of the chlorinated ethylenes was tested in batch experiments with an initial organics concentration of 20 ppm. The Fe-C particles were loaded with extremely small amounts of palladium (specifically 0.1 wt% Pd relative to Fe in this study) to enhance reactivity through the dissociative adsorption of

H₂ on the catalyst surface^{15, 31, 32, 58, 117}. In detail, 0.2 g of the freshly prepared Fe-C particles are dispersed in 20 mL water, followed by the addition of known quantities of diluted K₂PdCl₆ in water solution (0.0047M) and placed in a 40 mL reaction vial capped with a Mininert valve. The Pd catalyst loading is the same level used by other researchers.^{24, 45, 65} Accordingly, the final composition of Fe-C particles used in this study is 2.5g/L Fe, 7.5 g/L carbon, and 0.1wt% Pd (w/w Fe). To each vial, 20 µL of respective chlorinated ethylene stock solution (20 g/L of PCE, TCE 1, 2-DCE, or 1, 1-DCE in methanol) was spiked, resulting in an initial concentration of 20 ppm. In case of vinyl chloride, 200 µL of 2000 µg/mL (2000 ppm) in methanol was spiked into 20 mL particle suspension to make initial VC concentration of 20 ppm. The reactions were monitored through headspace analysis using a HP 6890 gas chromatography (GC) equipped with a J&W Scientific capillary column (30m × 0.32 mm) and flame ionization detector (FID). Samples were injected splitless at 220 °C. The oven temperature was held at 75 °C for 2 min, ramped to 150 °C at a rate of 25 °C /min and finally held at 150 °C for 15, 10, and 5 min for PCE, TCE and, 1,2-DCE, 1,1-DCE, VC respectively to ensure adequate peak separation between chlorinated and non-chlorinated reaction products.

4.3 Results and Discussion

4.3.1 Chemistry in a droplet

Figure 4.1a is a schematic of the aerosol reactor illustrating the aerosol-based process. A homogenous precursor solution containing sucrose and iron chloride was first atomized using an inexpensive commercial nebulizer (Micro Mist Nebulizer, Hudson RCI (REF 1883)) to form aerosol droplets that undergo a heating and drying step, generating submicron particles that are collected on a filter. We note the modification

over our earlier work^{93, 113, 114} in the use of extremely inexpensive pneumatic nebulizers, typically used in a hospital environment, as opposed to commercial atomizers that lead to sharper particle size distributions but are considerably more expensive. While our previous studies utilized the commercial atomizer (model 3076 TSI Inc., St. Paul, MN) with a stainless steel body, the present work uses simple plastic nebulizers. Our choice in switching to nebulizer use is also based on the fact that these plastic aerosol generating systems do not corrode, as with atomizers incorporating a stainless steel body when exposed to acidic conditions. Nebulizers are the oldest form of aerosol generation and require a pressurized gas supply as the driving force for liquid atomization.¹¹⁸⁻¹²⁰ The ease of use and low cost of nebulizers add to the feasibility of scaling up the aerosol process for potential commercialization.

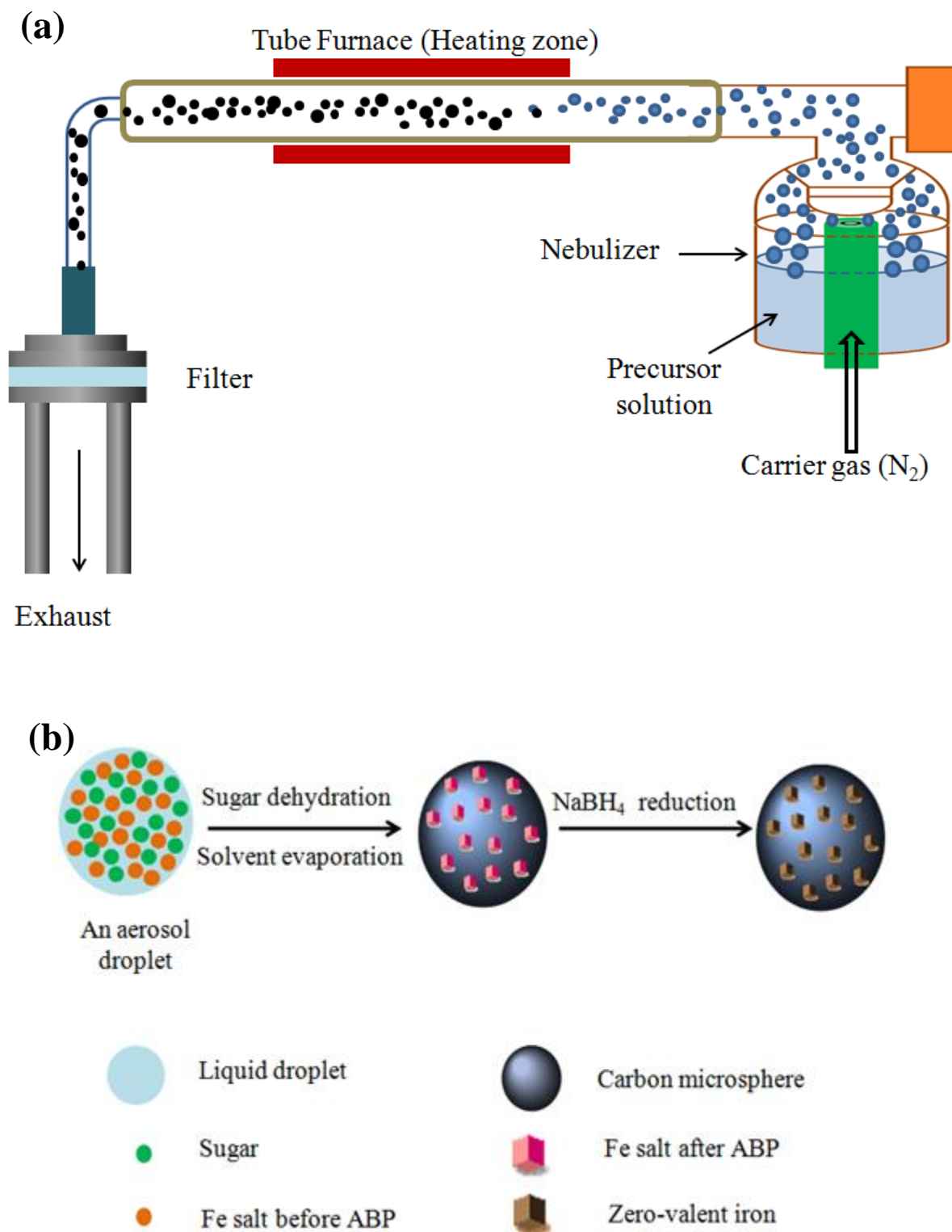


Figure 4.1 (a) Schematic showing the aerosol process for composite particle synthesis and (b) schematic of the reaction in an aerosol droplet.

Figure 4.1b is a representation of the formation process illustrating the “chemistry in a droplet” concept of producing the Fe-C composite particles. When the aerosol droplets pass through the heating zone, solvent evaporation and dehydration/carbonization of sucrose occurs. In addition, precipitation of solidified iron salt is concomitant with the dehydration of sucrose, generating a black powder of Fe salt-C composites. To obtain Fe-C composites, the collected powder is treated with sodium borohydride solution in excess to reduce ferrous ion to zero-valent iron.

4.3.2 Particle Characterization

Figure 4.2 illustrates the morphology and microstructure of the Fe-C composite particles analyzed using scanning and transmission electron microscopy. The composites are well-defined microspheres and are typically in the submicron (100 nm to 1000 nm) size range (Figures 4.2a and 4.2b). The inset in Figure 4.2a illustrates a single particle SEM while Figure 4.2c is a high resolution TEM. The micrographs clearly show a distribution of iron nanoparticles on the carbon support.

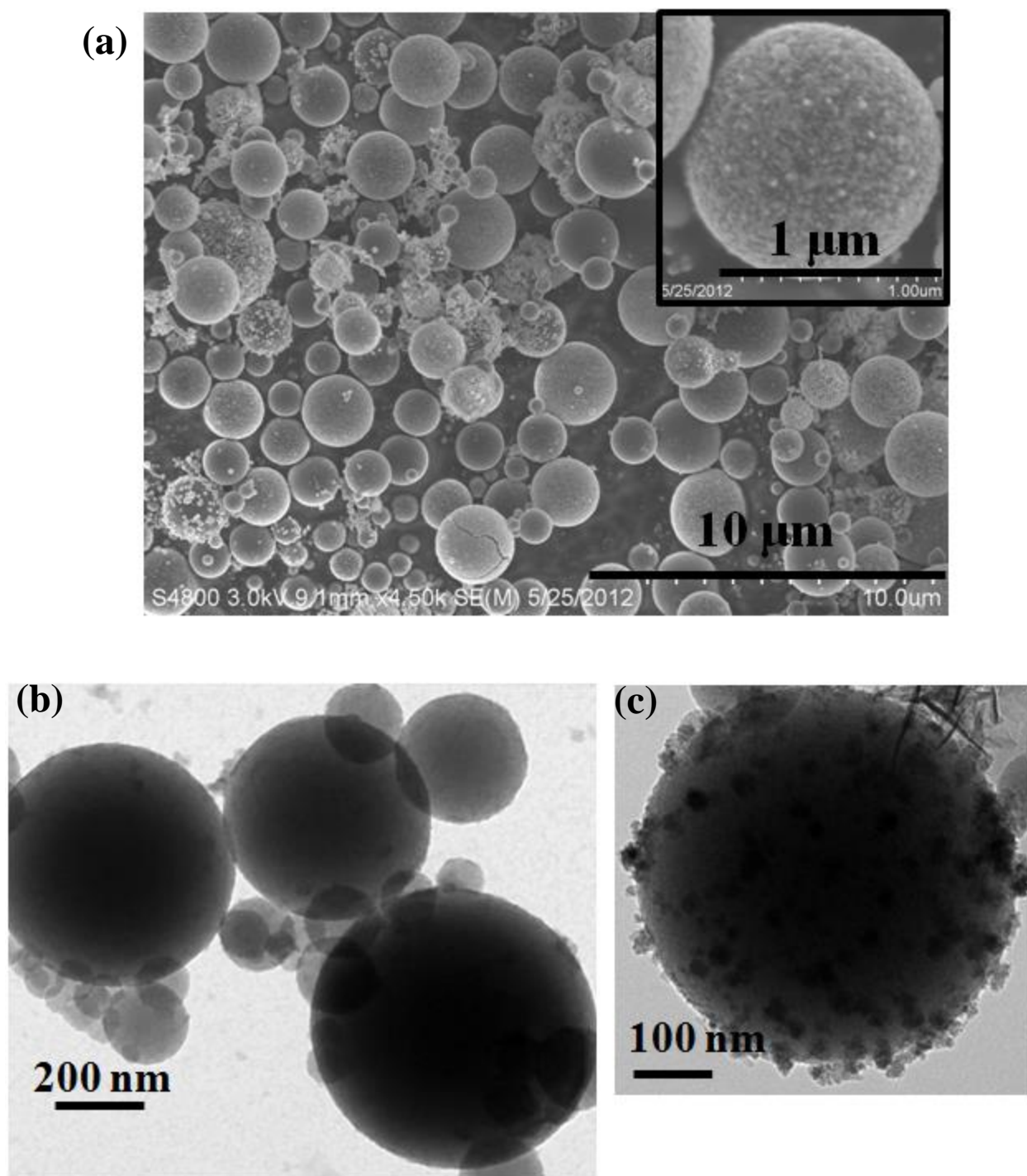


Figure 4.2 (a) SEM (b) TEM and (c) High resolution TEM of Fe-C composite particles prepared by the aerosol-based process. The inset in Figure (a) is the single particle SEM of the Fe-C composite.

4.3.3 Reactivity characteristics

Figures 4.3a and 4.3b show details of the product evolution for the reactions of PCE and TCE with the Fe-C composites. The following are consistent and notable aspects of the reaction (i) there is an immediate and sharp decrease in the reactant (PCE or TCE) peak upon contact with the Fe-C system (ii) the gas phase final products of ethane/ethylene evolve more gradually (iii) intermediates such as the di and mono chlorinated compounds are essentially negligible. The coupling of adsorption to reaction is therefore clearly observed and it is our hypothesis that the strongly adsorptive carbon sequesters all chlorinated compounds till final reduction to the volatile hydrocarbon products such as ethane and ethylene. Thus all chlorinated intermediates generated remain adsorbed on the carbons till they are reacted away to the light gases, primarily ethane and ethylene, but including a small amount of butane and butene (the other product peaks seen in the chromatograph).

To confirm this aspect of dechlorination of adsorbed intermediates by the Fe-C composites, separate batch experiments with DCEs and VC were performed. Reactions of the chlorinated ethylenes (PCE, TCE, 1, 2-DCE (a mixture of *cis*- and *trans*-compounds), 1, 1-DCE and VC) with the Fe-C composite particles are shown in Figures 4.4 (a-b) and Figures 4.5(a-c). An immediate sharp decrease of the respective chlorinated hydrocarbon (PCE, TCE, 1, 2-DCE, 1, 1-DCE or VC) peak is followed by a much slower decline in chlorinated ethylenes concentration. The initial sharp decrease is due to chlorinated ethylene partitioning from solution to the carbon through strong adsorption.

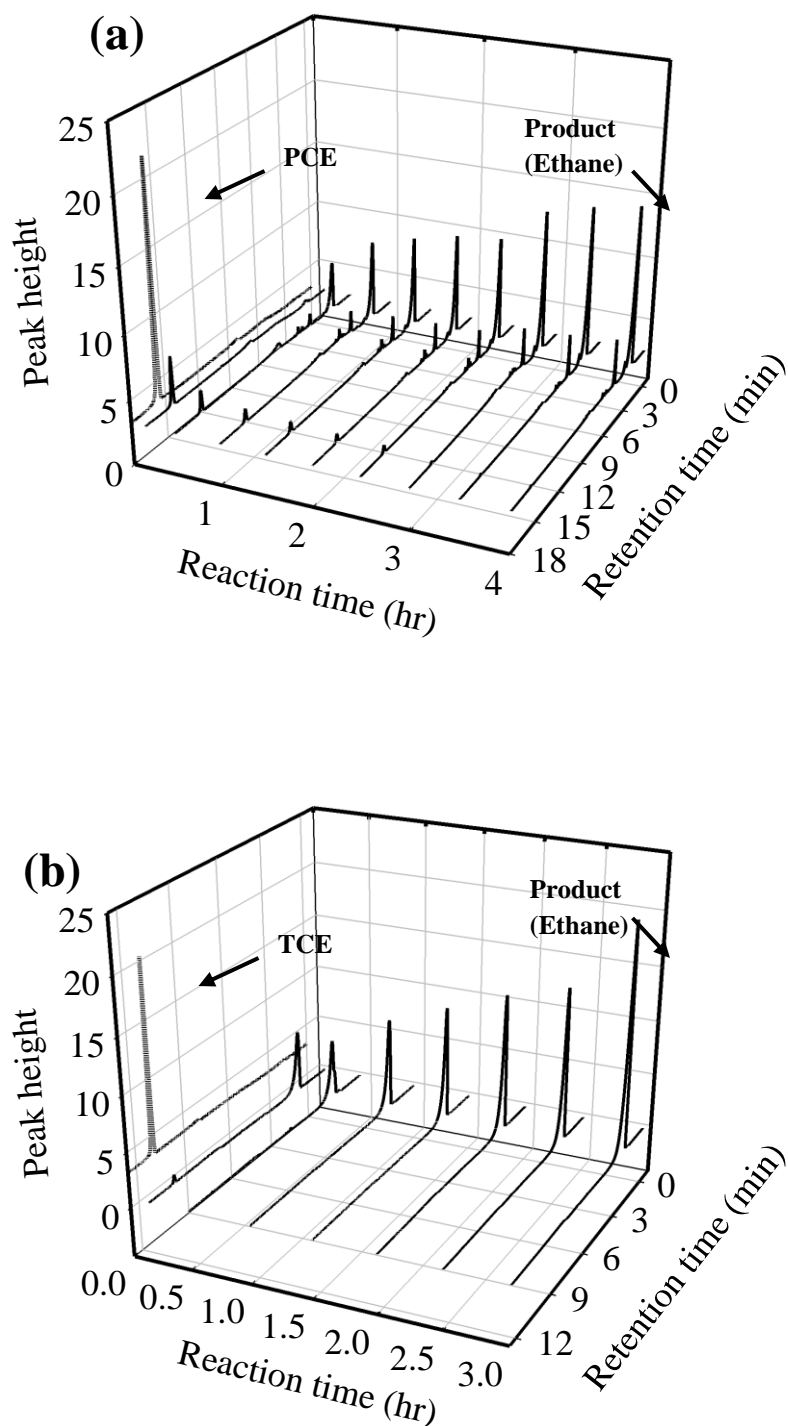


Figure 4.3 Representative headspace analyses using gas chromatography showing (a) PCE and (b) TCE degradation and reaction product evolution at various reaction times.

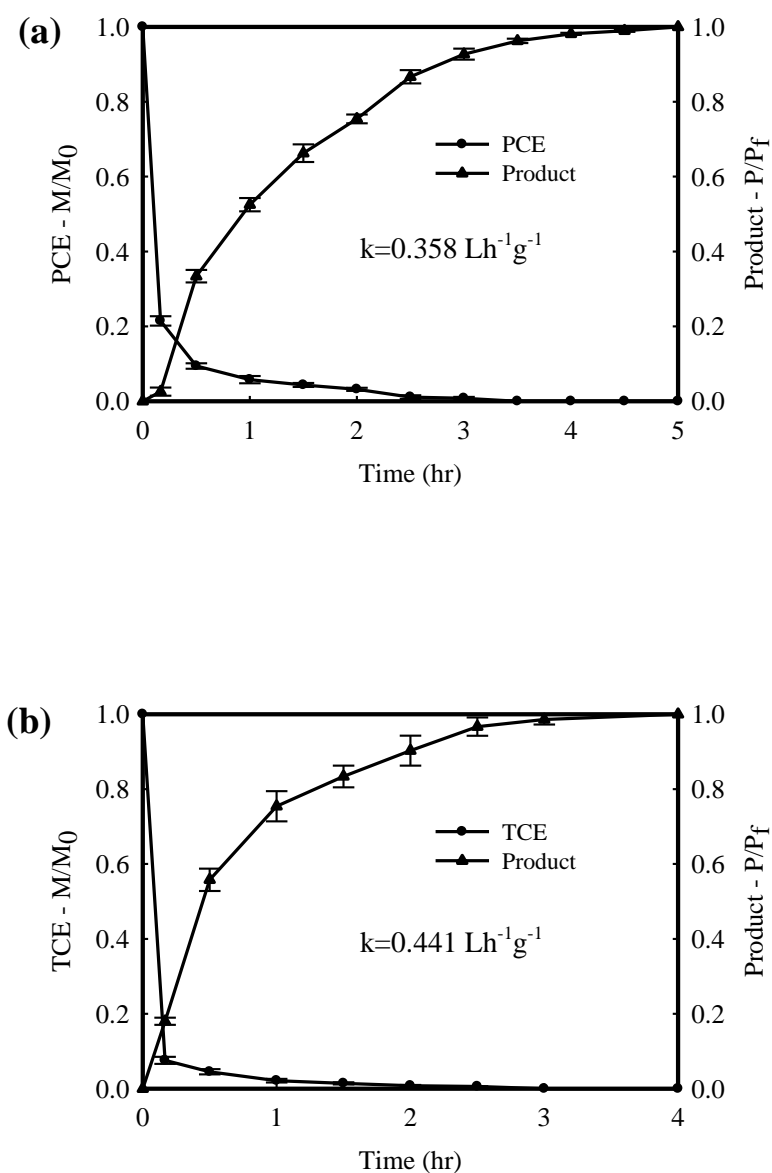


Figure 4.4 (a) PCE and (b) TCE removal from solution and gas product evolution rates for the Fe-C composites. M/M_0 is the fraction of the original chlorinated ethylene remaining and P/P_f is the ratio of the gas product peak to the gas product peak at the end of reaction.

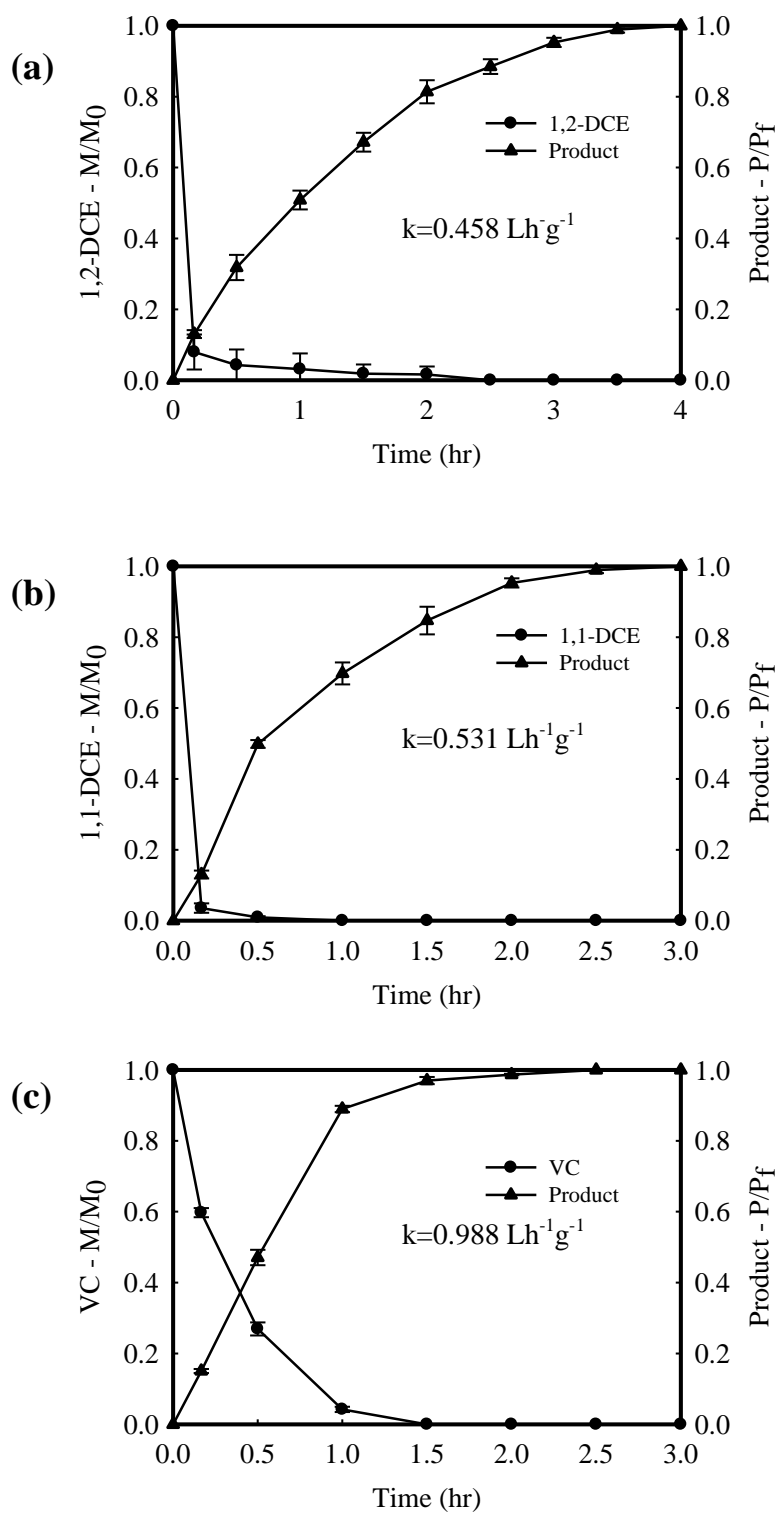


Figure 4.5 Reaction kinetics of the intermediate chlorinated ethylenes (a) 1, 2-DCE, (b) 1, 1-DCE, and (c) VC.

This is an important aspect to the design of these materials as the strong adsorption may lead to enhanced reactant concentrations in the vicinity of the reactive NZVI sites. The subsequent slow evolution of gas phase dechlorination products indicates that the dechlorination of chlorinated ethylene is responsible for the second, slower phase in the coupled adsorption+reaction sequence. Since the reaction is the slow step in the coupled sequence and therefore the rate controlling step, the overall kinetics of the reaction can be deduced by following the evolution of the lumped products. Table 4.1 lists the apparent first order rate constant k_{obs} and the mass-normalized reaction rate constant, k_{m} , based on the mass of zerovalent iron for all chlorinated hydrocarbons studied here.

4.3.4 Adsorption Characteristics

The adsorptive capacities of the aerosol-based Fe-C composites were compared with both humic acid and commercial activated carbon for the chlorinated hydrocarbons, PCE, TCE, 1, 2-DCE, 1, 1-DCE, and VC. The results are shown in Figure 4.6. In all experiments, 20 mL of a 20 ppm chlorinated ethylene solution and 0.2 g of particles were used. Clearly, the adsorption of chlorinated hydrocarbons on the Fe-C particles is higher than that of humic acid and comparable to that on commercially available granular and irregularly defined activated carbons. The comparison of adsorption capacities are given in Table 4.2.

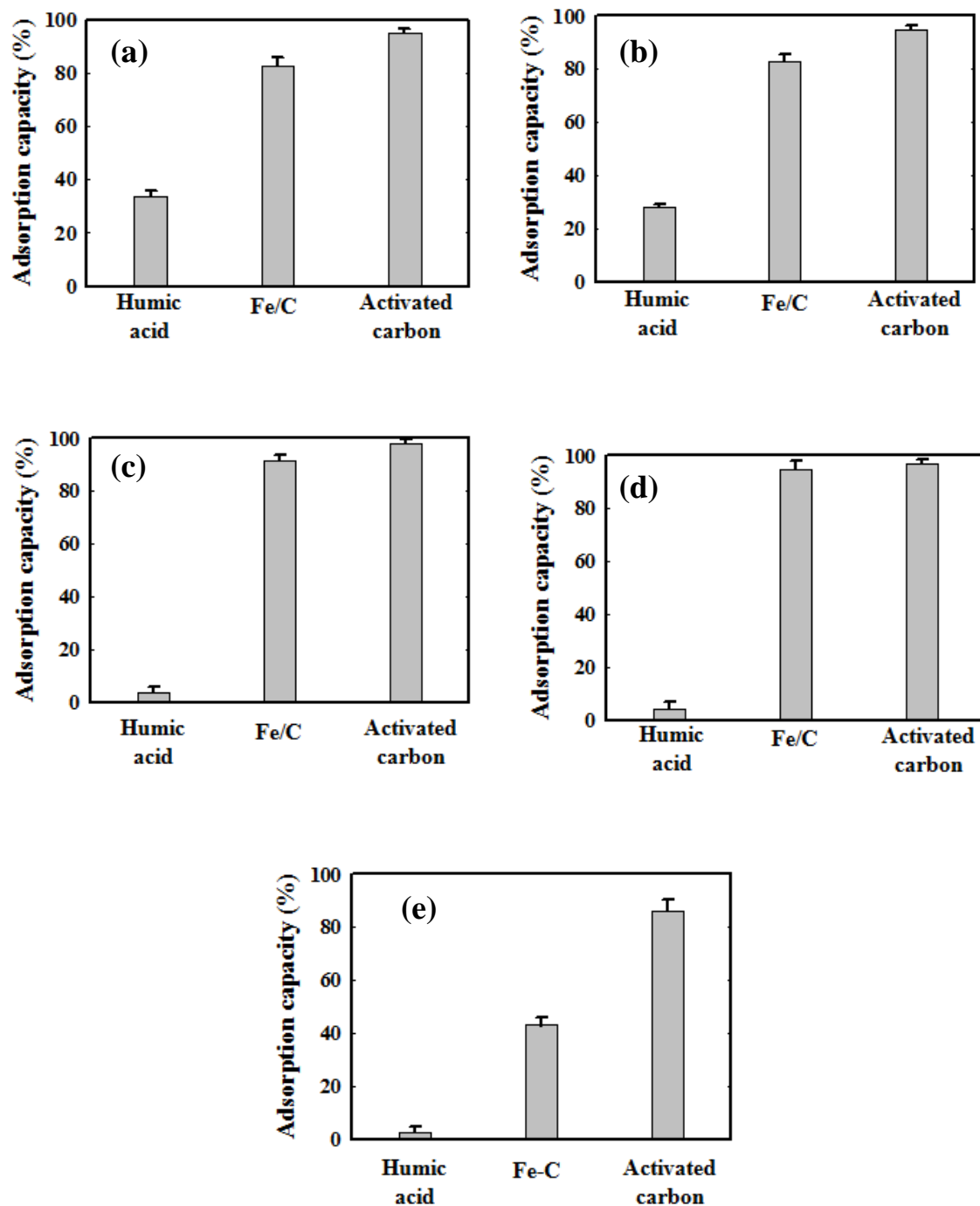


Figure 4.6 Comparison of the adsorption capacities of humic acid, Fe-C from the aerosol-based process and commercial activated carbon. In all experiments, 20 mL of a 20 ppm chlorinated ethylene ((a) PCE, (b) TCE, (c) 1, 2-DCE, (d) 1, 1-DCE, and (e) VC) solution and 0.2g of particles were used.

Chlorinated ethylene	Abbreviation, Formula	k_{obs} (apparent reaction rate constant) (h^{-1})	k_{m} (mass-normalized reaction rate constant) ($\text{Lh}^{-1}\text{g}^{-1}$)
Tetrachloroethylene	PCE, C_2Cl_4	0.895	0.358
Trichloroethylene	TCE, C_2HCl_3	1.101	0.441
1, 2-dichloroethylene (mixture of <i>cis</i> - and <i>trans</i> -)	1, 2-DCE, $\text{C}_2\text{H}_2\text{Cl}_2$	1.145	0.458
1, 1-dichloroethylene	1, 1-DCE, $\text{C}_2\text{H}_2\text{Cl}_2$	1.328	0.531
Vinyl chloride	VC, $\text{C}_2\text{H}_3\text{Cl}$	2.4709	0.988

Table 4.1 Reaction rate constants for reduction of the various chlorinated ethylenes using the aerosol-based Fe-C composite particles.

The implication of the strong adsorption on the aerosol-based carbon is the ability to establish a driving force for chlorinated hydrocarbons to desorb from natural organic matter and partition to the carbon containing NZVI, as a result of reactant depletion (through reaction) at the Fe-C sites. The establishment of this adsorption-reaction mechanism is expected to enhance the effectiveness of remediation.

We have calculated the partition coefficient for the adsorption of each chlorinated hydrocarbon on the Fe-C composites using the comprehensive definition of ⁷¹:

$$\frac{C_{CVOC}^{ads}}{C_{CVOC}^{water}} = K_p = \left\{ \frac{\left[(C_{CVOC}^{Air})_{ref} V_{hs} - (C_{CVOC}^{Air})_{ads} V_{hs} \right] + \left[\left(\frac{C_{CVOC}^{Air}}{K_H^{CVOC}} V_{water} \right)_{ref} - \left(\frac{C_{CVOC}^{Air}}{K_H^{CVOC}} V_{water} \right)_{ads} \right]}{\left(\frac{M_p}{\rho_p} \right) \left(\frac{C_{CVOC}^{Air}}{K_H^{CVOC}} \right)_{ads}} \right\}$$

Where C_{CVOC}^{ads} is the concentration of the respective chlorinated hydrocarbon (PCE, TCE, 1,2 DCE, 1,1-DCE and/or VC) on the adsorbent (mol/L), C_{CVOC}^{water} is the concentration of chlorinated hydrocarbon in the water phase (mol/L), C_{CVOC}^{Air} is the concentration of chlorinated hydrocarbon in the headspace (mol/L), V_{hs} and V_{water} are the volumes of the headspace and water, respectively (L), M_{ads} is the mass of the adsorbent (g), ρ_{ads} is the density of the adsorbent (g/L). The subscripts *ref* and *ads* refer to the system without and with the adsorbent. K_H^{CVOC*} is the Henry's law constant for the respective chlorinated hydrocarbon partitioning in water, with a value of 0.723 for PCE, 0.392 for TCE, 0.167 for cis – 1,2-DCE, 0.384 for trans – 1, 2-DCE and 1.137 for VC at 24.8°C ¹²¹.

Chlorinated ethylene	Adsorption capacity (%)		
	Humic acid	Aerosol Fe-C	Commercial activated carbon
Tetrachloroethylene	35	80	>90
Trichloroethylene	30	85	>95
1, 2-dichloroethylene (mixture of <i>cis</i> - and <i>trans</i> -)	<10	90	>95
1, 1-dichloroethylene	<10	95	>95
Vinyl chloride	<5	45	<85

Table 4.2 Comparison of adsorption capacities of the aerosol-based Fe-C composites with humic acid and commercial activated carbon. In all experiments, 20 mL of a 20 ppm chlorinated ethylene ((a) PCE, (b) TCE, (c) 1, 2-DCE, (d) 1, 1-DCE, and (e) VC) solution and 0.2g of particles were used.

The calculated partition coefficients for the chlorinated hydrocarbons on Fe-C composite particles are listed in Table 3. The results clearly indicate a high degree of chlorinated hydrocarbons adsorption on the Fe-C composite microspheres compared to various stabilizers used for preventing NZVI particles aggregation⁷¹. From the results presented in Table 3, the calculated partition coefficient for TCE adsorption on Fe-C composite microspheres ($K_p=1897$) is 22 fold higher than that for TCE adsorption on humic acid ($K_p=85$) and 126 fold higher than that for TCE adsorption on CMC ($K_p=14.5$)^{64, 71, 93, 112}.

Chlorinated ethylene	Partition coefficient (K_p) Aerosol Fe-C
Tetrachloroethylene	898
Trichloroethylene	1897
<i>cis</i> - 1, 2-dichloroethylene	5927
<i>trans</i> - 1, 2-dichloroethylene	3057
1, 1-dichloroethylene	4536
Vinyl chloride	145

Table 4.3 Calculated partition coefficient of chlorinated hydrocarbons adsorption on the aerosol-based Fe-C composite particles.

4.4 Summary

The present study is an extension of our earlier work describing the facile synthesis of Fe-C composite microspheres that are effective in the reductive dechlorination of TCE. The earlier work demonstrated an undetectable amount of intermediate release during the reductive process implying that the intermediates were strongly adsorbed on the carbon matrix. This work proves that the hypothesis is accurate, and that all chlorinated ethylenes are strongly adsorbed on the carbon matrix till final reduction to gas phase hydrocarbons. The results indicate the applicability of the Fe-C composite for reductive dechlorination and we list some of the advantages of such systems. (1) Aggregation of NZVI is inhibited by means of immobilization on the surface of carbon microspheres. In a sense, this immobilization also negates the deleterious implications of the environmental impact of nanomaterials as the nanoscale iron is strongly entrapped in a submicron matrix of carbon. (2) The Fe-C composite microspheres have strong adsorption characteristics, thereby significantly and rapidly reducing the dissolved chlorinated solvent concentration. (3) The highly adsorptive carbon prevents the release of any toxic chlorinated intermediates. (4) The aerosol-based process would be a promising approach to prepare adsorptive-reactive particulate systems for the *in situ* remediation of soil and groundwater DNAPL contaminants as the process is very simple and can be scaled up (due to its semi-continuous nature). Finally the Fe-C composite microspheres are prepared from inexpensive precursor materials (sugar and iron chloride in water).

Chapter 5

Carbon Supported Palladium Nanoparticles prepared through a facile Aerosol-Based Process for the Catalytic Hydrodechlorination of Trichloroethylene

5.1 Introduction

Trichloroethylene (TCE) is one of the most prevalent organic pollutants in groundwater and its contamination has been a significant environmental problem in the United States for decades.^{3, 5, 122} Catalytic hydrodechlorination is a promising method for the complete reduction of chlorinated compounds and is a well-established technique towards the environmental remediation of contaminated water.^{58, 123, 124} Hydrodechlorination is the process of converting chlorinated molecules to non-chlorinated ones by replacement of chlorine by hydrogen. The noble metal palladium (Pd) is a very effective catalyst and has been extensively used in the hydrodechlorination reactions as it is very active under ambient temperature and pressure.^{58, 122, 125} The catalyst Pd in the presence of hydrogen gas completely converts chlorinated solvents such as TCE into ethane.^{58, 125} Hydrodechlorination process is very promising for *ex situ* remediation of contaminated water.

The catalytic activity of Pd particles is greatly enhanced when they are prepared in nanoscale due to increase in surface area and the availability of more active sites. But Pd nanoparticles are thermodynamically unstable in solution and are difficult to separate from the aqueous phase and hence are used with a suitable support. Activated carbon and

alumina are the two most widely used supports for Pd nanoparticles.^{17, 58, 122, 124,}
¹²⁵ The typical preparation of supported Pd nanoparticles uses multi-step processes such as incipient wetness method.¹²⁶ These methods lack the advantage of scale-up as it involves not only multi-steps but also uses expensive and harmful chemicals for reducing palladium salts to zero-valent palladium. One other significant challenge with these multi-step processes is the uniform distribution of Pd particles in nanoscale throughout the support matrix. We address these problems in this study. Herein, we describe a simple one-step process to prepare nanoscale Pd particles distributed on well-defined carbon microspheres. We use an aerosol-based process to prepare carbon supported Pd nanoparticles for catalytic hydrodechlorination of chlorinated solvents such as TCE.

5.2 Experimental Section

5.2.1 Materials

All chemicals for synthesis were purchased from Sigma-Aldrich and used as received: Sucrose ($C_{12}H_{22}O_{11}$, ACS reagent), Iron (III) chloride hexahydrate ($FeCl_3 \cdot 6H_2O$, 97%, ACS reagent), potassium hexachloropalladate (IV) (K_2PdCl_6 , 99%) and trichloroethylene. Deionized (DI) water generated with a Barnstead E-pure purifier (Barnstead Co., Iowa) to a resistance of approximately 18.2 M Ω was used in all experiments.

5.2.2 Preparation of Palladium-Carbon (Pd-C) composite microspheres

The aerosol-based process was used to prepare Fe-C composite particles and follows the same procedure, described in our earlier work.^{93, 113, 114} In a typical synthesis, 2.0 g of sucrose and 0.2 g of K_2PdCl_6 salt were dissolved in 20 mL of water. To this solution, 0.1

g of concentrated H_2SO_4 was added as a catalyst for dehydration of sugar for carbonization reaction. The resulting solution was aged for 15 minutes under stirring to mix the solution completely. In the aerosol-based process, the precursor solution was first atomized to form aerosol droplets, which were then carried by an inert gas (nitrogen (N_2)) through a heating zone where solvent evaporation and carbonization occurs. The flow rate of the carrier gas was 2.5 L/min and the thermal treatment was carried out in a 120 cm tube (internal diameter of 4.45 cm) with a furnace length of 38 cm with a superficial velocity of 2.7 cm/s and a furnace residence time of 14 seconds. The flow rate of the carrier gas was obtained after bubbling the effluent gas through water at room temperature, and the superficial velocity calculations are done with flow rate conditions at standard temperature and pressure (1 atm, 298K). The temperature of the heating zone was held at 400 °C. The heating zone temperature was maintained using a commercial tube furnace unit (Type F21100 Tube Furnace, Barnstead International, Dubuque, IA). The resulting iron salt-carbon particles were collected over a filter maintained at 100 °C.

The as-synthesized palladium salt-carbon particles were reduced by H_2 at two different temperatures (300 °C and 400 °C) at a ramp rate of 10 °C/min for 3 hours to obtain palladium-carbon (Pd-C) composite microspheres.

5.2.3 Characterization and Analysis

Field emission scanning electron microscopy (SEM, Hitachi S-4800, operated at 20 kV), transmission electron microscopy (TEM; JEOL 2010, operated at 120 kV voltage), were used to characterize particle size and morphology. Energy-dispersive X-ray spectroscopy (EDS) is used for the elemental analysis and to confirm the presence of

palladium in the samples. In analysis, TCE dechlorination effectiveness was tested in batch experiments. In details, 0.02 g (20 mg) of the aerosol-based Pd-C was dispersed in 20 mL of water and placed in a 40 mL reaction vial and sonicated for 5 min. The particle suspension is then bubbled with H₂ gas for 15 minutes and the reaction vial is capped with a Mininert valve. To this vial, 20 µL of a TCE stock solution (20 g/L TCE in methanol) was spiked, resulting in an initial TCE concentration of 20 ppm. The reaction was monitored through a headspace analysis using the procedures described in our earlier work.^{64, 112, 113}

5.3 Results and Discussion

5.3.1 Chemistry in a droplet

Figure 5.1a is a schematic of the aerosol reactor illustrating the aerosol-based process. A homogenous precursor solution containing sucrose and palladium salt was first atomized using an inexpensive commercial nebulizer (Micro Mist Nebulizer, Hudson RCI (REF 1883) to form aerosol droplets that undergo a heating and drying step, generating submicron particles that are collected on a filter. Nebulizers are the oldest form of aerosol generation and require a pressurized gas supply as the driving force for liquid atomization¹¹⁸⁻¹²⁰. The ease of use and low cost of nebulizers add to the feasibility of scaling up the aerosol process for potential commercialization.

Figure 5.1b is a representation of the formation process illustrating the “chemistry in a droplet” concept of producing the Pd-C composites. When the aerosol droplets pass through the heating zone, solvent evaporation and dehydration/carbonization of sucrose occurs. In addition, precipitation of solidified palladium salt is concomitant with the

dehydration of sucrose, generating a black powder of Pd salt-C composites. To obtain Pd-C composites, the collected powder is treated under flowing H₂ at lower temperatures (300 °C and 400 °C) to reduce palladium salts to metallic or zero-valent palladium.

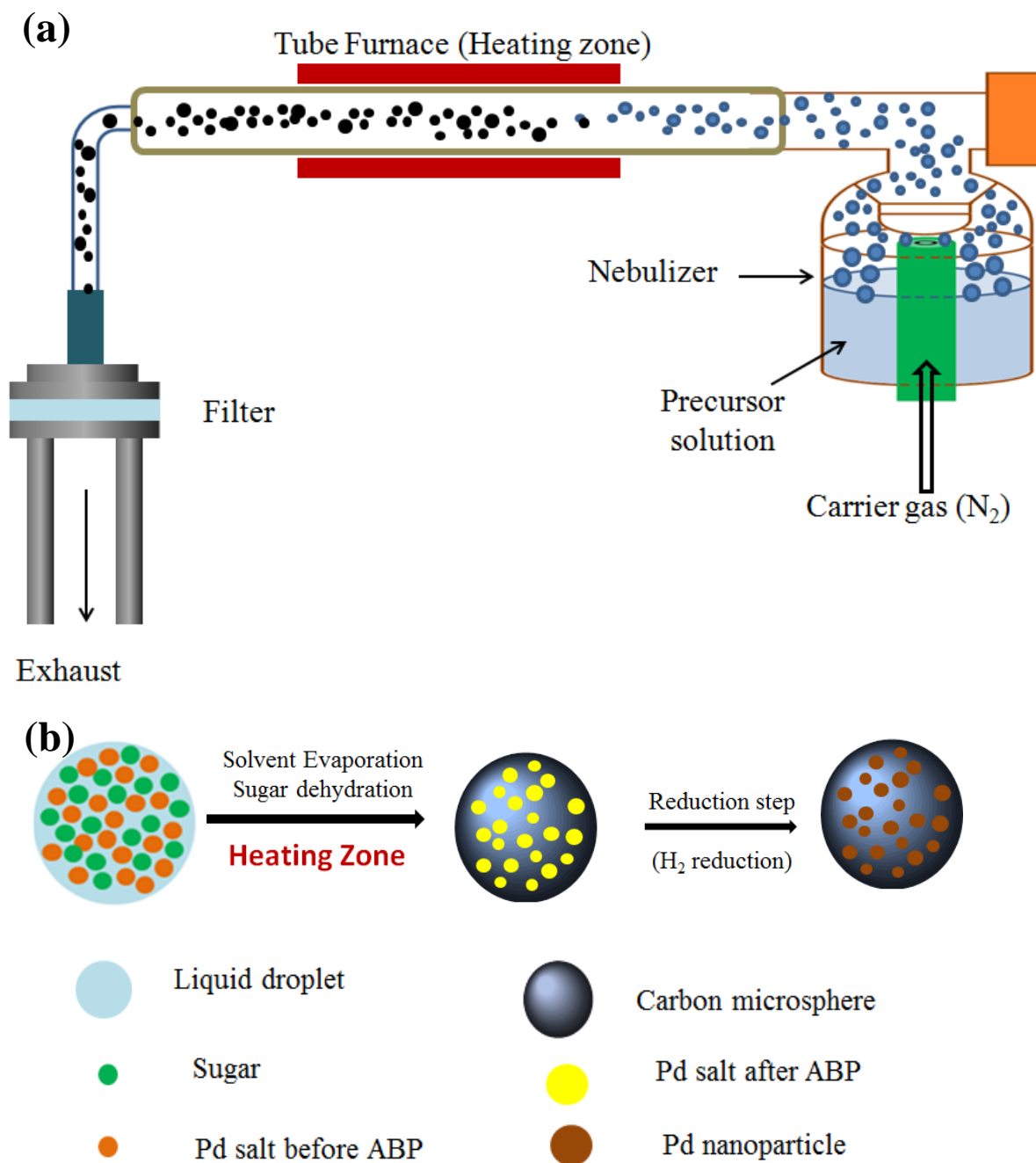


Figure 5.1 (a) Schematic showing the aerosol process for composite particles preparation and (b) schematic of the reaction in an aerosol droplet.

5.3.2 Particle Characterization

Figure 5.2 and 5.3 shows the SEM and TEM images of the Pd-C composite microspheres prepared at 400 °C aerosolization temperature and H₂ reduction at 300 °C and 400 °C, respectively. From Figure 5.2c and 5.3c, the presence of Pd nanoparticles with higher electron contrast on carbon microsphere indicates the distribution of nano-Pd throughout the surface of carbon microspheres with the size of Pd around 5-10 nm. The presence of Pd nanoparticles in the Pd-C composites is further confirmed by the EDS analysis (Figure 5.2d and 5.3d). From the SEM (Figure 5.2a and 5.3a) and TEM images (Figure 5.2b), the particles are spherical with a size range of 100 – 1000 nm.

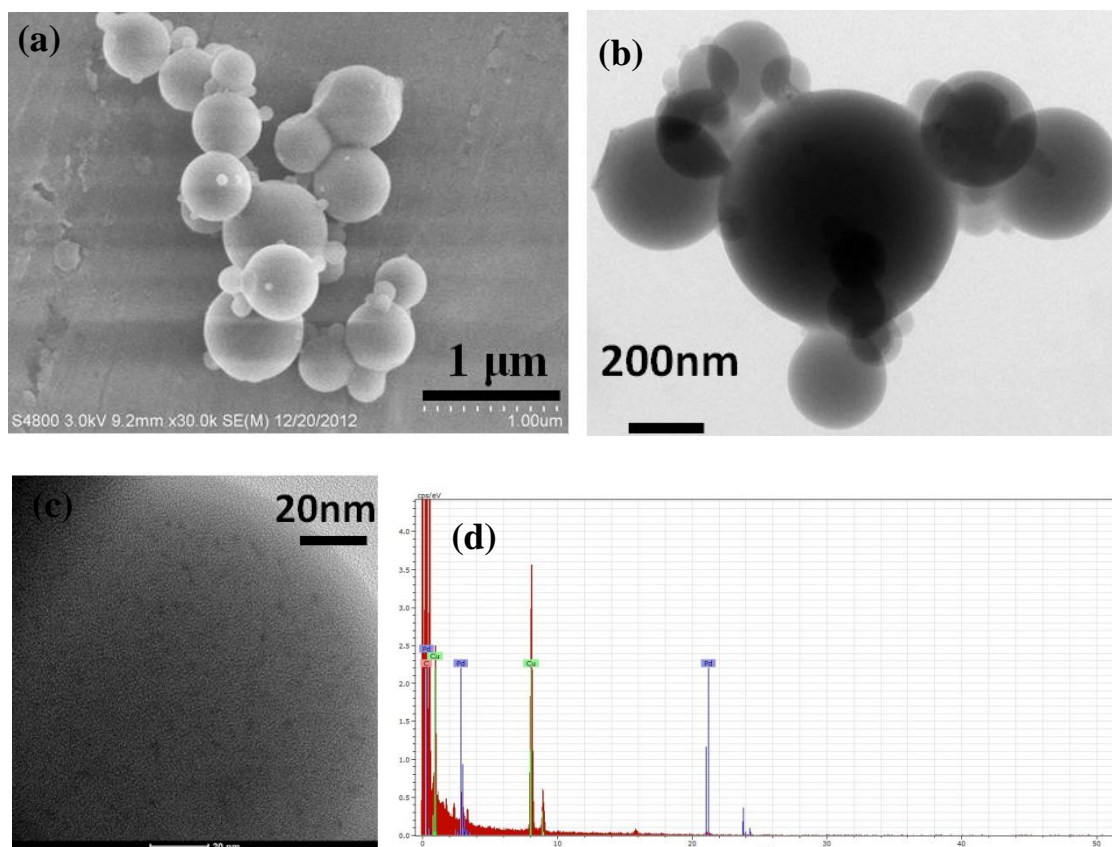


Figure 5.2 (a) SEM (b) TEM (c) high-resolution TEM of carbon supported palladium nanoparticles (Pd-C composite microspheres) prepared using aerosol-based process at 400 °C and H₂ reduction at 300 °C. (d) EDS spectrum of the Pd-C composites confirming the presence of palladium.

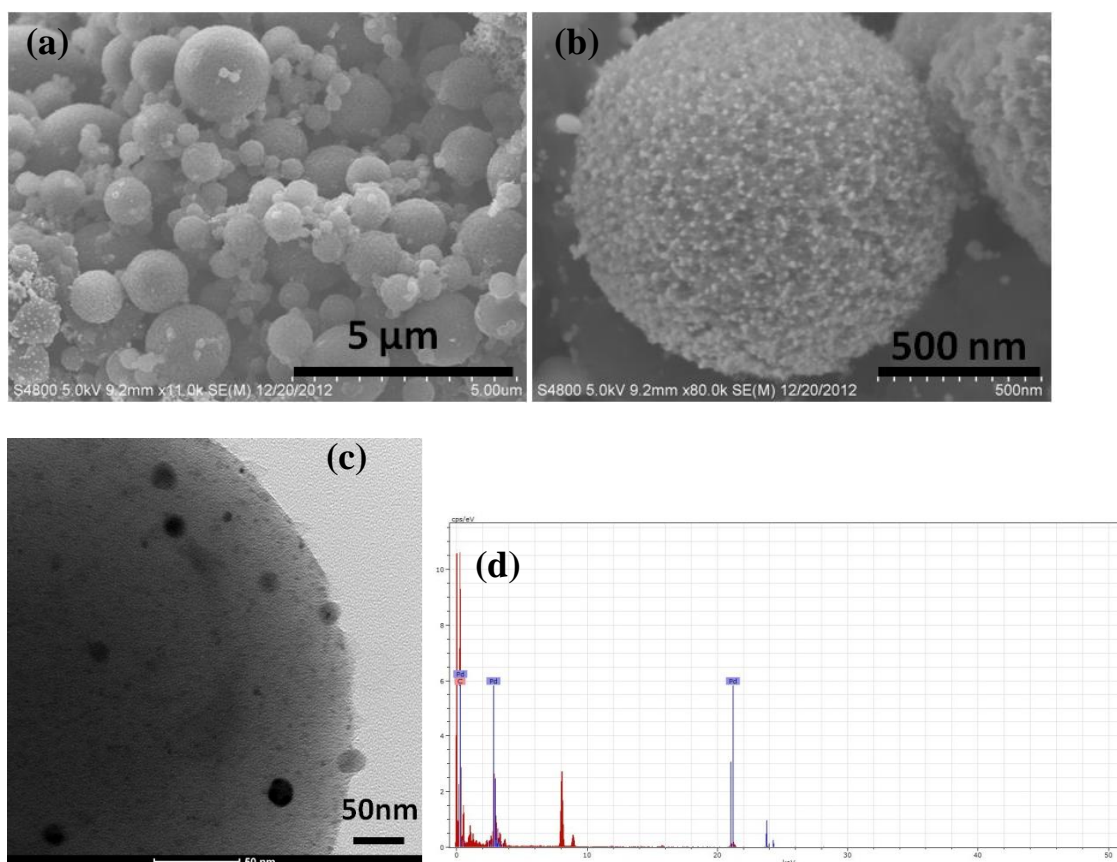


Figure 5.3 (a) SEM (b) single particle SEM (c) high-resolution TEM of carbon supported palladium nanoparticles (Pd-C composite microspheres) prepared using aerosol-based process at 400 °C and H₂ reduction at 400 °C. (d) EDS spectrum of the Pd-C composites confirming the presence of palladium.

5.3.3 Reaction characteristics

The reaction kinetics of TCE in the presence of Pd-C particles is shown in Figure 5.4. Figure 5.4 is the kinetic plot for TCE with Pd-C particles reduced by H₂ at 300 °C. From Figure 5.4, we can observe an immediate sharp reduction of the TCE peak followed by a much slower decline in TCE concentrations. This sharp reduction is not due to reaction but to TCE adsorption on the carbon, as the product generation follows a much slower rate. The subsequent slow evolution of gas phase TCE dechlorination products indicates that dechlorination of TCE is responsible for the second, slower phase in the combined adsorption+reaction sequence. Assuming that dechlorination of TCE is rate controlling for the second step, it is possible to calculate a pseudo-first order rate constant for TCE dechlorination from the evolution rate of gas phase products. The mass normalized rate constant for the Pd-C composite particles (H₂ reduction temperature is 300 °C), k_m is 0.788 Lg⁻¹h⁻¹.

In the case of Pd-C particles prepared at 400 °C reduction temperature, the particles are highly active and complete conversion of TCE to product ethane is achieved in less than 30 minutes (result not shown here). The reaction of TCE conversion to the product ethane is 30 times faster with the increase of H₂ reduction temperature from 300 °C to 400 °C. Although the conversion is slow for the system reduced at 300 °C, it is interesting to note that dissolved concentration of TCE is significantly reduced as soon as the particles are added. This is the advantage of using carbon-based system as it has adsorption which is not the case with other supports such as alumina. This is significant for the systems that have low catalytic activity. Because of the adsorption characteristic, carbons can not only reduce dissolved concentration but also enhance reaction kinetics by

increasing local concentrations of contaminants at the reactive catalytic sites. Hence this study demonstrates that adsorption can play an important role for the catalytic hydrodechlorination of chlorinated hydrocarbons and carbons would be better supports for Pd nanoparticles compared to other supports or stabilizers.

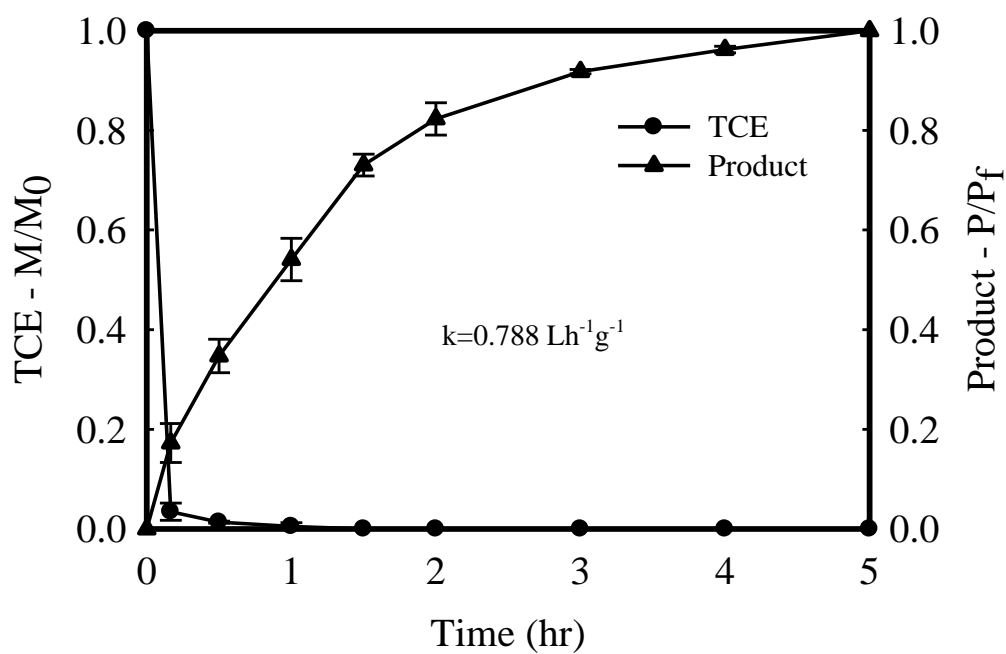


Figure 5.4 TCE removals from solution and gas product evolution rates for Pd-C particles (aerosol-based process at 400 °C and H₂ reduction at 300 °C). M/M_0 is the original TCE remaining, and P/P_f is the ration of gas product peak to the gas product peak at the end of 5 h.

5.4 Summary

In summary, nanoscale Pd particles supported on carbon microspheres are prepared using an aerosol-based process followed by H₂ reduction at lower temperatures. Although the actual preparation is a two-step process, the distribution of Pd species (salts) in nanoscale on carbon microspheres is achieved using the one-step aerosol-based process. The subsequent H₂ reduction converts the Pd-salts to metallic Pd particles. Nevertheless, aerosol-based process is a promising method for the synthesis of supported Pd nanoparticles due to its simplicity and its potential for scale-up. The materials prepared are highly active and demonstrated excellent reaction characteristics for the catalytic hydrodechlorination of TCE. The advantage of carbon-based system is its adsorption, which significantly reduces the bulk concentration of organic contaminants such as TCE.

Chapter 6

Conclusions and Future work

In this research, adsorptive-reactive composite microparticulate systems within the size range of 100 – 1000 nm were developed for the simultaneous adsorption and reduction of chlorinated hydrocarbons such as trichloroethylene (TCE). This work demonstrated two different approaches to prepare functional nanocomposites of zerovalent iron supported onto carbon microspheres. Both the iron-carbon composite microparticulate systems developed in this work have the requisite properties of reaction, adsorption, and transport which make them attractive and suitable for the *in situ* remediation technology.

The first study illustrates that the reduction of precursor iron salts to zerovalent iron does not necessarily take place through addition of a reductant such as sodium borohydride. Instead, reduction can occur through the carbothermal step to generate NZVI and generate porous adsorptive carbons. These Fe-C composite microspheres are highly uniform and monodisperse with particle size around 500 nm. The Fe-C composite microspheres prepared in the second study are polydisperse with particle size range of 100 – 1000 nm. The novelty of this study is the demonstration of the ability of the aerosol-based process in selectively controlling the placement of iron nanoparticles from the external surface of carbon microsphere to the interior.

The aerosol-based is used to synthesize carbon-supported palladium (Pd) nanoparticles for catalytic hydrodechlorination of trichloroethylene. The materials prepared are highly active and demonstrated excellent reaction characteristics.

In summary, the iron-carbon composite materials prepared in this research are very effective towards the simultaneous adsorption and reaction of the chlorinated hydrocarbon contaminants such as trichloroethylene (TCE). They are in the optimal size range for optimal transport through the subsurface and these composite materials are environmentally benign. Finally, the iron-carbon composite particles prepared through the aerosol-based process can be used for the *in situ* remediation technology as the process is conducive to scale-up and the materials are environmentally benign. The aerosol-based process is also very promising for the preparation of supported Pd nanoparticles for ex situ remediation of contaminated water.

The findings in this research suggest the following directions for future work:

The simple preparation method of aerosol-based process to develop carbon supported iron nanoparticles can be applied to prepare other carbon supported catalyst materials such as supported bimetallic nanoparticles. The fact that the aerosol-based process is amenable to scale-up is very encouraging in exploring the application of this process in preparing various carbon supported catalytic materials for environmental remediation and heterogeneous catalysis applications. Initial results in this direction are very encouraging and are discussed below.

The preliminary results of the carbon supported nanoscale iron-nickel bimetallic particles (Fe-Ni/C composite microspheres) prepared using the aerosol-based process is

shown in Figure 6.1. The preparation process is similar to the preparation of iron-carbon composite microspheres described in chapter 4, but with the addition of nickel salt to the precursor materials. Briefly, a homogeneous precursor solution containing 6g sucrose, 4g $\text{FeCl}_3 \cdot 6\text{H}_2\text{O}$ and 0.34g $\text{NiCl}_2 \cdot 6\text{H}_2\text{O}$ in 30mL of water was first atomized to form aerosol droplets, which were then carried by an inert gas (nitrogen (N_2)) through a heating zone where solvent evaporation and carbonization occurs. The weight ratio of nickel is 10% relative to iron in the precursor solution. The temperature of the heating zone was held at 700 °C. The resulting iron-nickel salt-carbon particles were collected over a filter maintained at 100 °C. The as-synthesized iron-nickel salt-carbon particles were reduced through liquid phase NaBH_4 reduction to obtain Fe-Ni/C composite particles. Figure 6.1a and 6.1b are the SEM and TEM micrographs of Fe-Ni/C composite particles. The particles are well-defined microspheres (SEM - Figure 6.1a) and the presence of bimetallic Fe-Ni nanoparticles with higher electron contrast can be seen in the Figure 6.1b (TEM). These Fe-Ni/C composite microspheres were tested towards the reductive dechlorination of TCE in batch experiments with an initial TCE concentration of 20 ppm and 0.2g Fe-Ni/C composite particles. The reaction was monitored through headspace analysis using the procedures described in earlier chapters (chapters 2-4). The reaction kinetics of TCE in the presence of Fe-Ni/C composite microspheres is shown in Figure 6.1c. These iron-nickel bimetallic particles supported on carbon microspheres show a rapid adsorption and reaction with complete conversion of TCE to product achieved in 8 hours. The mass normalized rate constant, k_m is $0.116 \text{ Lg}^{-1}\text{h}^{-1}$.

These initial results of carbon supported bimetallic nanoparticles (Fe-Ni/C) are very encouraging in fully exploring these systems towards the remediation of DNAPL

contaminants. Systematic and detailed experiments are needed to completely understand these systems and develop a new class of adsorptive-reactive particulate systems for environmental remediation applications.

One other very important research direction in the future would be to apply the iron-carbon composite systems developed in this research towards the remediation of other class of groundwater contaminants such as polychlorinated biphenyls (PCBs), metal ions including hexavalent chromium (Cr (VI)) and arsenic (As (V)).

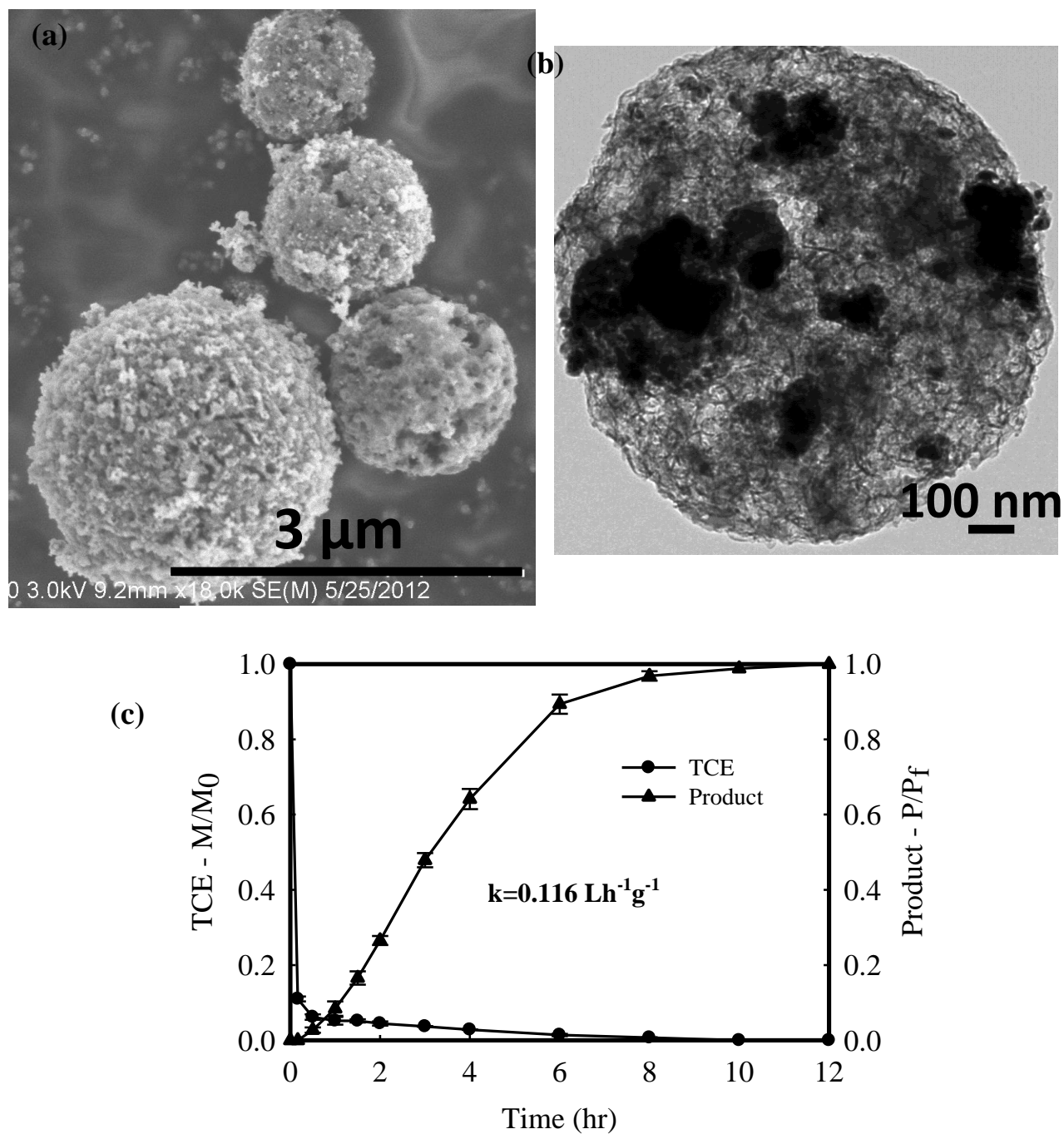


Figure 6.1 (a) SEM (b) TEM of carbon supported nanoscale Fe-Ni bimetallic particles (Fe-Ni/C) prepared using aerosol-based process at 700 °C. (c) TCE removal from solution and gas product evolution rates for Fe-Ni/C composite particles. M/M_0 is the fraction of the original chlorinated ethene remaining and P/P_f is the ratio of the gas product peak to the gas product peak at the end of 12 h.

Appendix

Adsorption Effect of Carbons on the Catalytic Hydrodechlorination of Trichloroethylene

1. Introduction

In this study, adsorption effect of carbons on the catalytic hydrodechlorination of trichloroethylene (TCE) using commercially available supported palladium (Pd) particles is investigated. The commercial systems selected in this study are palladium supported on activated carbon (Pd/AC) and palladium supported on alumina (Pd/Al). The amount of Pd on both of these supports is 1 wt% relative to the respective support weight. Commercially available activated carbon (AC) is added separately in systematic amounts to the suspensions of Pd/AC and Pd/Alumina to study the effect of carbon adsorption on the conversion of TCE to ethane during the catalytic hydrodechlorination reaction.

2. Experimental section

2.1. Materials

All chemicals for reaction kinetics were purchased from Sigma-Aldrich and used as received: 1 wt% palladium supported on activated carbon (1% Pd/AC, ACS reagent), 1 wt% palladium supported on alumina (1% Pd/Al, ACS reagent), Activated carbon (AC, 97%, ACS reagent), and trichloroethylene. Hydrogen (H_2) gas used to saturate the particle suspension is purchased from Airgas. Deionized (DI) water generated with a Barnstead E-pure purifier (Barnstead Co., Iowa) to a resistance of approximately 18.2 M Ω was used in all experiments.

2.2. Characterization and Analysis

Field emission scanning electron microscopy (SEM, Hitachi S-4800, operated at 20 kV), transmission electron microscopy (TEM; JEOL 2010, operated at 120 kV voltage), were used to characterize particle size and morphology. Energy-dispersive X-ray spectroscopy (EDS) is used for the elemental analysis and to confirm the presence of palladium in the samples. In analysis, TCE dechlorination effectiveness was tested in batch experiments. In details, 0.2 mg of the commercial supported catalytic material (Pd/AC or Pd/Al) is first dispersed in 20 mL of water and sonicated for 5 minutes. To this desired amount of activated carbon (1.8 mg or 9.8 mg) is added (in the systems where extra activated carbon is added to see the adsorption effect on the reaction) and sonicated for 15 minutes. The particle suspension is then bubbled with H_2 gas for 15 minutes and the reaction vial is capped with a Mininert valve. To this vial, 20 μ L of a TCE stock solution (20 g/L TCE in methanol) is spiked, resulting in an initial TCE concentration of

20 ppm. The reaction was monitored through a headspace analysis using the procedures described in our earlier work.^{64, 112, 113}

3. Results

The results (morphology, microstructure, elemental analysis and reaction kinetics) of this study are presented/shown in Figures (B.1 to B.8) and Table B.1. From the SEM and TEM images, the commercial Pd/AC and Pd/Al particles have irregular morphology and the EDS analysis confirms the presence of palladium in the samples. Figures B.5 to B.8 shows the reaction kinetics of TCE with the supported Pd particles (Pd/AC and Pd/Al) along with added activated carbon to the Pd/AC and Pd/Al systems. The reaction kinetics in this study illustrates that the extra activated carbon reduces the dissolved TCE concentration dramatically by means of adsorption. But more importantly, the adsorbed TCE desorbs from the activated carbon sites to the catalyst (Pd) sites to get reduced to the product ethane as the reaction proceeds. The mass normalized rate constants for the systems studied here are given in Table B.1.

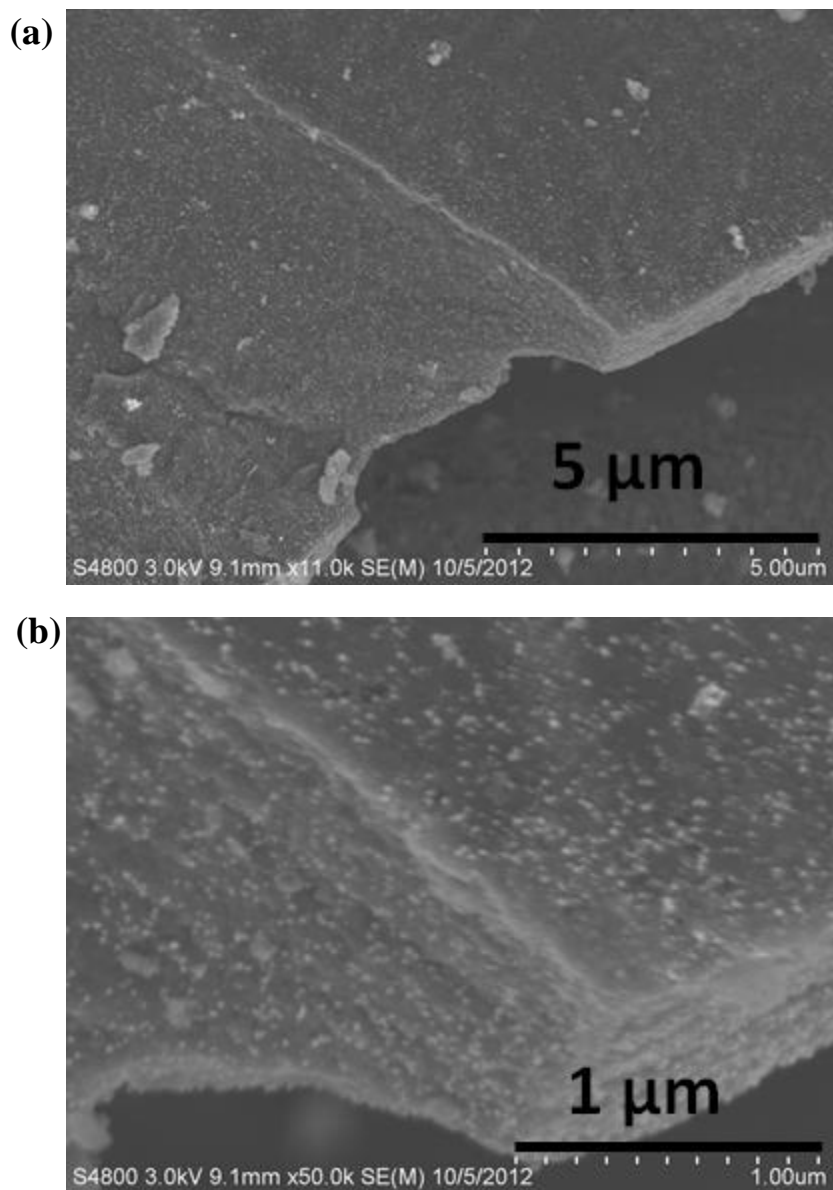


Figure B.1 (a) SEM and (b) high-resolution SEM of commercial palladium on activated carbon (Pd/AC) material.

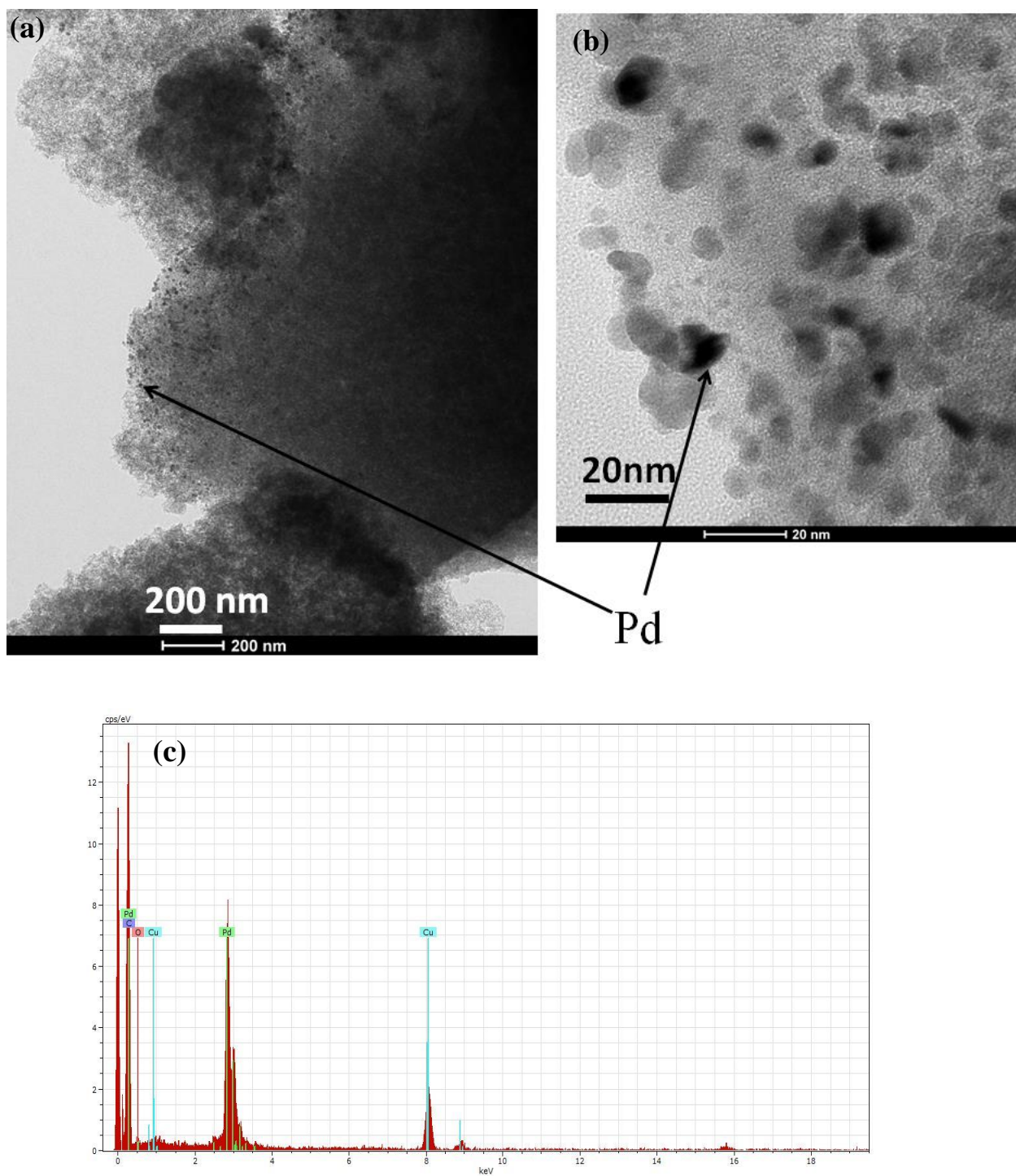


Figure B.2 (a) TEM and (b) high-resolution TEM of the commercial palladium on activated carbon (Pd/AC) material. (c) The EDS spectrum of the commercial Pd/AC confirming the presence of palladium.

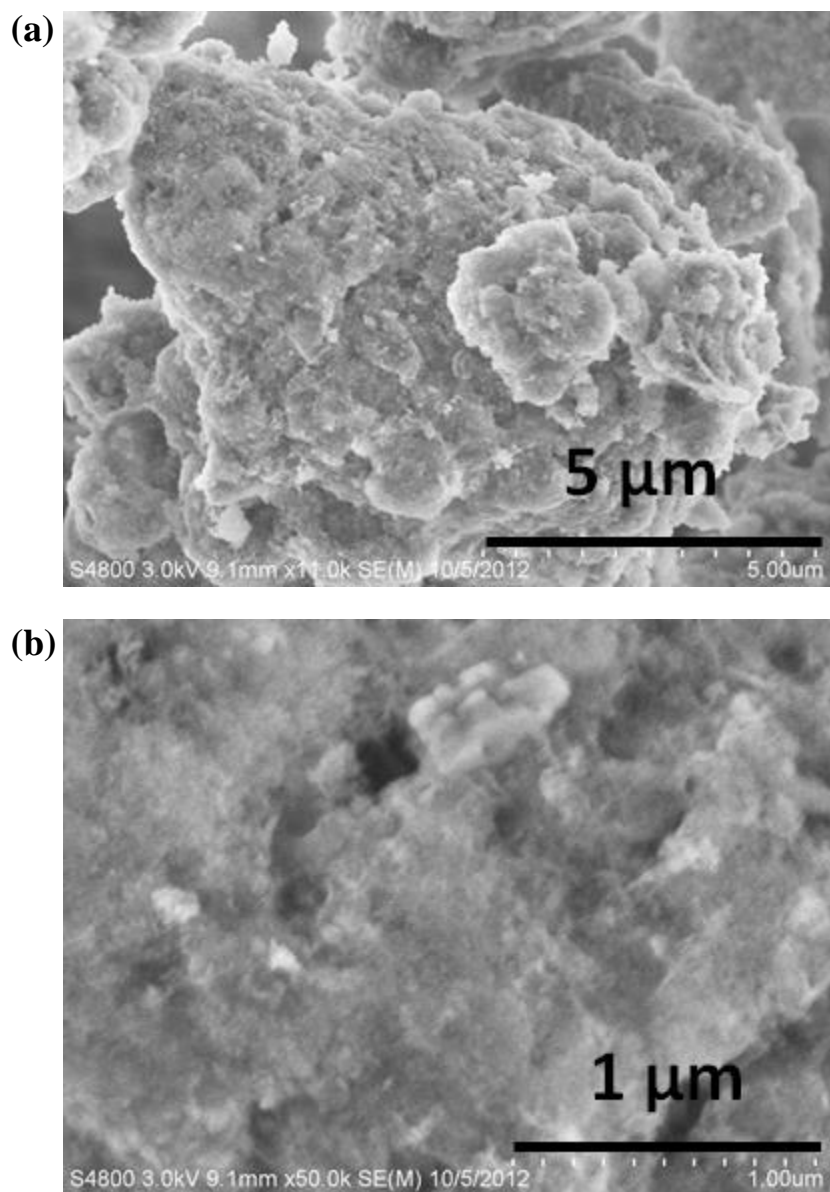


Figure B.3 (a) SEM and (b) high-resolution SEM of commercial palladium on alumina (Pd/Al) material.

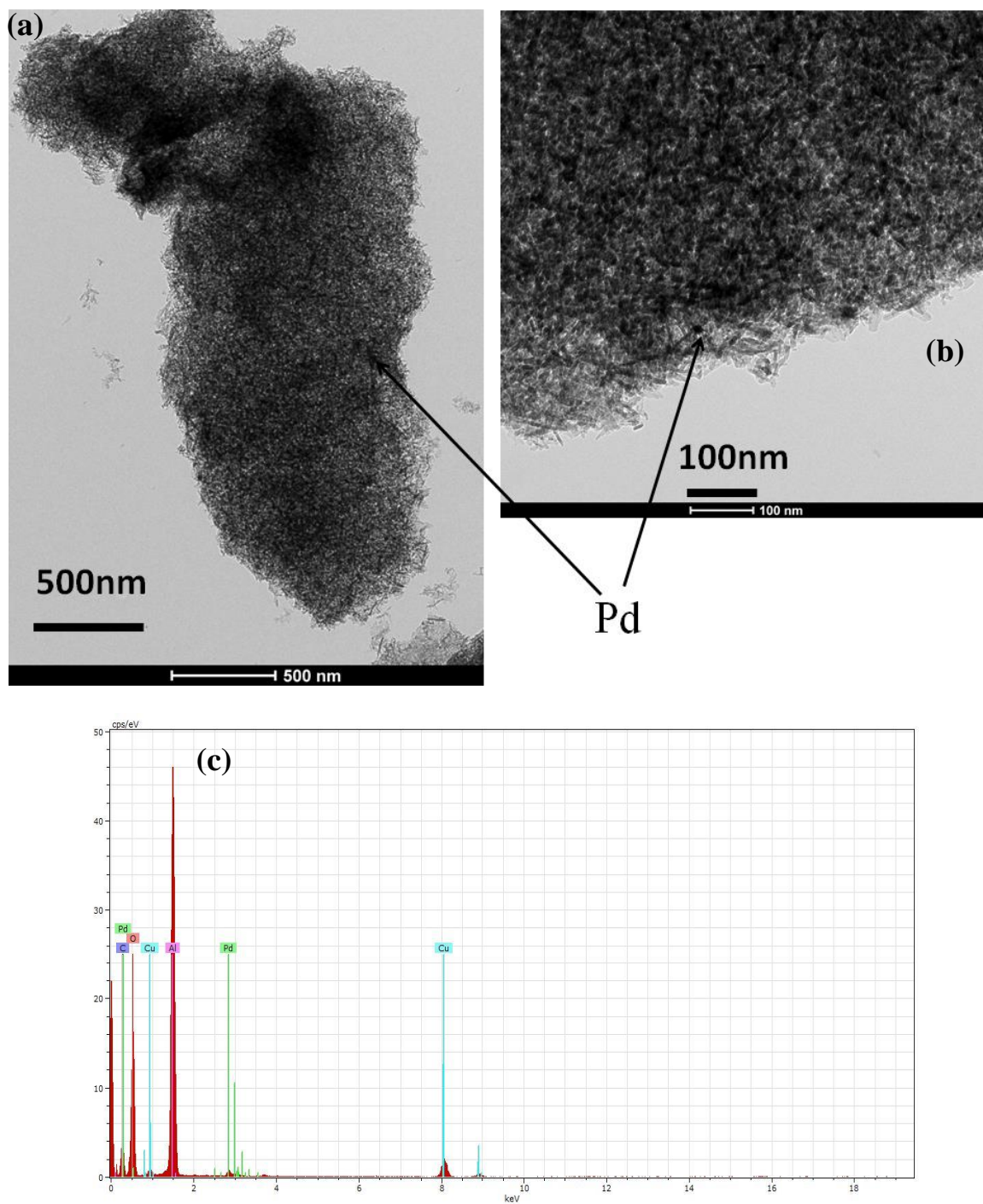


Figure B.4 (a) TEM and (b) high-resolution TEM of the commercial palladium on alumina (Pd/Al) material. (c) The EDS spectrum of the commercial Pd/Al material confirming the presence of palladium.

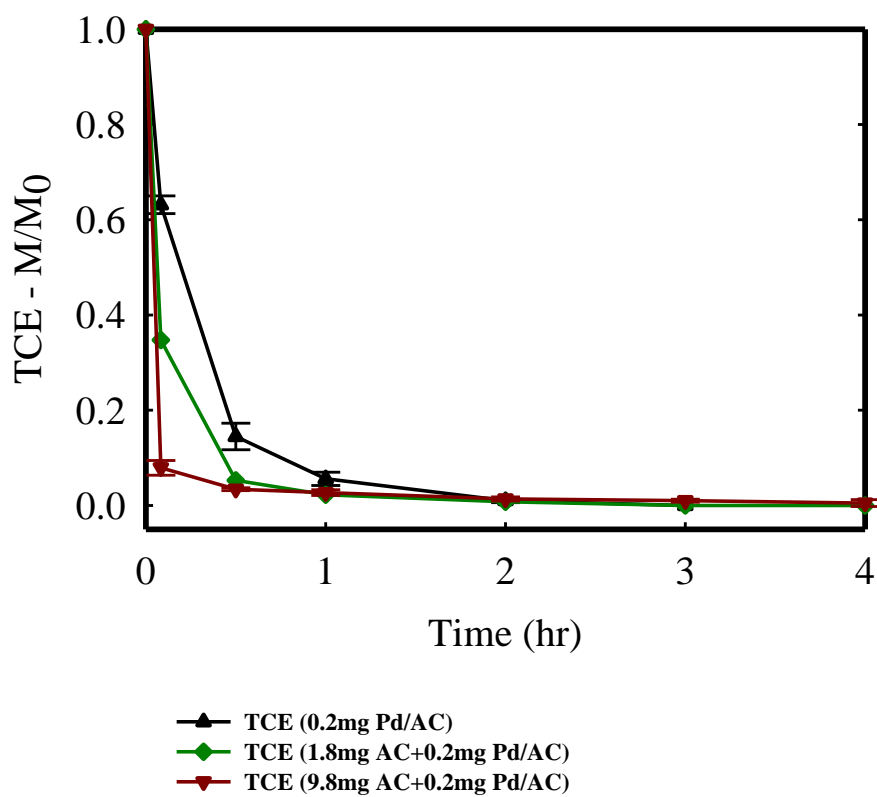


Figure B.5 TCE removal from solution Pd/AC systems with separate addition of activated carbon. M/M_0 is the original TCE remaining in the system.

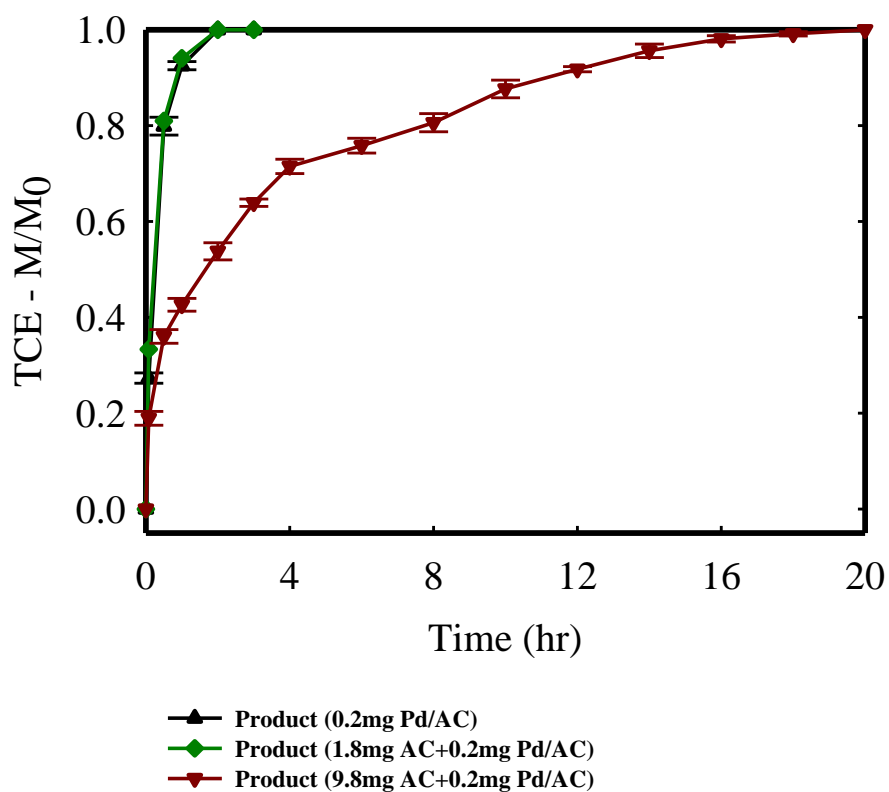


Figure B.6 Gas product evolution for Pd/AC systems with separate addition of activated carbon. P/P_f is the ration of gas product peak to the gas product peak at the end of the reaction.

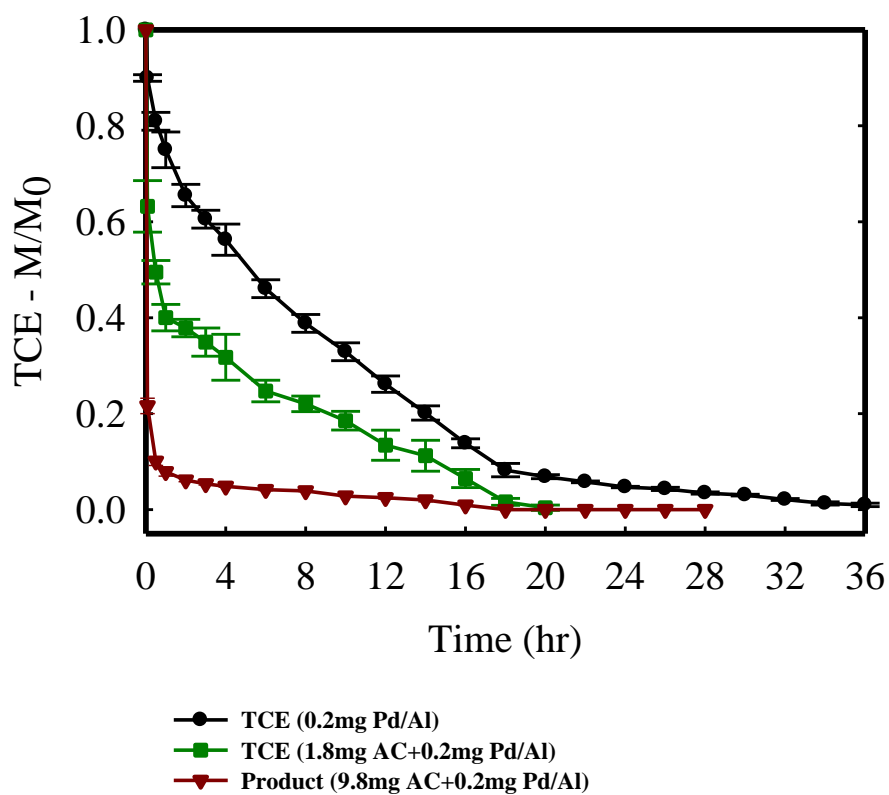


Figure B.7 TCE removal from solution Pd/Al systems with separate addition of activated carbon. M/M_0 is the original TCE remaining in the system.

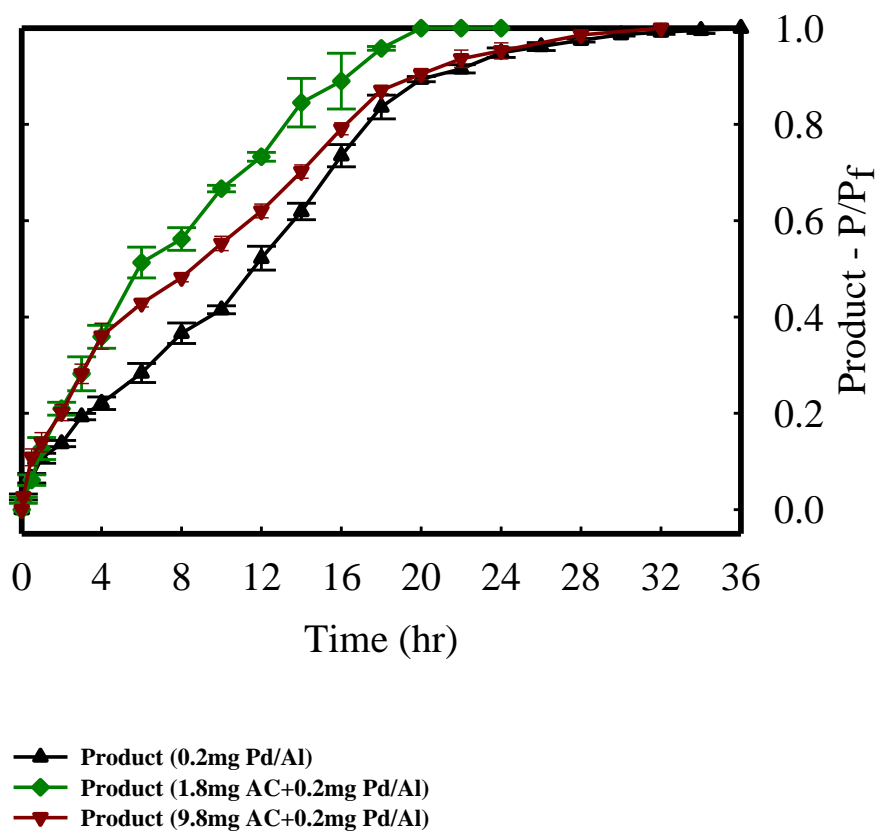


Figure B.8 Gas product evolution for Pd/Al systems with separate addition of activated carbon. P/P_f is the ration of gas product peak to the gas product peak at the end of the reaction.

Sample	Mass-normalized rate constant ($\text{Lg}_{\text{pd}}^{-1}\text{min}^{-1}$)
0.2 mg Pd/AC	328.8
1.8mg AC+0.2 mg Pd/AC	332.6
9.8mg AC+0.2 mg Pd/AC	39.8
0.2 mg Pd/Alumina	20.7
1.8mg AC+0.2 mg Pd/Alumina	22.01
9.8mg AC+0.2 mg Pd/Alumina	24.02

Table B.1 Reaction rate constants for the reduction of trichloroethylene (TCE) using the commercial Pd/AC and Pd/Al systems with separate addition of activated carbon to the particle suspensions.

References

- (1) Michael, M.; John, Z.; Paul, S. Chlorinated Solvents in groundwater of the United States. *Environ. Sci. Technol.* **2007**, *41*, 74-81.
- (2) JS, Z.; JM, C.; T, I.; WW, L.; MJ, M.; BL, R. *The quality of our nation's waters: volatile organic compounds in the nation's groundwater and drinking water supply wells*; US Geological Survey: Reston, VA, 2006.
- (3) Leeson, A.; Kavanaugh, M. C.; Marqusee, J. A.; Smith, B.; Stroo, H.; M, U. Remediating chlorinated Source Zones. *Environ. Sci. Technol.* **2003**, *37* (11), 224A-230A.
- (4) EPA, U. S. *Maximum Contaminants Levels and Regulatory Dates for Drinking Water*; U. S. EPA vs California: November 2008.
- (5) Orth, W. S.; Gillham, R. W. Dechlorination of Trichloroethene in Aqueous Solution Using Fe⁰. *Environ. Sci. Technol.* **1996**, *30* (1), 66-71.
- (6) *Cleaning Up the Nation's Waste Sites: Markets and Technology Trends*; The United States Environmental Protection Agency: 2004.
- (7) Heron, G.; Christensen, T. H.; Enfield, C. G. Henry's Law Constant for Trichloroethylene between 10 and 95 °C. *Environ. Sci. Technol.* **1998**, *32* (10), 1433-1437.
- (8) Mackay, D. M.; Cherry, J. A. Groundwater contamination: Pump-and treat remediation. *Environ. Sci. Technol.* **1989**, *23* (6), 630-636.

- (9) Nakano, Y.; Hua, L.; Nishijima, W.; Shoto, E.; Okada, M. Biodegradation of Trichloroethylene (TCE) Adsorbed on Granular Activated Carbon (GAC). *Wat. Res.* **2000**, *34* (17), 4139-4142n.
- (10) O'Hannesin, S. F.; Gillham, R. W. Long-term performance of an in situ "iron wall" for remediation of VOCs. *Ground Water* **1998**, *36* ((1)), 164-170.
- (11) Ritter, K.; Odziemkowski, M. S.; Gillham, R. W. An in situ study of the role of surface films on granular iron in the permeable iron wall technology. *J. Contam. Hydrol.* **2002**, *55*, 87-111.
- (12) Scherer, M. M.; Richter, S.; Valentine, R. L.; Alvarez, P. J. J. Chemistry and microbiology of permeable reactive barriers for in situ groundwater clean up. *Crit. Rev. Environ. Sci. Technol.* **2000**, *30*, 363.
- (13) Elliott, D. W.; Zhang, W. X. Field Assessment of Nanoscale Bimetallic Particles for Groundwater Treatment. *Environ. Sci. Technol.* **2001**, *35* (24), 4922-4926.
- (14) Phenrat, T.; Saleh, N.; Sirk, K.; Tilton, R.; Lowry, G. Aggregation and sedimentation of aqueous nanoscale zerovalent iron dispersions. *Environ. Sci. Technol.* **2007**, *41*, 284.
- (15) Wang, C.; Zhang, W. Synthesizing nanoscale iron particles for rapid and complete dechlorination of TCE and PCBs. *Environ. Sci. Technol.* **1997**, *31* (7), 2154-2156.
- (16) Xu, Y.; Zhang, W. Subcolloidal Fe/Ag particles for reductive dehalogenation of chlorinated benzenes. *Ind. Eng. Chem. Res.* **2000**, *39*, 2238.

- (17) Lowry, G.; Reinhard, M. Pd-Catalyzed TCE dechlorination in groundwater: Solute effects, biological control, and oxidative catalyst regeneration. *Environ. Sci. Technol.* **2000**, *34*, 3217.
- (18) Schrick, B.; Blough, J. L.; Jones, A. D.; Mallouk, T. E. Hydrodechlorination of Trichloroethylene to Hydrocarbons Using Bimetallic Nickel-Iron Nanoparticles. *Chem. Mater.* **2002**, *14* (12), 5140-5147.
- (19) Joo, S.; Feitz, A.; Waite, T. Oxidative degradation of the carbothioate herbicide, molinate, using nanoscale zero-valent iron. *Environ. Sci. Technol.* **2004**, *38*, 2242.
- (20) Dror, I.; Baram, D.; Berkowitz, B. Use of nanosized catalysts for transformation of chloro-organic pollutants. *Environ. Sci. Technol.* **2005**, *39*, 1283.
- (21) Liu, Y. Q.; Majetich, S. A.; Tilton, R. D.; Sholl, D. S.; Lowry, G. V. TCE dechlorination rates, pathways, and efficiency of nanoscale iron particles with different properties. *Environ. Sci. Technol.* **2005**, *39*, 1338-1345.
- (22) Liu, Y.; Choi, H.; Dionysiou, D.; Lowry, G. V. Trichloroethene Hydrodechlorination in Water by Highly Disordered Monometallic Nanoiron. *Chem. Mater.* **2005**, *17* (21), 5315-5322.
- (23) Lien, H. L.; Zhang, W. X. Nanoscale iron particles for complete reduction of chlorinated ethenes. *Colloids Surf., A* **2001**, *191*, 97-105.
- (24) He, F.; Zhao, D. Preparation and Characterization of a New Class of Starch-Stabilized Bimetallic Nanoparticles for Degradation of Chlorinated Hydrocarbons in Water. *Environ. Sci. Technol.* **2005**, *39* (9), 3314-3320.
- (25) Sakulchaicharoen, N.; O'Carroll, D. M.; Herrera, J. E. *J. Contam. Hydrol.* **2010**, *118*, 117.

- (26) Lien, H. L.;Zhang, W. X. Nanoscale Pd/Fe bimetallic particles: Catalytic effects of palladium on hydrodechlorination. *Applied Catalysis B-Environmental* **2007**, 77 (1-2), 110-116.
- (27) Zhang, W. X.;Nanoscaleironparticlesforenvironmentalremediation An overview. *J. Nanopart. Res.* **2003**, 5, 323-332.
- (28) Tratnyek, P. G.;Johnson, R. L. Nanotechnologies for environmental cleanup. *NanoToday* **2006**, 1, 44-48.
- (29) Nurmi, J. T.; Tratnyek, P. G.; Sarathy, V.; Baer, D. R.; Amonette, J. E.; Pecher, K.; Wang, C. M.; Linehan, J. C.; Matson, D. W.; Penn, R. L.;Driessen, M. D. Characterization and properties of metallic iron nanoparticles: Spectroscopy, electrochemistry, and kinetics. *Environ. Sci. Technol.* **2005**, 39, 1221-1230.
- (30) Matheson, L. J.;Tratnyek, P. G. Reductive dehalogenation of chlorinated methanes by iron metal. *Environ. Sci. Technol.* **1994**, 28, 2045-2053.
- (31) Muftikian, R.; Fernando, Q.;Korte, N. A method for the rapid dechlorination of low molecular weight chlorinated hydrocarbons in water. *Water Res.* **1995**, 29, 2434.
- (32) Nyer, E. K.;Vance, D. B. Nano-scale iron for dehalogenation. *Ground Water Monit. Remediat.* **2001**, 2, 41-46.
- (33) Farrell, J.; Kason, M.; Melitas, N.; Li, T.;Investigation Investigation of the long-term performance of zero-valent iron for reductive dechlorination of trichloroethylene. *Environ. Sci. Technol.* **2000**, 34, 514-521.
- (34) Gillham, R. W. Enhanced degradation of halogenated aliphatics by zero-valent iron. *Ground Water* **1994**, 32, 958-957.

- (35) Wust, W. F.; Kober, R.; Schlicker, O.; Dahmke, A. Combined zero- and first-order kinetics model of the degradation of TCE and cis-DCE with commercial iron. *Environ. Sci. Technol.* **1999**, *33*, 4304.
- (36) Tratnyek, P. G.; Johnson, T. L.; Scherer, M. M.; Eykholt, G. R. Remediating ground water with zero-valent metals: chemical considerations in barrier design. *Ground Water Monit. Rem.* **1997**, *Winter*, 108.
- (37) Bratsch, S. G. *J. Phys. Chem. Ref. Data* **18**, 1-21.
- (38) Ponder, S.; Darab, J.; Mallouk, T. Remediation of Cr(VI) and Pb(II) aqueous solutions using supported, nanoscale zero-valent iron. *Environ. Sci. Technol.* **2000**, *34*, 2564-2569.
- (39) Ponder, S. M.; Darab, J. G.; Bucher, J.; Caulder, D.; Craig, I.; Davis, L.; Edelstein, N.; Lukens, W.; Nitsche, H.; Rao, L.; Shuh, D. K.; Mallouk, T. E. Surface Chemistry and Electrochemistry of Supported Zerovalent Iron Nanoparticles in the Remediation of Aqueous Metal Contaminants. *Chem. Mater.* **2001**, *13* (2), 479-486.
- (40) Phenrat, T.; Saleh, N.; Sirk, K.; Tilton, R.; Lowry, G. Aggregation and sedimentation of aqueous nanoscale zerovalent iron dispersions. *Environ. Sci. Technol.* **2007**, *41* (1), 284-290.
- (41) Schrick, B.; Hydutsky, B. W.; Blough, J. L.; Mallouk, T. E. Delivery vehicles for zerovalent metal nanoparticles in soil and groundwater. *Chem. Mater.* **2004**, *16* (11), 2187-2193.
- (42) Saleh, N.; Phenrat, T.; Sirk, K.; Dufour, B.; Ok, J.; Sarbu, T.; Matyjaszewski, K.; Tilton, R. D.; Lowry, G. V. Adsorbed triblock copolymers deliver reactive iron nanoparticles to the oil/water interface. *Nano Lett.* **2005**, *5* (12), 2489-2494.

(43) Saleh, N.; Sirk, K.; Liu, Y.; Phenrat, T.; Dufour, B.; Matyjaszewski, K.; Tilton, R. D.; Lowry, G. V. Surface modifications enhance nanoiron transport and NAPL targeting in saturated porous media. *Environ. Eng. Sci.* **2007**, *24* (1), 45-57.

(44) Phenrat, T.; Saleh, N.; Sirk, K.; Kim, H. J.; Tilton, R. D.; Lowry, G. V. Stabilization of aqueous nanoscale zerovalent iron dispersions by anionic polyelectrolytes: Adsorbed anionic polyelectrolyte layer properties and their effect on aggregation and sedimentation. *J. Nanopart. Res.* **2008**, *10*, 795-894.

(45) He, F.; Zhao, D.; Liu, J.; Roberts, C. B. Stabilization of Fe-Pd Nanoparticles with Sodium Carboxymethyl Cellulose for Enhanced Transport and Dechlorination of Trichloroethylene in Soil and Groundwater. *Ind. Eng. Chem. Res.* **2007**, *46* (1), 29-34.

(46) Zhan, J.; Zheng, T.; Piringer, G.; Day, C.; McPherson, G. L.; Lu, Y.; Papadopoulos, K.; John, V. T. Transport Characteristics of Nanoscale Functional Zerovalent Iron/Silica Composites for in Situ Remediation of Trichloroethylene. *Environ. Sci. Technol.* **2008**, *42* (23), 8871-8876.

(47) Yao, K.-M.; Habibian, M. T.; O'Melia, C. R. Water and waste water filtration. Concepts and applications. *Environmental Science & Technology* **1971**, *5* (11), 1105-1112.

(48) Tufenkji, N.; Elimelech, M. Correlation equation for predicting single-collector efficiency in physicochemical filtration in saturated porous media. *Environ. Sci. Technol.* **2004**, *38* (2), 529.

(49) Zheng, T.; Zhan, J.; He, J.; Day, C.; Lu, Y.; McPherson, G. L.; Piringer, G.; John, V. T. Reactivity characteristics of nanoscale zerovalent iron--silica composites for trichloroethylene remediation. *Environ Sci Technol* **2008**, *42* (12), 4494-4499.

- (50) O'Carroll, D.; Sleep, B.; Krol, M.; Boparai, H.;Kocur, C. Nanoscale zero valent iron and bimetallic particles for contaminated site remediation. *Advances in Water Resources* **2013**, *51* (0), 104-122.
- (51) Al-abed, S. R.;Chen, J., Transport of trichloroethylene (TCE) in natural soil by electroosmosis. In *Physicochemical Groundwater Remediation*, Smith, J. A.; Burns, S. E., Eds. Kluwer academic/ Plenum: New York, 2001; pp 91-114.
- (52) Alessi, D. S.;Li, Z. Synergistic Effect of Cationic Surfactants on Perchloroethylene Degradation by Zero-Valent Iron. *Environ. Sci. Technol.* **2001**, *35* (18), 3713-3717.
- (53) Kanel, S. R.;Choi, H. Transport characteristics of surface-modified nano scale zero-valent iron in porous media. *Water Sci. Technol.* **2007**, *55*, 157-162.
- (54) Quinn, J.; Geiger, C.; Clausen, C.; Brooks, K.; Coon, C.; O'Hara, S.; Krug, T.; Major, D.; Yoon, W. S.; Gavaskar, A.;Holdsworth, T. Field Demonstration of DNAPL Dehalogenation Using Emulsified Zero-Valent Iron. *Environ. Sci. Technol.* **2005**, *39* (5), 1309-1318.
- (55) Lubick, N. Cap and degrade: a reactive nanomaterial barrier also serves as a cleanup tool. *Environ. Sci. Technol.* **2009**, *43* (2), 235-235.
- (56) Choi, H.; Agarwal, S.;Al-Abed, S. R. Adsorption and Simultaneous Dechlorination of PCBs on GAC/Fe/Pd: Mechanistic Aspects and Reactive Capping Barrier Concept. *Environmental Science & Technology* **2009**, *43* (2), 488-493.
- (57) Al-Abed, S. R.; Jegadeesan, G.; Scheckel, K. G.;Tolaymat, T. Speciation, characterization, and mobility of As, Se, and Hg in flue gas desulphurization residues. *Environmental Science & Technology* **2008**, *42* (5), 1693-1698.

- (58) Schreier, C.; Reinhard, M. Catalytic hydrodehalogenation of chlorinated ethylenes using palladium and hydrogen for the treatment of contaminated water. *Chemosphere* **1995**, *31*, 3475-3487.
- (59) Wang, Q.; Li, H.; Chen, L.; Huang, X. Monodispersed hard carbon spherules with uniform nanopores. *Carbon* **2001**, *39* (14), 2211-2214.
- (60) Wang, Q.; Li, H.; Chen, L. Q.; Huang, X. J. Novel spherical microporous carbon as anode material for Li-ion batteries. *Solid State Ionics* **2002**, *152*, 43-50.
- (61) Yang, R.; Qiu, X.; Zhang, H.; Li, J.; Zhu, W.; Wang, Z.; Huang, X.; Chen, L. Monodispersed hard carbon spherules as a catalyst support for the electrooxidation of methanol. *Carbon* **2005**, *43* (1), 11-16.
- (62) L'Vov, B. V. Mechanism of carbothermal reduction of iron, cobalt, nickel and copper oxides. *Thermochimica Acta* **2000**, *360* (2), 109-120.
- (63) Hoch, L. B.; Mack, E. J.; Hydutsky, B. W.; Hershman, J. M.; Skluzacek, I. M.; Mallouk, T. E. Carbothermal synthesis of carbon-supported nanoscale zero-valent iron particles for the remediation of hexavalent chromium. *Environmental Science & Technology* **2008**, *42* (7), 2600-2605.
- (64) Zhan, J.; Sunkara, B.; Le, L.; John, V. T.; He, J.; McPherson, G. L.; Piringir, G.; Lu, Y. Multifunctional Colloidal Particles for in Situ Remediation of Chlorinated Hydrocarbons. *Environ. Sci. Technol.* **2009**, *43* (22), 8616-8621.
- (65) Grittini, C.; Malcomson, M.; Fernando, Q.; Korte, N. Rapid Dechlorination of Polychlorinated Biphenyls on the Surface of a Pd/Fe Bimetallic System. *Environmental Science & Technology* **1995**, *29* (11), 2898-2900.

- (66) He, F.;Zhao, D. Hydrodechlorination of trichloroethene using stabilized Fe-Pd nanoparticles: Reaction mechanism and effects of stabilizers, catalysts, and reaction conditions. *Appl. Catal. B* **2008**, *84*, 533-540.
- (67) Atekwana, E. A.;Richardson, D. S. *Hydrol. Process.* **2004**, *18*, 2801.
- (68) Busenberg, E.; Plummer, L. N.; Doughten, M. W.; Widman, P. K.;Bartholomay, R. C., *Chemical and Isotopic Composition and Gas Concentrations of Groundwater and Surface Water from Selected Sites at and near the Idaho National Engineering and Environmental Laboratory*. 2000.
- (69) Brunauer, S.; Deming, L. S.; Deming, W. E.;Teller, E. On a Theory of the van der Waals Adsorption of Gases. *J. Am. Chem. Soc.* **2002**, *62* (7), 1723-1732.
- (70) S. Lowell, J. E. S., Martina A. Thomas and, Matthias Thommes, *Characterization of porous solids and powders: surface area, pore size and density*. Kluwer Academic Publishers: Dordrecht, 2004.
- (71) Phenrat, T.; Liu, Y. Q.; Tilton, R. D.;Lowry, G. V. Adsorbed Polyelectrolyte Coatings Decrease Fe-0 Nanoparticle Reactivity with TCE in Water: Conceptual Model and Mechanisms. *Environmental Science & Technology* **2009**, *43* (5), 1507-1514.
- (72) He, F.;Zhao, D. Manipulating the size and dispersibility of zerovalent iron nanoparticles by use of carboxymethyl cellulose stabilizers. *Environ. Sci. Technol.* **2007**, *41*, 6216.
- (73) Tufenkji, N.;Elimelech, M. Deviation from the Classical Colloid Filtration Theory in the Presence of Repulsive DLVO Interactions. *Langmuir* **2004**, *20* (25), 10818-10828.

- (74) Tufenkji, N.; Elimelech, M. Breakdown of Colloid Filtration Theory: Role of the Secondary Energy Minimum and Surface Charge Heterogeneities. *Langmuir* **2005**, *21* (3), 841-852.
- (75) Saleh, N.; Kim, H.-J.; Phenrat, T.; Matyjaszewski, K.; Tilton, R. D.; Lowry, G. V. Ionic Strength and Composition Affect the Mobility of Surface-Modified FeO Nanoparticles in Water-Saturated Sand Columns. *Environ. Sci. Technol.* **2008**, *42* (9), 3349-3355.
- (76) Hartley, P. A.; Parfitt, G. D. Dispersion of powders in liquids. 1. The contribution of the van der Waals force to the cohesiveness of carbon black powders. *Langmuir* **1985**, *1* (6), 651-657.
- (77) Bowker, M.; Nuhu, A.; Soares, J. High activity supported gold catalysts by incipient wetness impregnation. *Catalysis Today* **2007**, *122* (3-4), 245-247.
- (78) Itoh, M.; Saito, M.; Takehara, M.; Motoki, K.; Iwamoto, J.; Machida, K.-i. Influence of supported-metal characteristics on deNO_x catalytic activity over Pt/CeO₂. *Journal of Molecular Catalysis A: Chemical* **2009**, *304* (1-2), 159-165.
- (79) Li, Y.; Chen, Y.; Li, L.; Gu, J.; Zhao, W.; Li, L.; Shi, J. A simple co-impregnation route to load highly dispersed Fe(III) centers into the pore structure of SBA-15 and the extraordinarily high catalytic performance. *Applied Catalysis A: General* **2009**, *366* (1), 57-64.
- (80) Pooya, A.; Farnood, R.; Meier, E. Preparation of Multiwalled Carbon Nanotube-Supported Nickel Catalysts Using Incipient Wetness Method. *The Journal of Physical Chemistry A* **2010**, *114* (11), 3962-3968.

- (81) Choi, H.; Al-Abed, S. R.; Agarwal, S.; Dionysiou, D. D. Synthesis of Reactive Nano-Fe/Pd Bimetallic System-Impregnated Activated Carbon for the Simultaneous Adsorption and Dechlorination of PCBs. *Chemistry of Materials* **2008**, 20 (11), 3649-3655.
- (82) Dowideit, P.; von Sonntag, C. Reaction of ozone with ethene and its methyl- and chlorine-substituted derivatives in aqueous solution. *Environ. Sci. Technol.* **1998**, 32 (8), 1112-1119.
- (83) Nutt, M.; Hughes, J.; Wong, M. Designing Pd-on-Au bimetallic nanoparticle catalysts for trichloroethene hydrodechlorination. *Environ. Sci. Technol.* **2005**, 39 (5), 1346-1353.
- (84) Cowell, M.; Kibbey, T.; Zimmerman, J.; Hayes, K. Partitioning of ethoxylated nonionic surfactants in water/NAPL systems: Effects of surfactant and NAPL properties. *Environ. Sci. Technol.* **2000**, 34 (9), 1583-1588.
- (85) Alessi, D.; Li, Z. Synergistic effect of cationic surfactants on perchloroethylene degradation by zero-valent iron. *Environ. Sci. Technol.* **2001**, 35, 3713.
- (86) He, F.; Zhao, D. Manipulating the size and dispersibility of zerovalent iron nanoparticles by use of carboxymethyl cellulose stabilizers. *Environ. Sci. Technol.* **2007**, 41 (17), 6216-6221.
- (87) Choi, H.; Agarwal, S.; Al-Abed, S. R. Adsorption and Simultaneous Dechlorination of PCBs on GAC/Fe/Pd: Mechanistic Aspects and Reactive Capping Barrier Concept. *Environ. Sci. Technol.* **2009**, 43 (2), 488-493.
- (88) Sunkara, B.; Zhan, J.; He, J.; McPherson, G. L.; Piringer, G.; John, V. T. Nanoscale Zerovalent Iron Supported on Uniform Carbon Microspheres for the In situ

Remediation of Chlorinated Hydrocarbons. *ACS Applied Materials & Interfaces* **2010**, 2 (10), 2854-2862.

(89) Al-Abed, S. R.; Jegadeesan, G.; Scheckel, K. G.; Tolaymat, T. Speciation, characterization, and mobility of As, Se, and Hg in flue gas desulphurization residues. *Environ. Sci. Technol.* **2008**, 42 (5), 1693-1698.

(90) Choi, H.; Al-Abed, S. R.; Agarwal, S.; Dionysiou, D. D. Synthesis of Reactive Nano-Fe/Pd Bimetallic System-Impregnated Activated Carbon for the Simultaneous Adsorption and Dechlorination of PCBs. *Chem. Mater.* **2008**, 20 (11), 3649-3655.

(91) Hoch, L. B.; Mack, E. J.; Hydutsky, B. W.; Hershman, J. M.; Skluzacek, J. M.; Mallouk, T. E. Carbothermal Synthesis of Carbon-supported Nanoscale Zero-valent Iron Particles for the Remediation of Hexavalent Chromium. *Environ. Sci. Technol.* **2008**, 42 (7), 2600-2605.

(92) Zheng, T.; Pang, J.; Tan, G.; He, J.; McPherson, G.; Lu, Y.; John, V. T.; Zhan, J. Surfactant templating effects on the encapsulation of iron oxide nanoparticles within silica microspheres. *Langmuir* **2007**, 23 (9), 5143-5147.

(93) Zhan, J.; Kolesnichenko, I.; Sunkara, B.; He, J.; McPherson, G. L.; Piringer, G.; John, V. T. Multifunctional Iron–Carbon Nanocomposites through an Aerosol-Based Process for the In Situ Remediation of Chlorinated Hydrocarbons. *Environ. Sci. Technol.* **2011**, 45 (5), 1949-1954.

(94) Atkinson, J. D.; Fortunato, M. E.; Dastgheib, S. A.; Rostam-Abadi, M.; Rood, M. J.; Suslick, K. S. Synthesis and characterization of iron-impregnated porous carbon spheres prepared by ultrasonic spray pyrolysis. *Carbon* **2011**, 49 (2), 587-598.

- (95) Bystrzejewski, M.; Karoly, Z.; Szepvolgyi, J.; Kaszuwara, W.; Huczko, A.; Lange, H. Continuous synthesis of carbon-encapsulated magnetic nanoparticles with a minimum production of amorphous carbon. *Carbon* **2009**, *47* (8), 2040-2048.
- (96) Rongbo Zheng, X. M., Fangqiong Tang High-Density Magnetite Nanoparticles Located in Carbon Hollow Microspheres with Good Dispersibility and Durability: Their One-Pot Preparation and Magnetic Properties. *Eur. J. Inorg. Chem.* **2009**, (20), 3003-3007.
- (97) Yu, F.; Wang, J. N.; Sheng, Z. M.; Su, L. F. Synthesis of carbon-encapsulated magnetic nanoparticles by spray pyrolysis of iron carbonyl and ethanol. *Carbon* **2005**, *43* (14), 3018-3021.
- (98) Yu, G.; Sun, B.; Pei, Y.; Xie, S.; Yan, S.; Qiao, M.; Fan, K.; Zhang, X.; Zong, B. Fe₃O₄@C Spheres as an Excellent Catalyst for Fischer–Tropsch Synthesis. *Journal of the American Chemical Society* **2010**, *132* (3), 935-937.
- (99) Shin, Y.; Wang, L.-Q.; Bae, I.-T.; Arey, B. W.; Exarhos, G. J. Hydrothermal Syntheses of Colloidal Carbon Spheres from Cyclodextrins. *J. Phys. Chem. C.* **2008**, *112* (37), 14236-14240.
- (100) Zheng, M.; Liu, Y.; Xiao, Y.; Zhu, Y.; Guan, Q.; Yuan, D.; Zhang, J. An Easy Catalyst-Free Hydrothermal Method to Prepare Monodisperse Carbon Microspheres on a Large Scale. *J. Phys. Chem. C.* **2009**, *113* (19), 8455-8459.
- (101) Ryu, J.; Suh, Y.-W.; Suh, D. J.; Ahn, D. J. Hydrothermal preparation of carbon microspheres from mono-saccharides and phenolic compounds. *Carbon* **2010**, *48* (7), 1990-1998.

- (102) Mackenzie, K.; Schierz, A.; Georgi, A.;Kopinke, F.-D. Colloidal Activated Carbon and Carbo-Iron Novel Materials for In-Situ Groundwater Treatment. *Global NEST Journal* **2008**, *10* (1), 54-61.
- (103) Fennelly, J.;Roberts, A. Reaction of 1,1,1-trichloroethane with zero-valent metals and bimetallic reductants. *Environ. Sci. Technol.* **1998**, *32*, 1980.
- (104) Gotpagar, J.; Lyuksyutov, S.; Cohn, R.; Grulke, E.;Bhattacharyya, D. Reductive dehalogenation of trichloroethylene with zerovalent iron: surface profiling microscopy and rate enhancement studies. *Langmuir* **1999**, *15*, 8412.
- (105) Li, T.;Farrell, J. Reductive dechlorination of trichloroethene and carbon tetrachloride using iron and palladized-iron cathodes. *Environ. Sci. Technol.* **2000**, *34*, 173.
- (106) Uludag-Demirer, S.;Bowers, A. Adsorption/reduction reactions of trichloroethylene by elemental iron in the gas phase: the role of water. *Environ. Sci. Technol.* **2000**, *34*, 4407.
- (107) Butler, E.;Hayes, K. Factors influencing rates and products in the transformation of trichloroethylene by iron sulfide and iron metal. *Environ. Sci. Technol.* **2001**, *35*, 3884.
- (108) Doong, R.; Chen, K.;Tsai, H. Reductive dechlorination of carbon tetrachloride and tetrachloroethylene by zerovalent silicon-iron reductants. *Environ. Sci. Technol.* **2003**, *37*, 2575.
- (109) Dries, J.; Bastiaens, L.; Springael, D.; Agathos, S.;Diels, L. Competition for sorption and degradation of chlorinated ethenes in batch zero-valent iron systems. *Environ. Sci. Technol.* **2004**, *38*, 2879.

- (110) Arnold, W.; Roberts, A. Pathways and kinetics of chlorinated ethylene and chlorinated acetylene reaction with Fe(0) particles. *Environ. Sci. Technol.* **2000**, *34*, 1794.
- (111) Alessi, D.; Li, Z. Synergistic effect of cationic surfactants on perchloroethylene degradation by zero-valent iron. *Environ. Sci. Technol.* **2001**, *35* (18), 3713-3717.
- (112) Sunkara, B.; Zhan, J.; He, J.; McPherson, G. L.; Piringer, G.; John, V. T. Nanoscale Zerovalent Iron Supported on Uniform Carbon Microspheres for the In situ Remediation of Chlorinated Hydrocarbons. *ACS Appl. Mater. Interfaces.* **2010**, 2854-2862.
- (113) Sunkara, B.; Zhan, J.; Kolesnichenko, I.; Wang, Y.; He, J.; Holland, J. E.; McPherson, G. L.; John, V. T. Modifying Metal Nanoparticle Placement on Carbon Supports Using an Aerosol-Based Process, with Application to the Environmental Remediation of Chlorinated Hydrocarbons. *Langmuir* **2011**, *27*, 7854-7859.
- (114) Zhan, J.; Sunkara, B.; Tang, J.; Wang, Y.; He, J.; McPherson, G. L.; John, V. T. Carbothermal Synthesis of Aerosol-Based Adsorptive-Reactive Iron–Carbon Particles for the Remediation of Chlorinated Hydrocarbons. *Industrial & Engineering Chemistry Research* **2011**, *50* (23), 13021-13029.
- (115) Lien, H.-L.; Zhang, W.-x. Nanoscale iron particles for complete reduction of chlorinated ethenes. *Colloids and Surfaces A: Physicochemical and Engineering Aspects* **2001**, *191* (1-2), 97-105.
- (116) R.W. Gillham, S. F. O. H. In *Development of zero-valent iron as an in-situ reactant for remediation of VOC-contaminated ground-water*, Association of Groundwater Scientists and Engineers, , Las Vegas, Nevada, 9–12 October, 1994;

Groundwater Remediation: Existing Technology and Future Directions: Las Vegas, Nevada, 1994.

(117) Song, H.; Kim, Y.; Carraway, E. R.; Irene, M. C. L.; Surampali, R. Y.; Keith, C. K. L., *Zero-valent iron reactive materials for hazardous waste and inorganics removal*. 2007; p 206.

(118) Nerbrink O, D. M., Hansson HC. Why do medical nebulizers differ in their output and particle size characteristics? *J Aerosol Med* **1994**, 7 (3), 259-276.

(119) SP, N. Aerosol generators and delivery systems. *Respiratory care* **1991**, 36 (9), 939-951.

(120) Hess, D. R. Nebulizers: principles and performance. *Respiratory care* **2000**, 45 (6), 609-622.

(121) Gossett, J. *Environ. Sci. Technol.* **1987**, 21, 202.

(122) MJ, M.; JS, Z.;PJ, S. Chlorinated Solvents in groundwater of the United States. *Environ. Sci. Technol.* **2007**, 41, 74-81.

(123) Michael, W.; Pedro, A.; Yu-lan, F.; Nurgul, A.; Michael, N.; Jeffrey, M.;Kimberly, H. Cleaner water using bimetallic nanoparticle catalysts. *J Chem Technol Biotechnol* **2009**, 84, 158-166.

(124) Schuth, C.;Reinhard, M. Hydrodechlorination and hydrogenation of aromatic compounds over palladium on alumina in hydrogen-saturated water. *Applied Catalysis B: Environmental* **1998**, 18 (3), 215-221.

(125) Kovenklioglu, S.; Cao, Z.; Shah, D.; Farrauto, R.;Balko, E. Direct catalytichydrodechlorination of toxicorganics in wastewater. *AIChE J* **1992**, 38, 1003-1012.

- (126) Zhu, J.; Zhou, J.; Zhao, T.; Zhou, X.; Chen, D.; Yuan, W. Carbon nanofiber-supported palladium nanoparticles as potential recyclable catalysts for the Heck reaction. *Applied Catalysis A: General* **2009**, 352 (1–2), 243–250.

Biography

Bhanu kiran Sunkara was born in the town of Parkal, India. He pursued his bachelor's degree in Chemical Engineering with distinction from the University of Madras, Chennai, India. He came to the United States in the Fall of 2005 for higher education. He received his Master of Science degree in Chemical Engineering from the University of Louisiana at Lafayette. In 2007, he joined the Chemical & Biomolecular Engineering Department at Tulane University, New Orleans for his doctoral studies.

Research towards his doctoral degree was focused on the development of new class of iron-carbon composite materials and carbon-supported catalytic materials for applications in environmental remediation and heterogeneous catalysis. His research has resulted in two first author and six coauthor publications in peer-reviewed journals like ACS Applied Materials & Interfaces, Langmuir and other American Chemical Society journals. His research towards the breakdown of chlorinated solvents in groundwater was recognized with (a) first place in the Environmental Division Graduate Student Papers Awards for 2009 at AIChE (American Institute of Chemical Engineers) National Conference (b) Distinguished Graduate Student Award and Outstanding Research Award by the Department of Chemical and Biomolecular Engineering in 2010 (c) first place in the School of Science and Engineering Research Day Poster Award for 2011.